Dissertation

Sophisticated Analytical Methods for Lipidomics

submitted by

Alexander Triebl MSc BSc

for the academic degree of

Doctor of Medical Science

(Dr. scient. med.)

at the

Medical University of Graz
Center for Medical Research

under the Supervision of

Priv.-Doz. Dr. med.univ. Tatjana STOJAKOVIC

Mag. Dr. rer. nat. Harald KÖFELER

Dipl.-Ing. Dr. tech. Martin TRÖTZMÜLLER

2016

DECLARATION

I hereby declare that this thesis is my own original work and that I have fully acknowledged by name all of those individuals and organisations that have contributed to the research for this thesis. Due acknowledgement has been made in the text to all other material used. Throughout this thesis and in all related publications I followed the "Standards of Good Scientific Practice and Ombuds Committee at the Medical University of Graz".

Graz, 28.09.2016

FOREWORD

First, I would like to thank Priv.-Doz. Dr. med. univ. Tatjana Stojakovic for the uncomplicated supervision of this work.

Great thanks go to Mag. Dr. rer. nat. Harald Köfeler for his supervision and the opportunity to work in his group.

My deepest thanks go to Dipl.-Ing. Dr. tech. Martin Trötzmüller for providing invaluable help and assistance whenever I needed it.

Thanks to Ing. Stefanie Rappold, Ing. Birgit Reiter and Christine Pein for providing a very enjoyable working atmosphere.

I would also like to thank Dipl.-Ing. Dr. techn. Jürgen Hartler and Univ.-Ass. Dr. med. univ. Katharina Leithner, PhD for the great collaboration.

Last but not least, thanks to all my friends who have helped me make the time I have spent in Graz one that I will never forget.

ACKNOWLEDGEMENTS

This work was supported by the Austrian Science Fund (FWF): [P 26148-N19].

TABLE OF CONTENTS

DECLARATION ..... **I**
FOREWORD ..... **I**
ACKNOWLEDGEMENTS ..... **II**
TABLE OF CONTENTS ..... **III**
ABBREVIATIONS AND ACRONYMS ..... **V**
LIST OF FIGURES ..... **VII**
LIST OF TABLES ..... **IX**
KURZZUSAMMENFASSUNG ..... **X**
ABSTRACT ..... **XII**
1 INTRODUCTION **1**
1.1 The field of Lipidomics **1**
1.1.1 Classification of lipids 2
1.1.2 Lipid nomenclature 4
2 SCOPE OF WORK **6**
3 ANALYTICAL METHODS IN LIPIDOMIC RESEARCH **7**
3.1 Sample preparation **7**
3.1.1 Liquid-liquid extraction 7
3.1.2 Solid-phase extraction 8
3.2 High-performance liquid chromatography **9**
3.2.1 Basics of chromatography 9
3.2.2 A chromatogram 10
3.3 Mass spectrometry **10**
3.3.1 Information content of a mass spectrum 10
3.3.2 A simple mass spectrometer 12
3.3.3 Scan modes 21
3.4 LC/MS **23**
3.5 Other methods **24**
3.5.1 Ion mobility mass spectrometry 24
3.5.2 Mass spectrometry imaging 25
4 A GLOBAL LIPIDOMICS METHOD **26**
4.1 Introduction **26**
4.2 Materials and methods **27**
4.2.1 Lipid standards 27
4.2.2 Sample preparation 27
4.2.3 LC/MS 28
4.2.4 Data processing and quantitation 29
4.2.5 Method validation 29
4.3 Results and discussion **30**
4.3.1 Sample preparation and sample storage 30

4.3.2 Chromatography 31
4.3.3 Tandem mass spectrometry of lipids 33
4.3.4 Identification 51
4.3.5 Method validation 59
4.3.6 Common difficulties in lipidomic quantitation 67
4.4 Conclusion 69
5 ANALYSIS OF N-ACYLPHOSPHATIDYLETHANOLAMINES 71
5.1 Introduction 71
5.2 Materials and methods 72
5.2.1 Synthesis of NAPE 72
5.2.2 Liquid-liquid extraction 73
5.2.3 Solid-phase extraction 73
5.2.4 Chromatography 74
5.2.5 Mass spectrometry 74
5.2.6 Data processing 74
5.2.7 Method validation 74
5.3 Results and discussion 75
5.3.1 NAPE nomenclature 75
5.3.2 Synthesis of NAPE standards 76
5.3.3 Efficiency of sample preparation method 76
5.3.4 NAPE detection and quantification 77
5.3.5 Method validation 80
5.3.6 NAPEs detected in rat brain 81
5.4 Conclusion 82
6 HIGH RESOLUTION TANDEM MASS SPECTROMETRY IN CANCER METABOLISM RESEARCH 83
6.1 Introduction 83
6.2 Hypothesis and aim 83
6.3 Materials and methods 84
6.3.1 Sample preparation 84
6.3.2 Chromatography 84
6.3.3 Mass spectrometry 85
6.3.4 Data processing 85
6.4 Results and discussion 87
6.4.1 Determination of the location of the stable isotope label 88
6.4.2 Quantitative analysis and enrichment 90
6.5 Conclusion 93
7 DISCUSSION 94
8 REFERENCES 96
APPENDIX I

ABBREVIATIONS AND ACRONYMS

APCI	atmospheric pressure chemical ionization
APPI	atmospheric pressure photoionization
CCS	collision cross section
Cer	ceramide
CI	chemical ionization
CID	collision-induced dissociation
CL	cardiolipin
DART	direct analysis in real time
DC	direct current
DDA	data dependent analysis
DESI	desorption electrospray ionization
DG	diacylglycerol
ECN	equivalent/effective carbon number
EI	electron ionization
EIC	extracted ion chromatogram
ESI	electrospray ionization
FA	fatty acid
FAB	fast atom bombardment
FD	field desorption
FTICR	Fourier transform ion cyclotron resonance
FWHM	full width at half maximum
GL	glycerolipid
GP	glycerophospholipids
HCD	higher energy collision dissociation
HexCer	hexosylceramide
HILIC	hydrophilic interaction liquid chromatography
HPLC	high performance liquid chromatography
IDA	information-dependent analysis
IMS	ion mobility spectrometry
LC	liquid chromatography
LDA	Lipid Data Analyzer
LESA	liquid extraction surface analysis
LIPID MAPS	LIPID Metabolites and Pathways Strategy
LIT	linear ion trap
LLE	liquid-liquid extraction
LLOQ	lower limid of quantitation
LOD	limit of detection
LOQ	limit of quantitation
LPA	lysophosphatidic acid
LPL	lysophospholipid
LPS	lysophosphatidylserine

m/z	mass to charge ratio
MALDI	matrix-assisted laser desorption ionization
MG	monoacylglycerol
MS	mass spectrometry
MS/MS / MS^2	tandem mass spectrometry
MSI	mass spectrometry imatging
MTBE	methyl *tert* butyl ether
NAE	N-acylethanolamine
NAPE	N-acylphosphatidylethanolamine
NCI / NICI	negative ion chamical ionization
NP	normal phase
oaTOF	orthogonal acceleration time of flight
PA	phosphatidic acid
PC	phosphatidylcholine
PE	phosphatidylethanolamine
PG	phosphatidylglycerol
PI	phosphatidylinositol
PICI	positive ion chemical ionization
PIP	phosphatidylinositolphosphate
PLD	phospholipase D
ppm	part per million
PS	phosphatidylserine
QqQ	triple quadrupole
QTOF	quadrupole time of flight
RF	radio frequency
RP	reversed phase
RSD	relative standard deviation
RT	retention time
SFC	supercritical fluid chromatography
SIM	single ion monitoring
SIMS	secondary ion mass spectrometry
SM	sphingomyelin
SP	sphingolipid
SPE	solid-phase extraction
SPME	solid-phase microextraction
SRM	selected reaction monitoring
TG	triacylglycerol
TIC	total ion chromatogram
TOF	time of flight
UHPLC	ultrahigh performance liquid chromatography
ULOQ	upper limit of quantitation

LIST OF FIGURES

Figure 1: A chromatogram 10

Figure 2: Centroid and profile mass spectra 11

Figure 3: Determination of the charge state of ions 12

Figure 4: Schematic of a mass spectrometer 13

Figure 5: Mass peak at high mass resolution 20

Figure 6: Determination of the elemental composition of an ion using high resolution accurate mass spectrometry 21

Figure 7: Retention behaviour of lipids separated by reversed phase chromatogaphy 32

Figure 8: Fatty acyl carboxylate anions 36

Figure 9: Tandem mass spectrum of $[TG\ 16:0/16:0/18:1+NH_4]^+$ 37

Figure 10: Tandem mass spectrum of $[DG\ 12:0/12:0/0:0+Na]^+$ 38

Figure 11: Tandem mass spectrum of $[PC\ 16:0/18:1+H]^+$ 39

Figure 12: Tandem mass spectrum of $[PC\ 16:0/18:1+Na]^+$ 40

Figure 13: Tandem mass spectrum of $[PC\ 16:0/18:1+HCOO]^-$ 41

Figure 14: Tandem mass spectrum of $[PE\ 18:1/18:1+H]^+$ 41

Figure 15: Tandem mass spectrum of $[PE\ P\text{-}18:0/18:1+H]^+$ 42

Figure 16: Tandem mass spectrum of $[PE\ 18:1/18:1+Na]^+$ 43

Figure 17: Tandem mass spectrum of $[PE\ 18:0/18:1–H]^-$ 43

Figure 18: Tandem mass spectrum of $[PS\ 16:0/18:1+H]^+$ 45

Figure 19: Tandem mass spectrum of $[PS\ 16:0/18:1–H]^-$ 45

Figure 20: Tandem mass spectrum of $[PG\ 16:0/18:1+Na]^+$ 46

Figure 21: Tandem mass spectrum of $[PG\ 16:0/18:1–H]^-$ 47

Figure 22: Tandem mass spectrum of $[PI\ 17:0/14:1–H]^-$ 48

Figure 23: Tandem mass spectrum of $[SM\ 18:0+H]^+$ 49

Figure 24: Tandem mass spectrum of $[SM\ 18:0+Na]^+$ 49

Figure 25: Tandem mass spectrum of $[SM\ 18:0+HCOO]^-$ 50

Figure 26: Tandem mass spectrum of $[Cer\ 20:0+H–H_2O]^+$ 50

Figure 27: Tandem mass spectrum of $[Cer\ 20:0–H]^-$ 51

Figure 28: Extracted ion chromatograms (EIC) of PC 40:7 in positive and negative ion mode. 52
Figure 29: TG species and their contribution to total TG amount..... 53
Figure 30: Number of lipid molecular species detected 54
Figure 31: Separation of structural isomers belonging to different phospholipid classes... 55
Figure 32: Structural isomers of PE plasmalogen species separated by chromatography .. 56
Figure 33: Retention behaviour of PC structural isomers 57
Figure 34: LPC regioisomers..... 58
Figure 35: Linearity of PC..... 61
Figure 36: Determination of LLOQ 64
Figure 37: Matrix effect..... 65
Figure 38: Differences in response for lipid molecular species of varying chain length and number of double bonds..... 66
Figure 39: N-acylphosphatidylethanolamine (NAPE) 71
Figure 40: SPE efficiency for NAPE molecular species 76
Figure 41: Tandem mass spectra of internal standard PE 18:1/18:1-N-19:0 77
Figure 42: Extracted ion chromatograms of NAPE molecular species 78
Figure 43: Extracted ion chromatograms of isobaric NAPE structural isomers 79
Figure 44: EICs of PE 36:2-N-18:1 80
Figure 45: NAPE species quantified in rat brain 81
Figure 46: TIC of HILIC separation of an A549 cell extract 87
Figure 47: Full scan (A) and tandem MS scan 88
Figure 48: Tandem mass spectra of PC 88
Figure 49: PC head group fragment ions 89
Figure 50: Time-dependent incorporation of ^{13}C from glutamine into the glycerol backbone of PE, PE and PI 91
Figure 51: ^{13}C-enrichment in the glycerol backbone of phospholipids..... 92

LIST OF TABLES

Table 1: PE plasmalogen fragment ions 44

Table 2: Validation data for lipids 60

Table 3: SPE method for NAPE purification 73

Table 4: Proposed NAPE nomenclature. 75

Table 5: Validation data for NAPEs 80

Table 6: Structures of phospholipid head group fragment ions 86

HOCHENTWICKELTE ANALYTISCHE METHODEN FÜR LIPIDOMIK

Lipide sind Biomoleküle von großer struktureller Diversität, die eine Vielzahl biologischer Funktionen besitzen. Diese funktionelle Variabilität führt dazu, dass die Homöostase von Lipiden im Zuge vieler Krankheitsbilder, beispielsweise Diabetes, Morbus Alzheimer, oder auch bei verschiedenen Krebsarten, gestört ist. Das junge Forschungsfeld der Lipidomik beschäftigt sich ausschließlich mit der umfassenden Analyse von Lipiden und der Aufklärung all ihrer Funktionen und Interaktionen in biologischen Systemen. Diese Zielsetzung verlangt hochentwickelte analytische Methoden, um die verschiedenen Aufgaben von Lipiden aufzuklären.

Um den Anforderungen an die Methodologie im Feld der Lipidomik gerecht zu werden, werden hier drei analytische Methoden, basierend auf Flüssigkeitschromatographie gekoppelt mit Massenspektrometrie, vorgestellt.

Zuallererst wird eine analytische Methode zur globalen Analyse des Lipidoms vorgestellt. Sie beinhaltet eine einfache Flüssig-Flüssig-Extraktion als Probenvorbereitung, Hochleistungsflüssigkeitschromatographie mit dem Potential, strukturisomere und sogar positionsisomere Lipide aufzutrennen, und Detektion durch hochauflösende Massenspektrometrie, gemeinsam mit einer automatischen Software zur Datenauswertung. Nachdem absolute Quantifizierung eine essentielle Anforderung an lipidomische Methoden ist, wurde die Methode im biologisch relevanten Konzentrationsbereich validiert. Zusätzlich wurde das massenspektrometrische Fragmentierungsverhalten von Lipiden anhand von Standards umfassend untersucht.

Die zweite Methode dient zur quantitativen Analyse von N-Acylphosphatidyl-ethanolaminen, die wichtige Signallipide sind und nur in sehr kleinen Konzentrationen vorkommen. Die vorgestellte Probenvorbereitung mittels Flüssig-Flüssig-Extraktion und Festphasenextraktion isoliert selektiv die Zielanalyten, die folgend chromatographisch aufgetrennt und durch zwei N-acyl-spezifische SRM-Übergänge pro Analyt detektiert werden. Dies ermöglicht gleichzeitig quantitative und strukturelle Analyse von N-Acylphosphatidylethanolaminen.

Zuletzt wird die Relevanz lipidomischer Methodologie für das Feld der Krebsforschung vorgestellt. Durch einen hochspezialisierten Messansatz, wobei hochauflösende Tandem-Massenspektrometrie verwendet wird, kann ein Aspekt des Energiemetabolismus von

Krebszellen untersucht werden. Durch Verfolgung einer isotopenmarkierten Vorgängersubstanz kann der Einbau von Kohlenstoff in das Glycerol-Gerüst der Kopfgruppe von Phospholipiden selektiv detektiert und quantifiziert werden. Es wird gezeigt, dass Krebszellen unter Glucosemangel Aminosäuren verwenden, um Glycerol für den Einbau in Phospholipide zu synthetisieren.

SOPHISTICATED ANALYTICAL METHODS FOR LIPIDOMICS

Lipids are biomolecules with enormous structural diversity and encompassing a plethora of biological functions. In particular this wide functional variety manifests itself in lipids being dysregulated in a number of diseases and pathological states, such as diabetes, Alzheimer's, or various forms of cancer. The relatively young research field of lipidomics concerns itself exclusively with comprehensive analysis of lipids, including the elucidation of their functional pathways and interactions in biological systems. These goals demand sophisticated analytical methods to elucidate the various roles of lipids.

To tackle the diverse analytical requirements of the lipidomic field, three approaches for use in lipidomic research, all using the methodology of liquid chromatography coupled to mass spectrometry, are presented.

The first is a method for global analysis of the lipidome. It encompasses sample preparation using a simple liquid-liquid extraction method, high-performance liquid chromatography with the power to separate structural and even positional isomers of lipids, and high-resolution mass spectrometric detection together with a software package for automated data processing. Since quantitation is a crucial aspect of lipidomic analysis, the method has been validated in the biologically relevant range of lipids. Additionally, the tandem mass spectrometric behaviour of lipids has been extensively studied. This method is a prime choice for untargeted lipidomic analysis of even the most complex biological systems.

The second approach describes a method for analysis of N-acylphosphatidylethanolamines, which are important signaling lipids present only in minute amounts. The analytes of interest are selectively isolated from complex biological matrices using a combination of liquid-liquid extraction and solid phase extraction, and analysed using two selected reaction monitoring transitions. This method enables quantative and simultaneous structural analysis of N-acylphosphatidylethanolamines.

Finally, the applicability of lipidomic methodology in cancer research is presented. In a specialized approach using high resolution accurate mass tandem mass spectrometry, an aspect of energy metabolism of cancer cells is examined. By tracing a stable isotope labelled precursor, the incorporation of carbon from amino acids into the glycerol backbone of phospholipids is detected and quantified, showing that cancer cells are able to use amino acids as a glycerol source under low-glucose conditions.

1 INTRODUCTION

1.1 The field of Lipidomics

The central dogma of molecular biology, first formulated decades ago by Francis Crick (Crick 1958), states that genes encode proteins, which in turn synthesize and manipulate the chemical inventory of all small molecules, termed metabolites, found in cells, tissues and organisms. The study of nucleic acids – genomics – and the study of proteins – proteomics – are now complemented by metabolomics, the study of all metabolites. Lipidomics is a subdiscipline of metabolomics, and concerns itself exclusively with the system-level scale biochemical analysis of lipids and their functions and interactions (Wenk 2005).

Lipids are defined broadly as "*substances of biological origin that are soluble in nonpolar solvents*" (Moss et al. 1995); or, more precisely, as "*hydrophobic or amphipathic small molecules that (...) originate (...) by carbanion-based condensations of thioesters and/or by carbocation-based condensations of isoprene units*" (Fahy et al. 2005).

The classical functions of lipids are the formation of cellular membranes (a phospholipid bilayer) or of the myelin sheath around nerves, and energy storage (triacylglycerols). Vitamins A, D, E, and K are also lipids, and even other lipids such as sphingosine-1-phosphate or (lyso-)phosphatidic acid have important signalling functions in cell growth, migration, and death (Wenk 2005). These diverse functions of lipids lead to the simple fact that lipid metabolism is a delicately balanced system, which, if unbalanced, may manifest itself in a plethora of diseases. Indeed, lipids have been found to be dysregulated in a variety of pathological states, among them obesity, diabetes, Parkinson's and Alzheimer's disease, multiple types of cancer as well as neurodegenerative disorders (Li et al. 2014).

The principal aim of lipidomics is "*to study the pathways and networks of cellular lipids by characterization and quantitation of all lipids present in a biological system*" (Vaz et al. 2015). Lipidomic experiments may be designed in either a targeted manner, where only a specific lipid or a lipid class is investigated, or in a global or untargeted manner, where as many lipids as possible are analysed simultaneously (Griffiths et al. 2011). With this comes the difficulty of analysing the vast amount of data generated from large-scale lipidomic experiments, often with the help of extensive metabolite databases, before arriving at the point where an important biological pathway, or the specific role of a certain lipid in metabolism or disease has been elucidated (Ekroos 2012; Vaz et al. 2015).

1.1.1 Classification of lipids

According to their chemical nature, lipids are subdivided into eight categories (Fahy et al. 2005), which in turn consist of several classes and subclasses:

1.1.1.1 Fatty acids

Fatty acids (FA) constitute the simplest lipid class; they are hydrocarbons with a carboxylic acid group. Most fatty acids have 12-24 carbon atoms. Saturated fatty acids have no double bonds, while unsaturated or poly-unsaturated fatty acids contain one or more double bonds, typically in the *cis*-configuration. In the most commonly used shorthand form, fatty acids are designated as [number of carbon atoms] : [number of double bonds], e.g. "16:0" for palmitic acid. While eukaryotes predominantly contain fatty acids with an even number of carbon atoms, lower organisms may have fatty acids with an odd number of carbon atoms, branchings, or epoxy or other functional groups. They generally occur either as free fatty acids, or as fatty acyls in complex lipids (Fahy et al. 2005; Fahy et al. 2009).

1.1.1.2 Glycerolipids

Glycerolipids (GL) contain mono- di and tri-substituted glycerol. The most well-known glycerolipids are mono- di- and triacylglycerols (MG, DG, TG) which contain either one, two or three fatty acyls esterified to the hydroxyl groups of glycerol, respectively. Glycerolipids play an essential role in energy storage (Fahy et al. 2005; Fahy et al. 2009).

1.1.1.3 Glycerophospholipids

Glycerophospholipids (GP, or simply phospholipids, PL) consist of a glycerol backbone, to which a phosphate group is linked at the *sn*-3 position. Further attached to the phosphate group is a head group, which defines the phospholipid class. In this context, the term "phosphatidyl-" is often used synonymously with "glycerophospho-". Head groups are typically choline, ethanolamine, serine, glycerol, or inositol, with the corresponding classes glycerophosphocholine/phosphatidylcholine (PC), glycerophosphoethanolamine/ phosphatidylethanolamine (PE), glycerophosphoserine/phosphatidylserine (PS), glycerophosphoglycerol/phosphatidylglycerol (PG) and glycerophosphoinositol/ phosphatidylinositol (PI), while the simplest phospholipid class, phosphatidic acid (PA), has no head group, but only the terminal phosphate group. Typically, one or two of the two remaining hydroxyl groups of glycerol are acylated with a fatty acid, but also alkyl

linkages are possible. Plasmalogens (*sn*-1(1*Z*-alkenyl), *sn*-2 acyl phospholipids) are the specific case of a 1*Z*-double bond in the *sn*-1 alkenyl chain and an *sn*-2 acyl chain of a phospholipid. If only one of the hydroxyl groups of the glycerol is acylated, the lipid is called a lysophospholipid (LPL). Phospholipids are ubiquitous and most importantly constitute the lipid bilayer of cellular membranes (Fahy et al. 2005; Fahy et al. 2009).

1.1.1.4 Sphingolipids

Sphingolipids (SP) contain as structural backbone a sphingoid base (usually sphingosine, sphinganine or phytosphingosine). Most sphingolipids also contain a fatty acid (in the case of ceramides), or additionally a headgroup: Choline in the case of sphingomyelin (SM), or one or more hexoses in the cases of cerebrosides (hexosylceramides, HexCer) or gangliosides, respectively. Sphingomelin forms the myelin sheath around nerves, while simpler sphingolipids, such as sphingosine-1-phosphate, function as signalling lipids (Fahy et al. 2005; Fahy et al. 2009; Liebisch & Scherer 2012).

1.1.1.5 Sterols

Sterols are cholesterol and its derivatives. Steroids are hormones, such as estrogens, androgens or corticoids. Vitamin D also belongs to this group, as do bile acids (Fahy et al. 2005; Fahy et al. 2009).

1.1.1.6 Prenols

Prenols are all synthesized from the same two five-carbon precursors. This group contains the lipid vitamins E and K (Fahy et al. 2005; Fahy et al. 2009).

1.1.1.7 Saccharolipids

Saccharolipids are fatty acids linked to a sugar backbone, such as Lipid A, a component of the lipopolysaccharide of gram-negative bacteria (Fahy et al. 2005; Fahy et al. 2009).

1.1.1.8 Polyketides

Polyketides are a diverse group of lipids synthesized by polymerisation of acetyl and propionyl groups. Examples are the antibiotics erythromycin or tetracyclines (Fahy et al. 2005; Fahy et al. 2009).

This huge complexity results in a total of tens of thousands of different molecular species belonging to these eight lipid categories, their classes and subclasses. Indeed, over 40 000 different molecular species have been identified, classified, and stored in the LIPID

Metabolites And Pathways Strategy (LIPID MAPS) structure database, the most comprehensive lipidomics database to date (Sud et al. 2007).

1.1.2 Lipid nomenclature

Considering the vast complexity of lipids (containing positional and conformational isomers of fatty acids and/or double bonds), use of a uniform nomenclature is essential. The "gold standard" for chemical nomenclature is provided by the International Union of Pure and Applied Chemistry (IUPAC) and also includes lipids (Anon 1967; Anon 1970; Moss 1978), although these recommendations are somewhat outdated nowadays. The LIPID Metabolites And Pathways Strategy (LIPID MAPS) consortium, founded in 2003, has provided a widely accepted lipid nomenclature for lipidomics (Fahy et al. 2005; Fahy et al. 2009), describing lipids on various levels. On the simplest level, a lipid is only identified with its class and monoisotopic molecular mass. In contrast, for the most precise and unambiguous identification, the positions of the fatty acyls need to be known, as do the positions and conformations of the double bonds. The entire complexity however cannot always be deduced from lipidomic analyses. For example, the identities of fatty acyl constituents of phospholipids can never be deduced from single stage mass spectrometry. Further elucidating the structure of fatty acyls, especially the location or the conformations of double bonds, is tremendously difficult and requires specialized techniques such as MS^3 (Hsu & Turk 2010), or ozonolysis (Sun et al. 2013).

To unambiguously clarify the level on which a lipid has been identified, a shorthand nomenclature, based on the LIPID MAPS classification system, and specifically developed for mass spectrometric analyses, has also been proposed and widely accepted. The levels on which lipids may be identified are (Liebisch et al. 2013):

- The class level (e.g. PC 759): This level gives only the nominal mass of the uncharged molecule.
- The species level (e.g. PC 34:1): The sum of all carbon atoms and double bonds in both fatty acyl chains is identified.
- The bond type level (e.g. PC O-34:2): At this level, the bond type is identified, allowing distinction between diacyl phospholipids and nominally isobaric ether lipids, designated "PL O-". This can be accomplished using high resolution mass spectrometry.
- The fatty acyl/alkyl level (e.g. PC 16:0_18:1): tandem mass spectrometry is required to identify the fatty acyl/alkyl constituents. At this level, plasmalogens (*sn*-1(1*Z*-alkenyl),

sn-2 acyl phospholipids) can be distinguished from other ether linkages. E.g., "PC P-" denotes plasmalogens, while "PC O-" indicates a different type of ether linkage. The underscore indicates that the positions of the fatty acyls/alkyls are not yet identified.

- The fatty acyl/alkyl position level (e.g. PC 16:0/18:1): this can be accomplished by comparing the intensities of fatty acyl/alkyl-derived fragment ions in tandem mass spectra (see also chapter 4.3.3, p. 33ff). The forward slash indicates that the positions of the fatty acyls are identified.
- The fatty acyl/alkyl structure level (e.g. PC 16:0/18:1(9*Z*)): This is the most precise identification level, but also the most difficult to reach, as it requires identification of the positions and orientations of double bonds in fatty acyls, as well as identifying branches in fatty acyls (e.g. iso-/anteiso species).

It is essential that lipidomic results are reported on the correct identification level, and that as few assumptions as possible are made concerning the structure. In particular, automated tools used for data analysis of large-scale untargeted lipidomics or metabolomics studies often erroneously assume a deeper level than is actually reached and their matching algorithms may for example report results at the fatty acyl structure level, although the method is based only on full scan or tandem mass spectrometric measurement (Liebisch et al. 2015). Strictly speaking, this means that identifying a 20:4 fatty acid as "arachidonic acid" is in most cases incorrect, if the positions and orientations of the double bonds are not elucidated. However, for reasons of practicability, and taking into account biological knowledge of lipids, fatty acids are often identified based on the presumption that there are no branchings (i.e., an 18:0 fatty acid is assumed to be stearic acid, not iso-heptadecanoic acid), even if this is not specifically verified (Sokol et al. 2015).

2 SCOPE OF WORK

This work is divided into three parts. Following the aims of the field of lipidomics, it comprises methods for large-scale high throughput global analysis of the lipidome, as well as specialized targeted approaches to quantify a class of low-abundant analytes notoriously difficult to analyse with global approaches, and even the application of highly sophisticated tandem mass spectrometric methodology to analyse metabolomic fluxes in the field of cancer research.

The first part is the development of a general LC/MS method for global lipid profiling and quantitation, to be used for lipidomic analysis of even the most complex biological matrices. The method should be able to analyse and quantify as many glycerolipids, glycerophospholipids and sphingolipids as possible in a reasonable time frame, while also delivering in-depth structural information about as many lipids as possible. A manuscript containing the results of this work is in under review.

The second part is the development of an LC/MS/MS method for analysis of a particular phospholipid subclass – N-acylphosphoethanolamines (NAPEs). NAPEs are triacylated derivatives of phosphatidylethanolamine which represent only a minor component of the lipidome. The difficulty lies in the extremely low concentrations of NAPE compared to the vast excess of other sample components. Additionally, the high structural complexity, arising from the many combinatorial possibilities of three fatty acids, needs to be resolved. The full results of this work have been published (Triebl et al. 2016).

The last part is a special topic in cancer metabolic research. Current research strives to elucidate energy metabolism of lung cancer cells. For determination of metabolic pathways and their regulation, it is necessary to measure incorporation of stable isotope marked metabolites into the glycerol backbone of phospholipids. Particular challenges are precise location of the label within multiple phospholipid classes and quantitation of the isotopic enrichment. The results of this work are to be published in an appropriate journal.

3 ANALYTICAL METHODS IN LIPIDOMIC RESEARCH

Mass spectrometry coupled to chromatography has emerged as the preferred analysis method in lipidomic research. The versatility of this technique, in particular together with electrospray ionization, has greatly advanced research in the lipidomic field (Sandra & Sandra 2013). With this comes the necessity for appropriate sample preparation methods, all of which will be briefly explained in this chapter.

3.1 Sample preparation

Whether the choice of model organism is single-cell organisms, rodents or humans, sample preparation is always the first analytical step after formulating the biological hypothesis and conducting the biological experiment.

A crucial point of sample preparation is to stop all metabolic processes and inhibit all further chemical or enzymatic degradation of analytes, so that the metabolic state may be analysed. This involves both the sample preparation procedure, working rapidly and efficiently – on ice, if possible –, as well as sample storage – preferably in inert glass containers at low temperatures (Vaz et al. 2015).

3.1.1 Liquid-liquid extraction

Probably the most common technique in lipidomic sample preparation is lipid extraction by liquid-liquid extraction (LLE). LLE generally relies on the different solubility of analytes in two non-miscible phases (usually an aqueous phase and an organic phase) to separate different components of mixtures (Lottspeich 1998). Simply put, the organic phase then contains the lipids, while polar sample components such as salts and carbohydrates may be found in the aqueous phase.

Historically, the most common methods for lipid extraction are based on chloroform-water mixtures, such as the methods established by Folch (Folch et al. 1957) and Bligh & Dyer (Bligh & Dyer 1978). While these methods are still widely in use, chloroform is increasingly being replaced by other organic solvents, such as methyl-*tert*-butyl ether (MTBE) or 2-propanol, for several reasons: Firstly, chloroform is cancerogenic and needs to be handled with appropriate care. Secondly, since chloroform has a higher density than water, it forms the lower of the two phases, complicating sample handling (Matyash et al. 2008). Also, depending on the lipid class in question, different extraction methods differ

considerably in extraction yield, and chloroform-water protocols may not always be the best choice, especially for more polar lipid classes (Triebl et al. 2014). Finally, traditional two-phase systems may be too time-consuming for large-scale lipidomic studies requiring high sample throughput. To address this concern, simple monophasic extraction methods (Zhao & Xu 2010; Lydic et al. 2014; Pellegrino et al. 2014; Sarafian et al. 2014), as well as ultrasound extraction methods (Pizarro et al. 2013; Meullemiestre et al. 2016) have recently been established.

Whatever the choice of extraction method, one should bear in mind that different lipid classes may vary greatly in their extraction yield (Reis et al. 2013), and that probably no single extraction method is equally suitable for all lipid classes (Vaz et al. 2015).

3.1.2 Solid-phase extraction

Solid-phase extraction (SPE) is a sample preparation method which separates an analyte mixture dissolved in a liquid. SPE uses cartridges containing a solid sorbent as stationary phase, through which the liquid sample and the liquid mobile phase pass. Interaction between the different sample components with the stationary phase and the mobile phase results in separation of the sample components. Some sample components interact more strongly with the stationary phase than with the mobile phase and are retained, while others show little interaction with the stationary phase and pass through the cartridge together with the mobile phase (Hennion 1999).

SPE shows similarities to chromatography (Chapter 3.2), and may also be used on-line prior to chromatographic separation, which is then termed either on-line SPE or 2D-chromatography (Buszewski & Noga 2012; Bang & Moon 2013; Mena-Bravo et al. 2016). However, it is often used "off-line", as an additional sample preparation step, e.g. after liquid extraction. In this use, a major benefit is the potential to increase the effective concentration of low-abundance analytes (Triebl et al. 2016). SPE may also be used to separate a lipid extract into lipid classes (Fauland et al. 2013) so that these classes may be analysed separately.

A typical SPE extraction procedure consists of four steps: Conditioning of the cartridge, sample loading, rinsing and cleaning of the sample, and desorption and recovery of the analytes of interest. Prior to application of the sample, the cartridge is conditioned using an appropriate volume of sample solvent. Then the sample is loaded onto the preconditioned cartridge. The analytes of interest are separated from the unwanted sample components by

retention of one while the other is eluted, and the corresponding fraction is collected (Hennion 1999).

SPE is suited for both automation (Helle et al. 2011) and miniaturization (solid-phase microextraction, SPME) (Vas & Vékey 2004), thereby vastly increasing sample throughput and detection limits compared to traditional SPE.

3.2 High-performance liquid chromatography

3.2.1 Basics of chromatography

Chromatography is a separation technique which can, in a simplified way, be viewed as a mobile phase moving through a stationary phase. The analyte mixture is dissolved in the mobile phase and separation is based on the partitioning of the analytes between the mobile and the stationary phases (Meyer 2010).

Different combinations of stationary and mobile phases result in different separation principles and techniques, such as thin layer chromatography, size exclusion chromatography, gas chromatography or ion exchange chromatography.

A chromatography system consists of the stationary phase, usually packed in a column, through which the mobile phase is pumped. The analyte mixture is injected into the solvent flow and after separation, the different analytes reach a detector at different times. The time an analyte takes to travel through the chromatographic system before it reaches the detector is called retention time (RT).

The most common technique in bioanalytical LC/MS is high-performance liquid chromatography (HPLC), the evolution of "classical" liquid chromatography (LC) made possible by more sophisticated manufacturing of stationary phases which allows for separation of even the most challenging chromatographic problems.

In HPLC, separation is based on non-covalent interactions between the analytes and the mobile and stationary phases. If an apolar stationary phase and a polar mobile phase is used, this is termed reversed phase (RP) chromatography. The inverse – a polar stationary phase and an apolar mobile phase – is normal phase (NP) chromatography or hydrophilic interaction liquid chromatography (HILIC). NP chromatography uses a mobile phase completely free of water, while the separation mechanism of HILIC relies on the partitioning of analytes between the mobile phase, the stationary phase and a thin aqueous layer between the two (Meyer 2010; Buszewski & Noga 2012). While RP chromatography

separates analytes based on their overall hydrophobicity, which in the case of lipids is determined mainly by their fatty acyl residues, HILIC or NP chromatography is able to separate lipids into classes differing in the polar head groups.

3.2.2 A chromatogram

The result of every chromatographic separation is a chromatogram which shows the detector signal (y-axis) over time (x-axis). The signal (represented by the height or area of a peak) is proportional to the amount of analyte – an important characteristic which can be used for quantification. The chromatogram of a reversed phase separation of a lipid extract is shown in Figure 1. While phospholipids have retention times of 20-30 min, the very apolar triacylglycerols elute later.

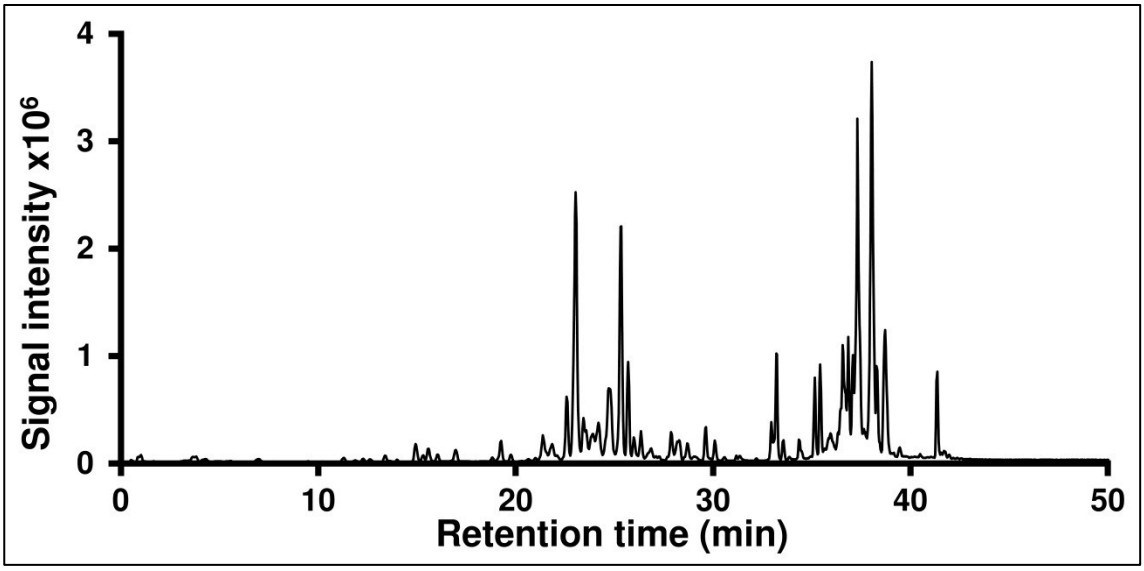

Figure 1: A chromatogram of a reversed phase separation of a lipid extract.

3.3 Mass spectrometry

3.3.1 Information content of a mass spectrum

Mass spectrometry is the determination of the mass-to-charge ratio of ions. Only ions can be analysed with mass spectrometry, never molecules, and the measured variable is always the mass-to-charge ratio (*m/z*), where *m* is the molecular mass of the ion and *z* is the number of elementary charges attached to the ion. Therefore, *m* can be any real number, while *z* is always a positive or negative integer. Despite being SI unit, "kg/C" (Cohen et al. 2008) is horribly impractical and virtually never used. The unit Th (in honour of

JJ Thomson) is sometimes used (Zubarev & Makarov 2013), but the dimensionless *m/z* remains most widespread (Gross 2013).

A mass spectrum is the two-dimensional representation of absolute or relative signal intensity (y-axis) and mass-to-charge ratio (x-axis), containing peaks at different *m/z* values. The highest peak in any mass spectrum (relative intensity = 100 %) is called the base peak (Gross 2013).

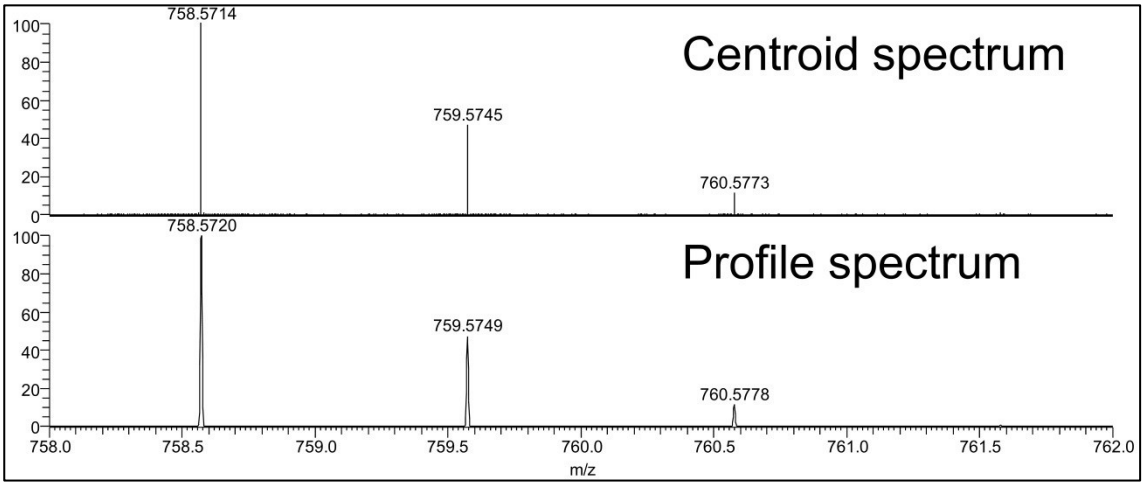

Figure 2: Centroid and profile mass spectra of protonated PC 34:2. The peak shape is conserved in profile spectra, but at the expense of data size.

The information content of a mass spectrum is no more than a list of *m/z* values and their respective intensities which can be displayed graphically as centroid or profile spectra. Profile spectra still display the shape and width of the peak while mass peaks in centroid spectra are essentially lines, with a weighted value for *m/z* and intensity (Figure 2). While centroid data contain fundamentally less information (about every single mass peak) than profile data, this leads to a significant reduction in file size (Urban et al. 2014).

Most biomolecules consist of only a handful of different elements, usually limited to carbon, hydrogen, oxygen, phosphorous and nitrogen. Of these elements, only carbon significantly contributes to observable isotopologues (molecules with the same elemental composition, but differing in isotopes (Nič et al. 2009)). For every carbon atom in a molecule, the natural abundance of ^{13}C results in the appearance of an isotopic peak of about 1.1 % intensity of the monoisotopic peak. An ion containing *n* carbon atoms therefore has an isotopic pattern for the first isotope (containing one ^{13}C) at a relative intensity of (1.1**n*) % and the second, third, etc. isotopes consecutively smaller (Wieser et al. 2013). This is also a simple way of estimating the number of carbon atoms in a

molecule/ion – which roughly corresponds to the relative intensity of the first isotopic peak compared to the monoisotopic *m/z*).

Due to the mere measurement of the mass-to-charge ratio, an ion with mass *m* and charge *z* cannot be distinguished from an ion with mass 2**m* and charge 2**z*. However, the charge state (number of charges) of biomolecules can be determined relatively easily from the isotopic pattern: Let's assume a molecule of cardiolipin (CL 72:8, M=1448.97223 g/mol), from which, in the process of ionization, either one or two protons are abstracted. A portion of the resulting ions is then singly charged ($[M–H]^-$, *m/z* 1447.96495), and the rest is doubly charged ($[M–2H]^{2–}$, *m/z* 723.47884). The resulting mass spectrum is shown in Figure 3, with the insets showing the isotopologues of the singly and doubly charged ions.

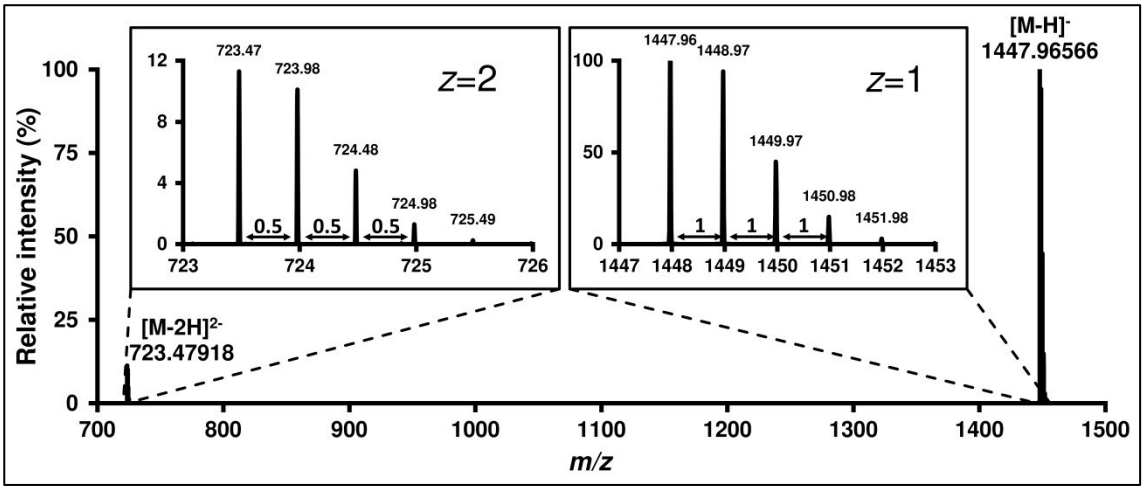

Figure 3: Determination of the charge state of ions. The spacing of the ^{13}C-isotopologues of cardiolipin is 1 *m/z* for singly charged ions and 0.5 *m/z* for doubly charged ions.

The charge state can be deduced from spacing of the isotope peaks: For the singly charged ion at *m/z* 1447.96, the ^{13}C-isotopologues are spaced by 1 *m/z*, while the ^{13}C-isotopologues of the doubly charged ion are 0.5 *m/z* apart. From this information, the charge state can be calculated and corresponds to the reciprocal value of the spacing of the ^{13}C-isotopologues (Tabb et al. 2006; Hsu et al. 2005).

3.3.2 A simple mass spectrometer

Simply put, a mass spectrometer consists of three parts: An ion source, a mass analyser and a detector (Figure 4). Ions generated in the ion source are passed through a system of lenses to a mass analyser, separated by mass-to-charge ratio, and measured by a detector.

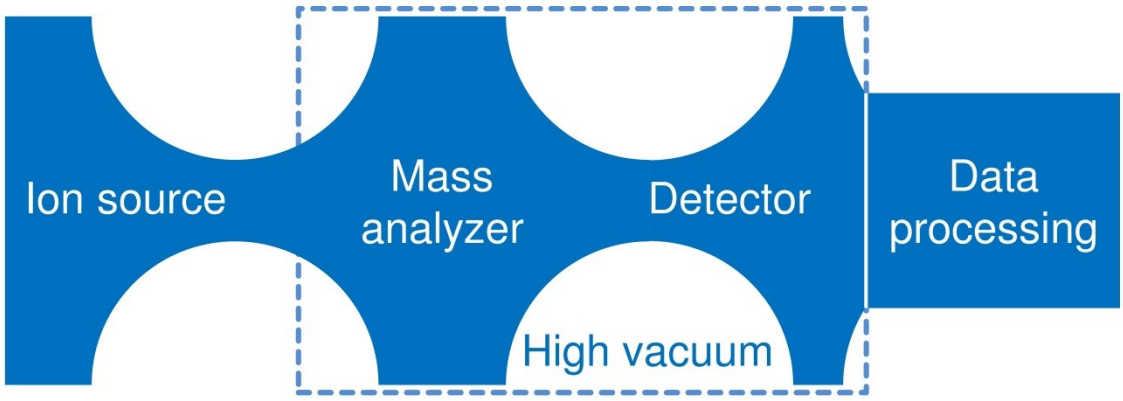

Figure 4: Schematic of a mass spectrometer. Ions generated in the ion source are separated by their mass-to-charge ratios in the mass analyser, detected, and the data is processed.

3.3.2.1 Ion source

Generation of suitable ions is a crucial step in mass spectrometry as only ions, and not molecules, may be detected. The choice of ionization technique largely depends on the physicochemical properties of the analytes to be measured. Furthermore, some ionization techniques such as electron ionization or chemical ionization, are not or at least not fully (Cappiello et al. 2005) compatible with chromatographic separation prior to mass spectrometric analysis.

Ions may originate from different molecules, but also different types of ions (adducts) may originate from the same molecule. For example, glycerolipids are observable as protonated, ammoniated and sodiated forms in positive ion mode, but form no detectable ions in negative ion mode. Some phospholipids may form protonated molecules, sodium and ammonium adducts in positive ion mode, and deprotonated molecules as well as formate or chloride adducts in negative ion mode. Ionization may be regulated by the choice of solvent additive (a weak organic acid promotes protonation of analyte molecules, LiOH suppresses protonation, and addition of a formate promotes the formation of formate adducts) (Han et al. 2012).

Only the most commonly used ionization techniques in the field of LC/MS analysis, as well as historically important techniques, are explained here, while other types such as fast atom bombardment (FAB), field desorption (FD) or atmospheric pressure photoionization (APPI) are not widely used nowadays (Bruins 1991; Gross 2013).

3.3.2.1.1 Electron ionization

The classical ionization technique is electron ionization (EI). EI is commonly coupled with gas chromatography, as it requires the analytes to be in the gas phase. The principle of EI is relatively simple – a heated wire filament emits electrons which are accelerated to 70 eV and lead to abstraction of an electron from the molecule, forming a radical cation, $M^{+\bullet}$ (Gross 2013). Note that the thermal electrons do not impact the molecule, as the probability of single electrons actually impacting any electron in a molecule is infinitely improbable, and therefore the term "electron impact", albeit being quite widely used, is obsolete, misleading and simply wrong (Todd 1991). The energy of 70 eV is enough to induce not only ionization (removal of an electron) but also, in most cases, bond cleavage. Therefore, while an EI spectrum may still contain the molecular ion, fragment ions are prominently visible, making EI a *hard* ionization technique. A big advantage of using standardized ionization with 70 eV is that spectra are reproducible across different instruments and manufacturers, enabling creation of comprehensive spectral libraries and databases for thousands of analytes (McLafferty et al. 1999).

3.3.2.1.2 Chemical ionization

Chemical ionization (CI) uses a reactant gas, such as methane, which is primarily ionized and in turn ionizes analyte molecules. CI exists as positive-ion-CI (PICI) and negative-ion-CI (NICI, NCI), which are competing reactions taking place at the same time. In contrast to EI, CI is a *soft* ionization technique, meaning that molecular ions largely stay intact and do not dissociate during ionization (Gross 2013).

3.3.2.1.3 Electrospray ionization

The use of electrospray (Taylor 1964) as a ionization method in the form of electrospray ionization (ESI) (Dole 1968) proved a breakthrough in mass spectrometric analysis of biomolecules, as it allowed for analysis of large biomolecules and coupling with chromatography. It is also a soft ionization technique forming quasi-molecular ions, has very low chemical specificity and is unlimited in mass (Fenn et al. 1989; Wilm 2011).

Electrospray ionization operates under the condition that analyte ions are already present in the sample solvent which must only be released. To achieve this, the sample solvent is passed through a stainless steel needle, to the tip of which a potential of several kV is applied. Two competing forces, surface tension and Coulomb attraction towards the counter electrode, form the *Taylor Cone* from which droplets of liquid containing multiple

charged analytes are sprayed into a fine aerosol. The droplets grow smaller through successive evaporation of solvent. As the solvent evaporates, the surface of the droplets grows smaller while the charge remains the same. When the field density reaches the *Rayleigh stability limit*, a new Taylor Cone forms at the surface, and even smaller droplets are released. The final formation of gas-phase ions is explained by two competing models: According to the *ion evaporation model*, solvated ions are expelled from the droplet at sufficiently high field strength. The *charge residue model* claims that solvent is successively evaporated from droplets containing only one analyte ion, until only the ion is left. This would explain the formation and stability of non-covalent complexes ("adducts"), which would be cooled by solvent evaporation. As ESI requires large volumes of solvent to be evaporated, it is beneficial to use volatile liquids such as methanol or acetonitrile or their mixtures with water. Drying/nebulizing gas flows and high temperatures can additionally be employed to assist desolvation (Gibson et al. 2009).

ESI produces singly or multiply charged ions with approximately one charge per thousand mass units. A common limitation of ESI is the limited linear range of around three orders of magnitude, with the upper limit often cited at 10^{-5} M (Tang et al. 2004; Zook & Bruins 1997; Cech & Enke 2001), although this value should be expected to vary between analytes and precise conditions.

ESI is nowadays the most prevalent of the atmospheric pressure ionization methods, particularly in the field of LC/MS (Holčapek et al. 2012).

Variations of ESI are nano-ESI, which uses very small flow rates to improve ionization efficiency (Gibson et al. 2009), and desorption electrospray ionization (DESI), where an electrospray is directed at the surface of the sample to be analysed (Takats 2004).

3.3.2.1.4 Atmospheric pressure chemical ionization

In atmospheric pressure chemical ionization (APCI), the sample solvent is pneumatically sprayed to form an aerosol which is then vaporized at high temperatures (~500 °C). Ionization occurs when the solution mist passes by a corona discharge electrode. Ionized solvent then reacts with analyte molecules to yield their ionized forms.

APCI can often be performed in a modified ESI source, but differs from ESI in that the ions are created in the gas phase (Prakash et al. 2007) and that higher flow rates (over 200 µL/min) are necessary for efficient vaporization. A big advantage of APCI over ESI is

that apolar molecules may be ionized, while ESI exhibits a distinct advantage for polar molecules (Gross 2013).

3.3.2.1.5 Matrix-assisted laser-desorption ionization

In the case of matrix-assisted laser-desorption ionization (MALDI), the sample is embedded in a matrix and targeted by a UV laser using a short burst in the nanosecond range. Suitable matrices are often dihydroxybenzoic acid, or cinnamic acid derivatives, which all contain several conjugated double bonds to absorb UV light, are of low molecular weight, and are acidic to aid in protonation of analytes. The exact mechanism of ion formation has so far not been completely elucidated but it is generally believed that the matrix absorbs most of the energy from the laser burst and in turn ionizes the analytes (Knochenmuss 2006; Gross 2013).

MALDI is more commonly combined with a time-of-flight analyser (section 3.3.2.2.4) than with any other mass analyser, as both work in a "pulsed" manner (as opposed to the continuous operation of ESI). MALDI is often used for proteomic analysis, but is also very well suited for imaging mass spectrometry, as it is capable to scan an area of sample, such as a tissue cross section, in two dimensions with sub-µm resolution (Murray et al. 2016).

3.3.2.2 Mass analyser

All mass analysers rely on the movement of gas phase ions in an electromagnetic or electrostatic field. While the ion source may operate at atmospheric pressure (e.g. when using ESI, MALDI or APCI), the mass analyser needs to be kept at a high vacuum ($<10^{-1}$ Pa) by a series of pumps to ensure that the movement of ions is not influenced by collision with surrounding gas molecules (Gross 2013).

3.3.2.2.1 Sector

In the oldest type of mass spectrometer, ions are deflected by a magnetic field based on their *m/z* value. During a scan over a certain *m/z* range, the magnetic field strength is varied so that only ions of certain *m/z* reach the detector at each time (Gross 2013).

3.3.2.2.2 Quadrupole

A quadrupole mass analyser consists of four, ideally hyperbolic, metal rods. A radio frequency (RF) voltage, offset with a direct current (DC) voltage is applied to each pair of opposing rods. Ions travelling between the rods follow paths described by the Mathieu differential equation. Only ions of a certain *m/z* follow a stable path through the

quadrupole field, while ions of all other *m/z* collide with one of the rods and are discharged. A quadrupole therefore operates as a mass filter, allowing only ions of one specific *m/z* value to reach the detector (selective stability). Quadrupole mass spectrometers are somewhat standard equipment for mass spectrometry laboratories, as they are affordable, relatively uncomplicated to use, and (as triple quadrupole hybrid instruments, chapter 3.3.2.2.7, p. 19) allow various types of scan modes (Gross 2013).

3.3.2.2.3 Ion trap

In a three-dimensional ion trap, ions are trapped between two end cap electrodes and a cylindrical ring electrode. A damping gas is used to "cool" the ions which have high kinetic energy after they enter the trap. Ion traps operate on the same physical principles as quadrupole mass analyzers, but on the basis of selective instability, meaning that ions of only one *m/z* are ejected towards a detector, while all others remain trapped in the quadrupole field. In a linear ion trap (LIT, quadrupole ion trap, Paul trap), ions are trapped by two end cap electrodes in a quadrupole and ion packets are passed back and forth along the quadrupole. The ability to trap and thereby accumulate ions for a relatively long time leads to increased sensitivity. In contrast to quadrupoles, ion traps do not operate continuously, as the processes of ion injection, *m/z* analysis by selective instability, and ion ejection towards the detector are not separated in space (Gross 2013). An important characteristic of ion traps is "low mass cut-off", which is their inability to simultaneously trap ions of both high and low *m/z* values. While ions of higher *m/z* values are efficiently trapped, ions of only a quarter to a third of their *m/z* value are unstable and cannot be detected (Y.-H. Yang et al. 2009).

3.3.2.2.4 Time-of-flight

In time-of-flight (TOF) mass analysers, ions are accelerated by an electric field so that they all have the same kinetic energy, regardless of *m/z* value. As they move through a field-free region, their velocity and thus the time they take to reach a detector, is only dependent on their *m/z* (with k being a proportionality constant):

$$t = k\sqrt{m/z}$$

To correct for differences in kinetic energy of the ions, a reflectron may be used. Of two ions of identical *m/z* but differing in kinetic energy, the ion with higher kinetic energy will penetrate deeper into the reflectron, and thus both ions will reach the detector at the same

time. Reflectron-TOFs also have the advantage of a longer drift tube, which leads to higher mass resolution.

TOF mass analyzers are ideal to use with MALDI, as both work in a pulsed manner and every time an ion packet is created, it can be analysed. They can however also be used with other ion sources – TOFs with orthogonal acceleration (oaTOFs) pulse a continuous ion beam (e.g. generated by ESI) orthogonally (Gross 2013).

3.3.2.2.5 Fourier-transform ion cyclotron resonance

A fourier-transform ion cyclotron resonance (FTICR) mass spectrometer is based on the Penning-type ion trap design: Ions injected into a magnetic field follow a circular trajectory along the axis of the magnetic field whereby their rotational frequency (ICR frequency) only depends on the *m/z* ratio. However, ions of identical *m/z* do not necessarily travel in packets –they may be evenly spaced along the entire circular trajectory and they still may have different velocities and radii. All ions are then excited by an electric field perpendicular to the magnetic field. This forces all ions of the same *m/z* to orbit coherently and in phase. This movement is then detected by two detector plates. Signals from different frequencies (originating from different ion packets of different *m/z* values) simply add up at the detector, and all ions are detected at the same time. Using Fourier transformation, *m/z* values and intensities are then calculated from the measured time domain. Resolution, which is inversely correlated with *m/z*, can be improved by increasing the magnetic field strength or increasing measurement time. Using superconducting magnets cooled with liquid helium, FTICR mass spectrometers are able to reach resolutions above 1 000 000 (Marshall & Hendrickson 2002; Scigelova et al. 2011; Holčapek et al. 2012; Gross 2013).

3.3.2.2.6 Orbitrap

The newest type of mass spectrometer was introduced in 2005 (Makarov 2000; Hu et al. 2005), and is based on the much older design of the Kingdon trap (Kingdon 1923), using an electrostatic field to confine ions in space. In contrast to FTICR instruments, this design omits the need for expensive cooling of superconducting magnets. The actual Orbitrap analyser consists of two cup-shaped outer electrodes around a spindle-like central electrode.

Ions injected with a slight offset from the centre into the electrostatic field move in all three dimensions – along and around the central electrode. Most importantly, the frequency of the axial motion ω is independent of all parameters except for *m/z*:

$$\omega = \sqrt{\frac{z}{m} * \mathrm{k}}$$

Analogously to FTICR detection, Fourier transformation is employed to obtain a mass spectrum from the measured transients. Modern Orbitrap instruments are capable of very high mass resolution (500 000 FWHM at *m/z* 200) (Thermo Fisher Scientific Inc. n.d.; Gross 2013; Makarov 2000; Scigelova et al. 2011; Zubarev & Makarov 2013; Eliuk & Makarov 2015).

3.3.2.2.7 Hybrid instruments

There are many combinations of the aforementioned types of mass analysers, the most common ones being quadrupole-time-of-flight (QTOF), quadrupole-linear ion trap (QTRAP) and triple quadrupole instruments (QqQ – although strictly speaking, only two quadrupoles in a triple quadrupole are used as mass analysers while the third functions solely as a collision cell) (Holčapek et al. 2012).

3.3.2.3 Detector

Detectors in mass spectrometry are usually Faraday cups, secondary electron multipliers, microchannel plates or conversion dynodes. They are destructive detectors, meaning that ions are discharged in order to produce a signal. They also cannot discriminate between ions of different masses and rely on prior separation of ions by their *m/z*. The exception is fourier transform mass spectrometry (either in FTICR or Orbitrap instruments), where ions are not discharged during detection and the mass analyser simultaneously functions as detector (Gross 2013).

3.3.2.4 Mass resolution and mass accuracy

Mass spectrometric resolution (or resolving power) is the ability of an instrument to distinguish between two ions of different *m/z*. There are two ways of measuring resolution – the "10 per cent valley definition" and the "peak width definition" (Todd 1991).

- Using the 10 per cent valley definition, two neighboring peaks of equal height are mass separated if the valley between them is no higher than 10 %. Resolution R=$m/\Delta m$.

However, the 10 per cent valley definition is seldomly used today since it is of little use if the two peaks in question are not of identical height.

- The peak width definition calculates resolution using the peak width at a given fraction of its height, most commonly at 50 %, thereby full width at half maximum (FWHM). FWHM is the predominant way of expressing mass spectrometric resolution.

Regardless of how resolution is calculated, it is always important to state the *m/z* at which it is calculated, e.g. R=100 000 at *m/z* 200, since for some types of mass analyser (such as Orbitraps), resolution changes with *m/z* (Zubarev & Makarov 2013).

Different types of mass analysers differ strongly in their maximum resolution. Quadrupole and ion trap mass spectrometers typically offer only "unit resolution", meaning that their *m/z* value should be treated as an integer. TOF instruments typically reach resolutions between 10 000 and 80 000, Orbitrap analysers offer resolutions between 100 000 and 500 000, and the highest values above 1 000 000 are reached by FTICR instruments. Generally, mass resolutions above 10 000 are referred to as "high-resolution" (Holčapek et al. 2012).

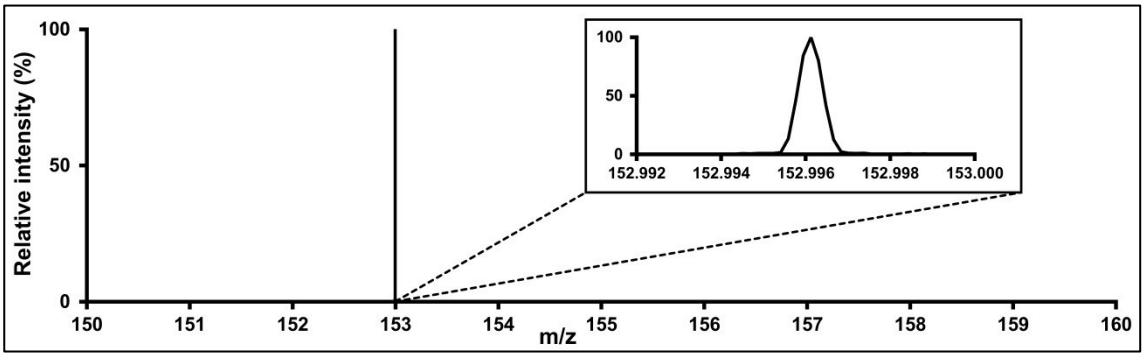

Figure 5: Mass peak at high mass resolution. The peak width at base is less than 0.002 Da; mass resolution exceeds 200 000 (FWHM).

Equally important as mass resolution is mass accuracy, the difference between the measured and the theoretical *m/z* value. Mass accuracy is usually expressed in ppm (parts per million). For typical high-resolution instruments, values for mass accuracy of below 5 ppm are standard (Holčapek et al. 2012). Figure 5 shows the mass spectrum of deprotonated cyclic glycerol phosphate ($[C_3H_6O_5P]^-$) acquired on an Orbitrap instrument. Mass deviation from the theoretical value is 1.810 ppm and the calculated resolution (FWHM) is 230 000.

Mass accuracy is achieved and maintained through regular external calibration of the instrument. When using internal calibration, the mass spectrometer is calibrated even

during a measuring run. The calibrant is then either constantly infused with the analyte or using a second inlet system (such as a second ESI source). Internal calibration leads to extremely high mass accuracy, typically below 1 ppm (Holčapek et al. 2012; Gross 2013).

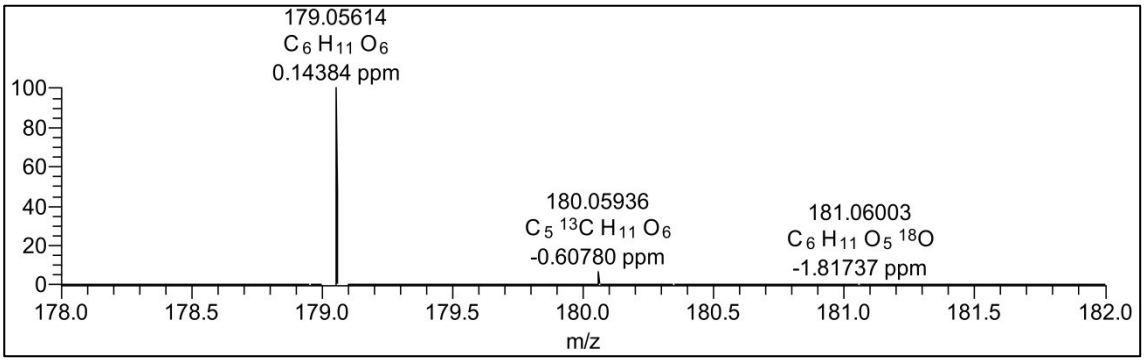

Figure 6: Determination of the elemental composition of an ion using high resolution accurate mass spectrometry. The most likely elemental compositions are automatically calculated by the data processing software Xcalibur. Shown here are deprotonated glucose ($[C_6H_{11}O_6]^-$), and its most abundant isotopologues, containing ^{13}C and ^{18}O.

Since only ^{12}C has a molecular mass of an integer (exactly 12 Da) (Wieser et al. 2013), the exact mass of a molecule (or an ion) is virtually never an integer. Using sufficient mass resolution and mass accuracy, the molecular composition can be determined (with some uncertainty) from the exact *m/z* value (Gross 2013). Figure 6 shows such an approach using the software Xcalibur: The screenshot shows the mass spectrum of an analyte at measured *m/z* 179.05608, and two smaller peaks at *m/z* 180.05936 and *m/z* 181.06015. Limiting expected molecular composition to 0-20 carbon atoms, 0-20 hydrogen atoms, 0-1 phosphorous atoms, 0-1 nitrogen atoms, 0-1 ^{13}C isotopes and 0-1 ^{18}O isotopes, the possible elemental compositions with a mass tolerance of 10 ppm are automatically calculated. The ions within these constraints are deprotonated glucose (theoretical *m/z* 179.05611) and its natural occurring isotopologues containing ^{13}C and ^{18}O (theoretical *m/z* 180.05947 and *m/z* 181.06036, respectively). However, this approach depends greatly on resolution and mass accuracy, and grows more unreliable with growing *m/z* value due to the sheer number of possible molecular formulas (Gross 2013).

3.3.3 Scan modes

3.3.3.1 Full scan, single ion monitoring and tandem MS

A full scan is a measurement of all ions over a given *m/z* range.

Single ion monitoring (SIM) refers to analysis of only a single ion or *m/z* value. SIM is usually used for targeted quantification and has the advantage of higher sensitivity (as time is only spent observing the ion of interest in the case of quadrupole instruments, and ion traps are not filled with additional background ions) (Gross 2013).

Tandem mass spectrometry (MS/MS, MS^2) is the technique of not only analysing ions, but also their fragments. Fragmentation takes place in a collision cell, where ions collide with a collision gas (CID, collision-induced dissociation). Note that only ions can be analysed, and when a singly charged ion dissociates, only the one fragment still carrying the charge can be directly monitored, while the mass of the neutral that is lost (neutral loss) may be calculated.

Tandem mass spectrometry relies on monitoring intact precursor ions and their fragments (product ions) and requires either specific type of mass analyser or a combination of two mass analysers. *Tandem in space* instruments (QqQ, QTOF, LIT-Orbitrap, Q-Orbitrap) have two mass analysers separated by a collision cell which allows separate analysis of precursor and product ions. *Tandem in time* instruments (ion traps, penning traps) isolate all ions of one *m/z* (by ejecting ions of all other *m/z* values) which are then fragmented. The processes of selection of precursor ions, fragmentation, and detection of the fragment ions all occur in the same space. Usually, tandem in space instruments are limited to two-stage mass spectrometry (MS^2), while MS^n, (with n limited only by fragmentation efficiency and sensitivity of the instrument) is possible on tandem in time instruments (de Hoffmann 1996; Gross 2013).

In the following sections, different tandem mass spectrometry analysis methods are explained for a tandem in space instrument, such as a triple quadrupole (although most analysis methods are also possible for a tandem in time instrument):

3.3.3.1.1 Product ion scan

A product ion scan is the analysis of all product ions that are generated from one precursor ion. The first mass analyser is fixed to a particular *m/z*, while the second analyser scans the whole mass range. The resulting product ion spectrum contains all fragment ions originating from one precursor ion. Product ion scans are often used for structure elucidation (de Hoffmann 1996).

3.3.3.1.2 Precursor ion scan

In a precursor ion scan, the first mass analyser scans the mass range and the second mass analyser is fixed to one *m/z* value. The resulting spectrum contains all precursor ions which generate one particular product ion (de Hoffmann 1996).

3.3.3.1.3 Neutral loss scan

Both mass analysers scan the mass range but are offset by a certain *m/z* value. The spectrum contains all ions which lose the same neutral fragment (de Hoffmann 1996).

3.3.3.1.4 Selected reaction monitoring

Selected reaction monitoring (SRM) is analysis of one or more specific fragmentation reactions. The dissociation of one precursor ion to one product ion is observed. SRM is often used in trace analysis because of its high sensitivity and higher selectivity compared to SIM (de Hoffmann 1996).

3.3.3.2 Data dependent acquisition/information-dependent acquisition

Using data dependent acquisition (DDA) or information-dependent acquisition (IDA), predefined scans are only performed if certain criteria, such as signal thresholds or the occurrence of certain ions, are met. For example, one might want to perform product ion scans on a group of analytes, but only if the corresponding analytes are of sufficient abundance. Or one might perform a survey precursor or neutral loss scan and then, targeted SRM analysis only of those analytes that have been found in the survey scan, for quantitation purposes (Baker et al. 2014; Almeida et al. 2015).

3.4 LC/MS

For a long time, LC methods were not compatible with existing ionization methods (FAB, EI), as these required a constant vacuum, which would immediately be lost as soon as the solvent vaporized and multiplied in volume. Chromatographic systems were therefore usually limited to fairly unspecific physico-chemical or optical detectors, such as resistivity, UV, or evaporative light scattering detectors.

The necessary advance in ionization methods was the development of ESI by the Fenn group (Fenn et al. 1989). In contrast to other ionization methods, ESI is applicable to a wide range of flow rates (from nanolitres to millilitres per minute). Additionally, it usually does not require derivatisation as EI often does. The final big advantage is that it is a soft

ionization technique, so the pseudo-molecular ions (protonated or deprotonated molecules, ammonium, sodium or other adducts) as well as fragment ions may be investigated using tandem mass spectrometry. ESI is therefore the predominant ionization technique for LC/MS methods (Holčapek et al. 2012).

On the side of mass spectrometers, tandem mass spectrometers are the most prevalent, with triple quadrupole and ion trap instruments viewed as "standard equipment" for LC/MS laboratories, as they combine robustness and versatility within an affordable price range. More expensive Orbitrap and FTICR instruments are rare, but offer significant advantages, particularly in terms of mass resolution and mass accuracy (Holčapek et al. 2012).

3.5 Other methods

While the vast majority of lipidomic methods relies on LC/MS as described in the previous chapters, other related techniques occupy a small, albeit interesting, niche. Among them are mass spectrometry imaging and ion mobility coupled to mass spectrometry. These techniques may even be coupled, for example to examine the spatial distribution of nominally isobaric compounds in tissue slices (McLean et al. 2007).

3.5.1 Ion mobility mass spectrometry

Ion mobility spectrometry (IMS) is an analytical technique which separates gas phase ions in the presence of gas collisions. In all variations and instrumental setups of IMS, such as drift time ion mobility, traveling wave ion mobility, asymmetric field ion mobility, or differential ion mobility analysis, the principle is always the same – an electrical field "pulls" ions towards an electrode, while the ions' trajectories are otherwise influenced by collisions with a damping gas. The key parameter influencing the movement of the ions is the collision cross section (CCS). CCS depends on the three-dimensional structure of the ions which defines the "contact area" between an ion and the gas through which it passes. It is a characteristic physicochemical property of a molecule/ion which can be calibrated, quantified, and searched against databases (Kanu et al. 2008; Kliman et al. 2011; Paglia et al. 2015).

Since IMS also requires an ion source and an ion detector, coupling with mass spectrometry is easy to achieve. Coupling ion mobility to mass spectrometry has the benefit that the ion mobility separation needs little additional time of only a few milliseconds. Ion mobility then is able to quickly provide an additional level of separation

– separation based on the ions' three-dimensional structure – in addition to *m/z* and possibly chromatography.

Ion mobility in lipid analysis is especially beneficial for shotgun lipidomics (where there is no chromatographic separation), as it may allow for separation of isobaric lipids, which cannot be separated by *m/z* alone. Thereby it is possible to separate isobaric lipids by their head group (Lintonen et al. 2014; Shvartsburg et al. 2011; Hankin et al. 2015), and even separate fatty acyl (Maccarone et al. 2014) and double bond (Groessl et al. 2015) positional isomers of phospholipids. IMS can also be used as a third separation criterion, alongside chromatography and mass spectrometry, to provide truly three-dimensional lipidomic analysis (Baker et al. 2014).

3.5.2 Mass spectrometry imaging

When samples (organs, cells, etc.) are subjected to classical lipidomic sample preparation, i.e. lipid extraction, all information about the spatial distribution of individual analytes is lost. In contrast, mass spectrometry imaging (MSI) allows for surface analysis of whole cells, histological slices of organs, etc. (Rohner et al. 2005; McDonnell & Heeren 2007).

Traditional ionization techniques used with MSI are MALDI (chapter 3.3.2.1.5, p. 16) and secondary ion mass spectrometry (SIMS). A drawback of these ionization techniques is that they operate in a vacuum, which may compromise the integrity of the tissue investigated. Ambient ionization methods, such as desorption electrospray ionization and direct analysis in real time (DART), allow for faster and uncomplicated analysis of samples (Ellis et al. 2013). Liquid extraction surface analysis (LESA) combines a short extraction step of analytes from the sample surface and subsequent ionization with nano-ESI, all using the same needle tip. Spatial resolution is also an important factor when considering ionization methods – where the vacuum ionization methods (MALDI, SIMS) have a clear advantage over the ambient ionization methods, since they offer spatial resolutions of as low as 1-5 µm. This allows for analysis of single cells and even subcellular compartments (Yang et al. 2015; Passarelli & Winograd 2011; Eberlin et al. 2011; Murphy et al. 2011). When using laser-based methods, such as MALDI or SIMS, a TOF is the ideal mass analyser, as it is capable to work synchronously with the short burst of the ions generated, while still generating informative, high-resolution spectra. The advantage of spray-based methods (DESI, LESA) is that they deliver a prolonged signal, which allows for acquisition of multiple MS or even MS/MS spectra (Ellis et al. 2013).

4 A GLOBAL LIPIDOMICS METHOD

4.1 Introduction

Following the aims of the research field of lipidomics (Wenk 2005; Griffiths et al. 2011; Quehenberger et al. 2010), one of the most essential requirements is comprehensive and quantitative analysis of the lipidome. However, the vast complexity of lipids (Chapter 1.1.1, p. 2ff) limits the ability of a single LC/MS method to analyse the complete lipidome. Hence, many or even most "global" lipidomic methods focus on the most abundant lipid classes – glycerolipids, glycerophospholipids, sphingolipids and sterols.

There are two main approaches to the task of "global" analysis of lipids – separation approaches and shotgun approaches. Separation of lipids prior to mass spectrometric analysis is usually achieved by HPLC (RP or HILIC), although supercritical fluid chromatography (SFC) is also being used. Depending on the type of chromatography used, lipids are either separated into classes using HILIC (Cífková et al. 2012; Zheng et al. 2010; Zhu et al. 2012; Schwalbe-Herrmann et al. 2010) or separated by their overall polarity using reversed phase chromatography (Fauland et al. 2011; Knittelfelder et al. 2014). There are several advantages of separation approaches: Firstly, less ion suppression is to be expected, since the sample being analysed is separated into its constituents. Secondly, chromatography has the potential to separate isobaric lipids (e.g., structural or even positional isomers) – which have the same elemental composition and therefore identical *m/z* values and cannot be separated solely by their *m/z* (Lísa & Holčapek 2013; Lisa et al. 2009; Triebl et al. 2016). The disadvantages of chromatographic approaches are usually a longer run time per sample (although very short analysis times of a few minutes have been reported using SFC (Lísa & Holčapek 2015)). Another disadvantage is that when gradient elution is used, differences in solvent composition at the time of elution may result in different ionization efficiencies, and therefore signal intensity for different analytes.

Shotgun approaches rely on stable infusion of the sample into the mass spectrometer without prior separation. Therefore, ionization is not influenced by gradient, and all analytes experience the same level of ion suppression. However, ionization efficiencies are not necessarily identical for all lipids, but instead depend on the lipid class, as well as on the number of carbon atoms and the degree of unsaturation (Koivusalo et al. 2001). Shotgun approaches therefore omit the need for HPLC instrumentation. Data interpretation from shotgun spectra is a complex task, necessitating specialized software packages. Not

only do the resulting spectra contain signals from all ionisable sample components, but isomeric components are also not separated. For example, odd-carbon PE and even-carbon PC form protonated molecules with identical *m/z* and can only be distinguished by their fragment spectra. Shotgun lipidomics require either high resolution mass spectrometers (Schuhmann et al. 2012; Kalvodova et al. 2009; Ejsing et al. 2009), or a combination of lipid class specific precursor or neutral loss scans (Wang et al. 2015; K. Yang et al. 2009; Bowden et al. 2014) to identify and quantify lipids. Flow-injection analysis (Liebisch et al. 2004; Liebisch et al. 2006) uses an HPLC setup without an analytical column, but instead relies on injecting the sample into the HPLC flow, resulting in elution of the whole sample over a few seconds or minutes, but without chromatographic separation.

In between these two main lipidomic approaches are in-source separation techniques. "Intrasource separation and selective ionization", made popular by X. Han (Han et al. 2006), relies on the use of modifiers (Li^+, Na^+, or NH_4^+) added to the infusion solvent, so that only some lipid classes are ionised, while ionization of other classes is almost completely suppressed. Another technique is ion mobility mass spectrometry, which exploits the physicochemical properties of ions to separate lipid classes, or even structural or positional isomers of lipids (Maccarone et al. 2014; Shvartsburg et al. 2011; Kliman et al. 2011; Lintonen et al. 2014; Baker et al. 2014; Hankin et al. 2015; Groessl et al. 2015).

The method developed and described here uses a simple liquid-liquid extraction method, and "classical" RP-HPLC coupled to high resolution mass spectrometric detection with parallel generation of fragment spectra for in-depth analysis of lipids. It is able to structurally and quantitatively analyse hundreds of glycerolipids, glycerophospholipids, and sphingolipids from even the most complex biological matrices in a single run.

4.2 Materials and methods

4.2.1 Lipid standards

Lipid standards used for controlled generation of tandem mass spectra are listed in Supplementary Table 1 (p. iii), and LIPID MAPS quantitative internal standards are listed in Supplementary Table 2 (p. vi).

4.2.2 Sample preparation

A whole murine liver was homogenized using a BioPulverizer (BioSpec Products, Bartlesville, OK, USA) and an aliquot of approximately 50 mg was taken. For lipid

extraction, an MTBE extraction protocol modified after Matyash et al. (Matyash et al. 2008) was employed. To the samples (50 mg liver homogenate, 100 mg of *C. elegans* embryos, or one million A549 adenocarcinomic human alveolar basal epithelial cells) were added 1.5 mL methanol and 5 mL MTBE and the mixture was incubated for 10 minutes in an overhead shaker at room temperature. 1.25 mL deionized water was added to induce phase separation and the mixture was shaken for 10 minutes. After centrifugation (3 min, 1250 x g, 21 °C), the upper MTBE phase was collected and the lower aqueous phase was re-extracted with 2 mL of the upper phase of MTBE/methanol/deionized water 10:3:2.5 (v/v/v). The combined upper phases were evaporated in a vacuum centrifuge. The dried lipid film was resuspended in chloroform/methanol 1:1 (v/v) and stored at -20 °C. Prior to analysis, the storage solvent was replaced with the injection solvent 2-propanol/chloroform/methanol 90:5:5 (v/v/v).

4.2.3 LC/MS

Chromatographic separation was performed on a Waters BEH C8 column (100x1 mm, 1.7 µ), thermostatted to 50 °C in a Dionex Ultimate 3000 RS UHPLC system. Mobile phase A was deionized water containing as additives 1 vol% of 1 M aqueous ammonium formate and 0.1 vol% of formic acid. Mobile Phase B was a mixture of acetonitrile/2-propanol 5:2 (v/v) with the same additives. Gradient elution started at 50 % mobile phase B, rising to 100 % B over 40 minutes; 100 % B were held for 10 minutes and the column was reequilibrated with 50 % B for 8 minutes before the next injection. Flow rate was 150 µL/min, the samples were kept at 8 °C and the injection volume was 2 µL.

The Orbitrap Velos Pro hybrid mass spectrometer (Thermo Fisher Scientific Inc., Waltham, MA, USA) was operated in Data Dependent Acquisition (DDA) mode using a HESI II ion source. Prior to experiments, lens settings were tuned and source parameters were optimized to the signal of PE 16:0/18:1 using the protonated and the deprotonated molecules in positive and negative ion mode, respectively. Ion source parameters for positive polarity were as follows: Source Voltage, 4.5 kV; Source Temperature, 275 °C; Sheath Gas, 25 arbitrary units; Aux Gas, 9 arbitrary units; Sweep Gas, 0 arbitrary units; Capillary Temperature, 300 °C. Ion source parameters for negative ion mode were: Source Voltage, 3.8 kV; Source Temperature, 325 °C; Sheath Gas, 30 arbitrary units; Aux Gas, 10 arbitrary units; Sweep Gas, 0 arbitrary units; Capillary Temperature, 300 °C. Full scan profile spectra from *m/z* 400-1 200 for positive ion mode and from *m/z* 400-1 600 in negative ion mode were acquired in the Orbitrap mass analyzer at a resolution setting of

100 000 (FWHM at *m/z* 400). For MS^2 experiments in both polarities, the 10 most abundant ions of the full scan spectrum were sequentially fragmented in the ion trap using He as collision gas (Normalized Collision Energy, 50; Isolation width, 1.5 *m/z*; Activation Q, 0.2; Activation Time, 10 ms) and centroid product spectra were collected. Exclusion time was set to 10 s.

4.2.4 Data processing and quantitation

LC/MS data was processed using Lipid Data Analyzer (LDA), as previously described (Hartler et al. 2011). Briefly, the algorithm identifies lipids with a 3D algorithm, using the three dimensions *m/z*, retention time, and intensity to correctly integrate peaks, while also taking into account the isotopic distribution. MS/MS spectra (displayed, but not automatically interpreted by the program) were manually inspected to obtain information about characteristic head group fragments and fatty acid composition, as described previously (Hsu & Turk 2009; Murphy et al. 2007; Griffiths 2003). Lipid species contributing a sum of less than 1 % to the total amount of the respective lipid class were omitted from the analysis.

In positive polarity, PC, PE, PG, PS, PG, LPC, LPE, LPS and SM were analysed as $[M+H]^+$ ions, Cer and HexCer as $[M–OH]^+$, DG and TG as $[M+NH_4]^+$ ions. In negative ion mode, PE, PS, PG, PI, LPE, LPS and CL were analysed as $[M–H]^–$ ions, and PC, LPC and SM as $[M+HCOO]^–$ ions.

Lipids were quantified using Lipid MAPS internal standards containing odd-chain fatty acids. To 60 µL of the liver extract and the A549 cell extract, all internal standards listed in Supplementary Table 2, p. vi were added at concentrations of 1.5 µM prior to measurement. To 60 µL of the *C. elegans* sample, only PC 25:0, PE 25:0, PG 25:0, PI 25:0, the deuterated TG and DG mix, and sphingolipid internal standards were added at concentrations of 5 µM. Quantitation of naturally occurring lipids was performed using a one-point calibration.

4.2.5 Method validation

A liver lipid extract was spiked with non-endogenous synthetic-standards (PC 12:0/12:0, PE 12:0/12:0, PS 12:0/12:0, PG 12:0/12:0, LPC 15:0, LPS 17:1, LPE 17:1, Cer 17:0, SM 17:0, TG 17:0/17:0/17:0 and DG 12:0/12:0/0:0) to 14 concentration levels ranging from 1 nM to 100 µM. Each concentration level, along with an unspiked lipid extract, was analyzed in triplicate to assess linearity range and limits of quantitation.

To gain insight about the fragmentation behaviour of lipids, 78 synthetic lipid standards with known fatty acyl compositions (19 glycerolipids from two classes, 51 glycerophospholipids from 10 classes and 9 sphingolipids from two classes; see also complete list in Supplementary Table 1, p. iii) were purchased. A mixture containing all these lipids at concentrations of 5 µM was prepared and analysed in quintuplicate by LC/MS/MS as described in chapter 4.2.3, p. 28f. To perform in-depth studies on the fragmentation behaviour, the experiments were also performed using higher-energy collision dissociation (HCD) with high-resolution accurate mass detection in the Orbitrap analyser HCD parameters were: Normalized Collision Energy, 25 for positive ion mode, 50 for negative ion mode; Activation Time, 0.1 ms; otherwise identical DDA settings as described in chapter 4.2.3, but only the four most abundant precursors were selected for MS^2 fragmentation.

4.3 Results and discussion

4.3.1 Sample preparation and sample storage

The presented sample preparation method is applicable to a wide variety of biological matrices. It has been successfully applied to multiple tissue (liver, brain, muscle) liquid (serum, lymph), as well as to cell culture samples without major modifications. For some sample types (e.g. those with a high amount of connective tissue), it is beneficial to homogenize the sample in the extraction solvent using a rotor-stator homogenizer. In contrast to classical Folch or Bligh and Dyer extraction protocols (Folch et al. 1957; Bligh & Dyer 1978), the biggest advantage of using MTBE as extraction solvent – besides reduced toxicity and cancerogenity compared to chloroform – is that the organic phase forms the upper layer, with precipitated proteins and other insoluble debris at the very bottom of the container. This greatly simplifies sample collection and minimizes the danger of contaminations.

When whole organs are to be analysed, great care must be taken to ensure that a representative aliquot is taken, since only a small part (e.g. 50 mg of a 1500 mg murine liver) of the organ is extracted. If the whole organ is homogenized – which can be easily achieved with a mortar and a pestle under liquid nitrogen –aliquots taken vary far less in their lipid content and composition than when pieces of the liver are cut with a scalpel. Indeed, different lobes of the same liver vary substantially in their phospholipid composition (unpublished observation). While liver or muscle are a relatively

homogeneous tissue, other organs such as brain vary greatly in their structure and contain different types of tissue (connective tissue or fat) in varying amounts next to the actual nerve parenchyma, making sampling of a representative aliquot even more important.

Sample storage is another critical point and a big potential error source. Biological samples, especially tissues, should always be flash-frozen in liquid nitrogen to stop enzymatic as well as chemical degradation processes. Recommended storage conditions for pure lipid standards are a temperature of -20 °C and a non-aqueous solvent (Avanti Polar Lipids n.d.), and these conditions should also be met for lipid extracts. Typical storage artefacts are hydrolysis and chemical oxidation. Hydrolysis can lead to cleavage of fatty acyls whereas oxidation mainly affects unsaturated fatty acyls, which causes an artificial increase in lipid oxidation products. Since oxidized lipids are important biomarkers for cellular oxidative stress (McIntyre et al. 1999; Bochkov et al. 2010; Ashraf & Srivastav 2012), any artificial increase of their levels prior to measurement should be avoided by all means. Analysis of other potential degradation products such as phosphatidic acid (which can be generated by cleavage of the head group from any diacyl phospholipid) or lysophosphatidic acid (which can be generated from any phospholipid through cleavage of the head group and one fatty acyl) is also prone to artefacts and sample preparation and storage should be carefully evaluated (Triebl et al. 2014).

Generally, storing biological material before sample preparation or lipid extracts after sample preparation for excessively long periods of time is never beneficial and samples should always be processed and analysed as quickly as possible.

4.3.2 Chromatography

During method development, multiple HPLC columns (comprising different manufacturers, different phases, and column dimensions) were tested, until the BEH C8 column was found to give more than satisfactory results. The ethylene-bridged C8 material provides sufficient retention and separation of all relevant lipid classes.

The chromatographic method is able to separate the very polar analytes LPC 13:0 and LPC 14:0 (which both elute well after the solvent peak), while there is more than three minutes of elution time left for even longer-chain triacylglycerols after elution of TG 60:1.

The chromatographic setup is robust and reproducible. Retention time of the analyte PC 34:1 remained constant over 50 consecutive injections of a liver extract, with an RSD of only 0.1 %. RSD of the peak area of PC 34:1 in five replicate injections of murine liver,

C. elegans and A549 cell lipid extracts was 6.8 %, 5.3 % and 2.2 % respectively; and retention time was unaffected by the difference in sample matrix (overall RSD 0.4 %).

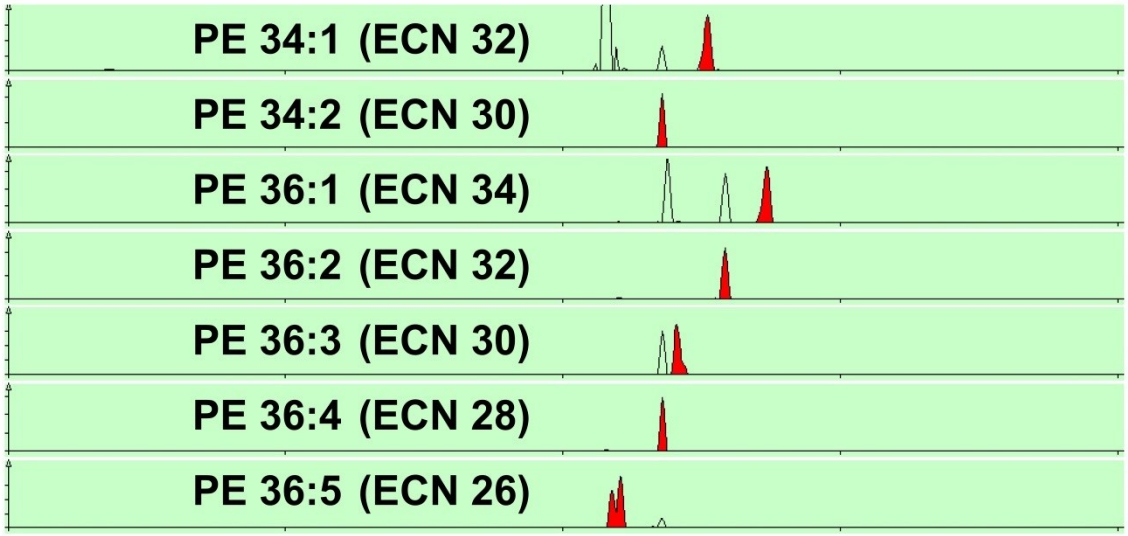

Figure 7: Retention behaviour of lipids separated by reversed phase chromatogaphy. Additional carbon atoms in the fatty acyls increase retention, while double bonds decrease retention of PE molecular species. Correct peaks are marked in red by Lipid Data Analyzer, the rest are quasi-isobaric interferences from other compounds. Green background denotes that tandem MS spectra of the corresponding lipids are available.

A well-described characteristic of reversed-phase separation of lipids is the applicability of the equivalent/effective carbon number (ECN) model for lipidomics (Lísa et al. 2011; Schwalbe-Herrmann et al. 2010; Fauland et al. 2011). ECN is calculated as [number of carbon atoms]–2*[number of double bonds]. As already indicated by the formula, additional carbon atoms in the fatty acyl chains cause an overall increase in hydrophobicity and increase retention, whereas conversely, double bonds decrease overall hydrophobicity and thereby retention. The effect of chain length and double bonds on retention is most likely explained by the *cis*-double bonds causing a curvature in the three-dimensional structure of the fatty acyls, which inhibits hydrophobic interaction with the column material. Longer acyl chains provide more area for hydrophobic interactions between the fatty acyls and the column material. Figure 7 shows chromatograms of PE molecular species. Generally, species with higher ECN elute later, although for molecular species with more than three double bonds, ECN alone does not accurately describe retention behaviour (e.g. PE 34:2 and PE 36:4 have almost identical retention time, but differ in ECN). Also, structural isomers have identical ECN, but are chromatographically separated in many cases (see also chapter 4.3.4.1, p. 54ff).

The reversed phase method presented delivers excellent results for more than 10 lipid classes. However, there remain some "problematic" classes: Phosphatidic acid (PA) and phosphatidylinositolphosphates (PIP), which both contain a terminal phosphate group, show strong tailing of the chromatographic peak. This is attributed to interactions of the free phosphate groups with stainless steel surfaces ubiquitous in HPLC systems (injection system, ESI spray capillary, etc.) (Wakamatsu et al. 2005; Asakawa et al. 2008). Should these lipid classes need to be analysed, specialized techniques are required, such as addition of a phosphate salt to the HPLC mobile phase (Knittelfelder et al. 2014), chemical derivatization (Wakelam 2014), or a different mode of chromatography such as HILIC (Triebl et al. 2014).

4.3.3 Tandem mass spectrometry of lipids

In the following chapter, the tandem mass spectrometric behaviour of lipids is discussed in detail. Emphasis is put on fragment ions characteristic of the head groups and of fatty acyls, while also discussing the relative intensity distributions of fragment ions indicative of the fatty acyls, from which their *sn*-positions can often be deduced. Both positive and negative polarity, as well as multiple informative adducts per lipid class are considered. The elemental composition of all fragment ions has been confirmed with high-resolution accurate mass detection (mass tolerance in tandem mass spectra 0.02 Da), and conform to existing literature (Pulfer & Murphy 2003; Murphy 2015; Hsu & Turk 2009).

Note that the tandem mass spectrometric behaviour described here may not necessarily be identical when other types of mass spectrometers are used. Already the occurrence and relative intensities of different adduct ions of the same lipid strongly depends on the geometry of the ion source and precise electrospray ionization settings used. E.g. while formate adducts may be the predominant ionized form of choline lipids in negative ion mode on one instrument, on other types of instruments they may be observable solely as their demethylated forms. Furthermore, the type of fragmentation used may have great influence on the occurrence and relative distribution of fragment ions. A quadrupole-type fragmentation is inherently different from an ion trap-type fragmentation in terms of internal energy distribution. This may result in different fragment spectra for the same analyte (Larsen et al. 2001). However, when appropriate and "reasonable" settings are used, the fragmentation process results in largely similar and comparable tandem mass spectra (at least concerning the main fragmentation pathways); even when different types of instruments are used.

Also, one should bear in mind that any tandem mass spectrum is always the cumulative result of the dissociations of thousands of precursor ions, and that fragmentation of one singly charged precursor ion can only give rise to a single detectable fragment ion, since the number of charges remains the same. When multiple fragment ions arise from one precursor ion, this is due to the fact that not all precursor ions follow the same fragmentation pathway. Instead, during the fragmentation process, more energy is transferred to some ions than to others. This difference in internal energy then results in the cleavage of different chemical bonds. Thus, if a fragment spectrum contains two mass peaks of the same intensity, half of the precursor ions have followed one fragmentation pathway and the other half the other pathway.

Finally, the following is not to be viewed as a mechanistic approach clarifying the underlying fragmentation mechanisms and pathways. Often, two fragment ions separated by 18 Da are here simply referred to as a "water loss", although mechanistically, these two fragment ions may have originated from different precursors or intermediates, and not directly from each other. For in-depth analysis of lipid fragmentation pathways and mechanisms, the detailed publications of Hsu and Turk are recommended. The aim of the following chapter instead is to identify characteristic fragment ions for many lipid classes, the knowledge of which can be used for very sophisticated lipidomic measurements (for an example, see chapter 6).

4.3.3.1 General rules for lipid fragmentation

Some general rules apply to the fragmentation of all lipids and are not discussed separately for every class:

Lysophospholipids, like all other compounds with a free hydroxyl group, usually show an unspecific neutral loss of water (-18 Da), just as formate adducts show a prominent neutral loss of formic acid (-46 Da), and tandem mass spectra of chloride adducts are usually dominated by a loss of hydrochloric acid (-36 Da). However, these neutral losses are unspecific and therefore should never be used for identification or quantification purposes.

Different adducts of the same lipid do not necessarily fragment the same way. This is especially true for sodium adducts, which usually differ substantially in their tandem mass spectra from protonated forms of the same lipid. For example, the tandem mass spectrum of protonated PC contains essentially only one type of ion (protonated phosphocholine, *m/z* 184, Figure 11, p. 39), indicating that only one major fragmentation pathway exists for

protonated PC, and that the charge always remains on the quaternary nitrogen of the choline moiety. In contrast, a MS^2 spectrum of the corresponding sodium adduct shows at least three prominent fragment ions of comparable intensity (Figure 12, p. 40): A small neutral loss of trimethylamine (meaning that the charge remains on the remaining part of the molecule which is still associated with sodium), a phosphocholine neutral loss (again indicating that the charge as well as the sodium remain on the diacylglycerol-like part), and a low abundance ion at *m/z* 147 corresponding to a sodiated form of phosphoglycerol (indicating that the charge as well as the sodium is associated with the head group moiety). The occurrence of four fragment ions indicates that four different fragmentation pathways take place. It is also reasonable to assume that localization of the charge provided by the sodium may be variable, which would also influence the fragmentation process the adduct ion subsequently undergoes.

For almost all lipid classes investigated, the typical ions derived from collisional activation are to be found in one of four categories:

- Neutral losses of the head group or parts of the head group: These neutral losses have a very wide range of 30-300 Da. They include small unspecific neutral losses (formaldehyde, methanol), as well as large portions of the head group (e.g. sodiated phosphoinositol). Characteristic head group neutral losses are usually in the range of 140-200 Da.
- Small charged head group ions: In the range of *m/z* 88-320; the very small fragments below *m/z* 200 often fall victim to low-mass cut-off in ion trap spectra.
- Neutral losses of the fatty acids, alone or together with a part of the head group: These fragment ions occur in both polarities and their relative intensities can often be used to assign the *sn*-positions on diacyl phospholipids.
- Charged fatty acid ions: These include fatty acyl carboxylate anions detectable for almost all lipids in negative ion mode, as well as the low abundant, dehydroxylated positive ions originating from the fatty acyls of triacylglycerols.

Tandem mass spectra of positive lipid ions and adducts are usually dominated by head group ions (charged or neutral losses), while ions deriving from cleavage of fatty acyls are of lower abundance. The notable exceptions are sodiated and ammoniated forms of glycerolipids (which have no head group) and protonated PE plasmalogens. PE plasmalogens essentially show only fragment ions derived from cleavage of the *sn*-1 1*Z*-alkenyl and the *sn*-2 acyl chains. Aside from these exceptions, assignment of fatty

acyl compositions and positions is usually more reliable in negative ion mode, where fatty acyls are observable as abundant carboxylate anions ($RCOO^-$).

Carboxylate anions of long chain polyunsaturated fatty acyls, such as arachidonic acid (20:4) or docosahexaenoic acid (22:6), often undergo an additional spontaneous loss of carbon dioxide (-44 Da), leading to a second observable ion, which is usually of lower intensity than the carboxylate anion (Figure 8).

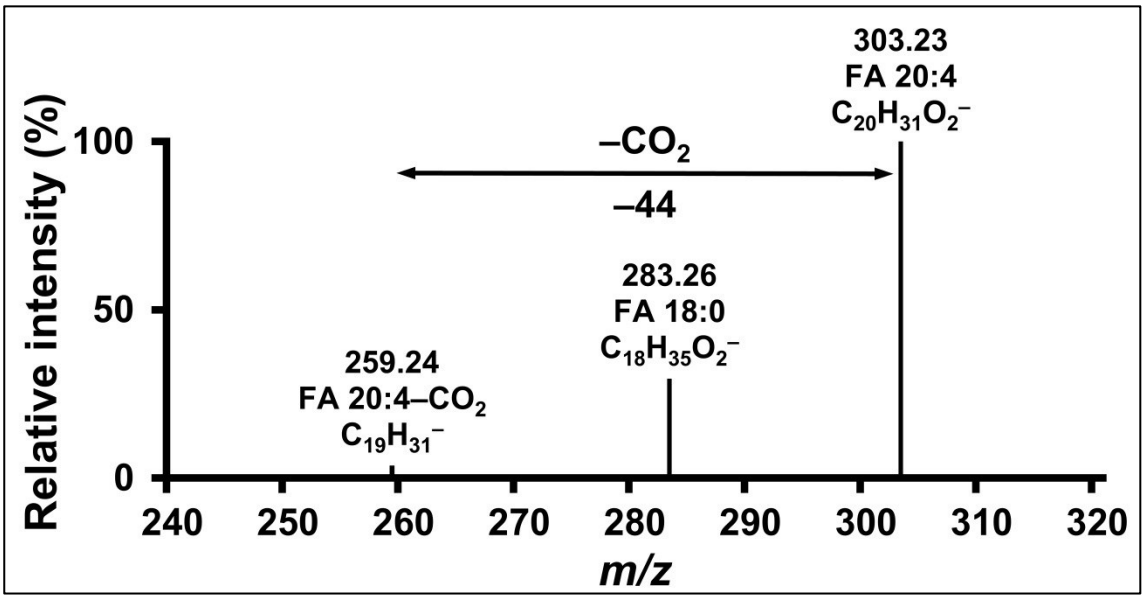

Figure 8: Fatty acyl carboxylate anions. The long chain polyunsaturated 20:4 fatty acyl carboxylate anion at *m/z* 303.23 additionally loses CO_2, leading to occurrence of an additional fatty acyl-derived ion at *m/z* 259.24. Shown here is an 18:0/20:4 PE species, where the position of the fatty acyls can be determined by comparing the relative intensities of the carboxylate ions.

In negative ion mode, all glycerophospholipids may show ions corresponding to cyclic glycerol phosphate (*m/z* 171) and the corresponding water loss (*m/z* 153), while ions at *m/z* 97 and *m/z* 79 originate from the phosphate group. However, these ions are often lost due to low mass cut-off.

The nitrogen rule also is very useful for interpreting tandem mass spectra of lipids. Since most lipids (with the exception of SM) usually do not contain more than one nitrogen atom (choline lipids or ammonium adducts), most ions with an even-numbered nominal *m/z* contain exactly one nitrogen atom (e.g. $[PC\ 34:1+H]^+$, *m/z* 760), while ions with an odd-numbered nominal *m/z* usually do not contain nitrogen (e.g. $[PI\ 38:4–H]^-$, *m/z* 885) (Gross 2013). Furthermore, the neutral loss of an odd *m/z* indicates that the number of nitrogen atoms differs between the precursor and the parent ion (e.g. neutral loss of trimethylamine, -59 Da).

4.3.3.2 TG

Triacylglycerols are only detectable in positive ion mode, as ammoniated adducts if an ammonium salt is present in the solvent, and as the ubiquitous sodium adducts. If acetonitrile is used as solvent, they also form ethylamine adducts $[M+C_2H_8N]^+$. Ethylamine adducts are particularly misleading, as they are structural isomers of ammonium adducts of other TG species. E.g., $[TG\ 52:1+NH_4]^+$ and $[TG\ 50:1+C_2H_8N]^+$ both have an *m/z* of 890.81712. However, they are easily differentiated by retention time.

Triacylglycerols have very characteristic tandem mass spectra. Ammonium adducts (Figure 9) readily lose ammonium plus a neutral fatty acid while showing almost no other fragment ions. Sodium adducts lose a neutral fatty acid as well as a neutral fatty acid together with sodium or ammonium. Usually, these spectra are dominated by neutral losses of fatty acids. Collisional activation with higher energy also results in small signals from a single charged fatty acyl fragment, generated by loss of a hydroxyl group from the neutral fatty acid, as well as a series of ions separated by 14 Da, similar in appearance to EI fragments of fatty acids. Under the conditions employed, no informative tandem mass spectra can be generated from TG ethylamine adducts despite high precursor intensities, indicating that these adducts are not sufficiently stable.

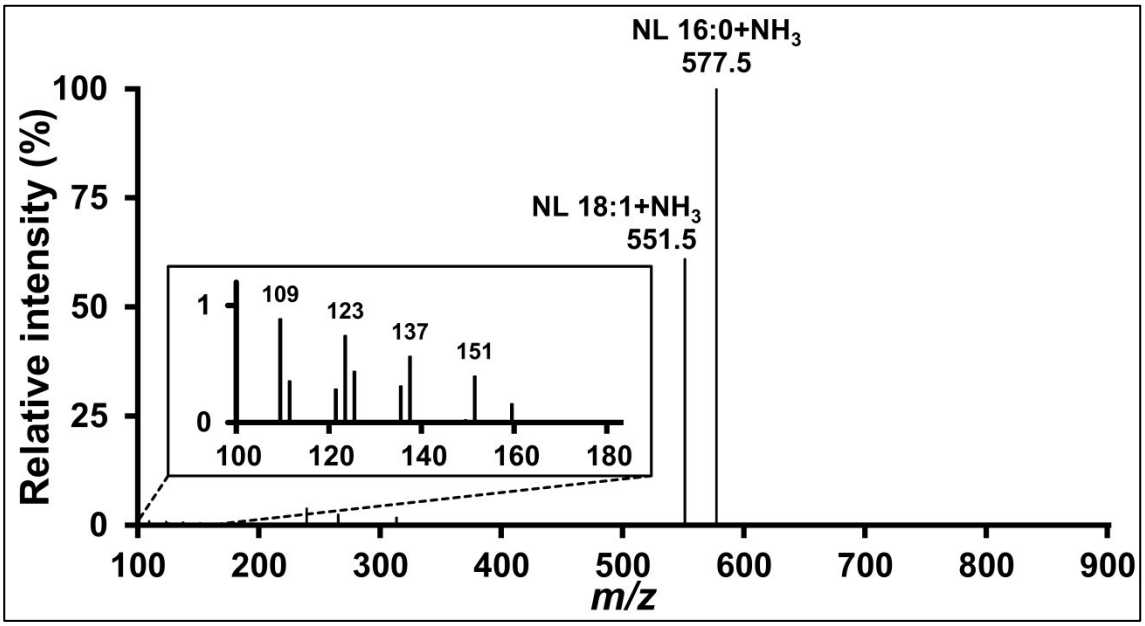

Figure 9: Tandem mass spectrum of $[TG\ 16:0/16:0/18:1+NH_4]^+$ (*m/z* 850.78578). Inset shows the EI-like fragment ions in the low mass range.

Assignment of the fatty acyl positions is almost impossible for TGs, as the loss of the fatty acyl at the *sn*-1 position occurs just as likely as the loss of the fatty acyl at the *sn*-3

position, while the probability for cleavage of the *sn*-2 fatty acyl is much lower. Therefore a fragment ion arising from cleavage of the *sn*-1 fatty acyl cannot be distinguished from one arising from *sn*-3 cleavage, impeding positional assignment.

4.3.3.3 DG

Diacylglycerols are very similar to TGs in terms of their ionization behaviour. In positive ion mode, they form ammoniated and sodiated adduct ions, as well as the potentially misleading ethylamine adducts with acetonitrile, while forming no detectable ions in negative ion mode.

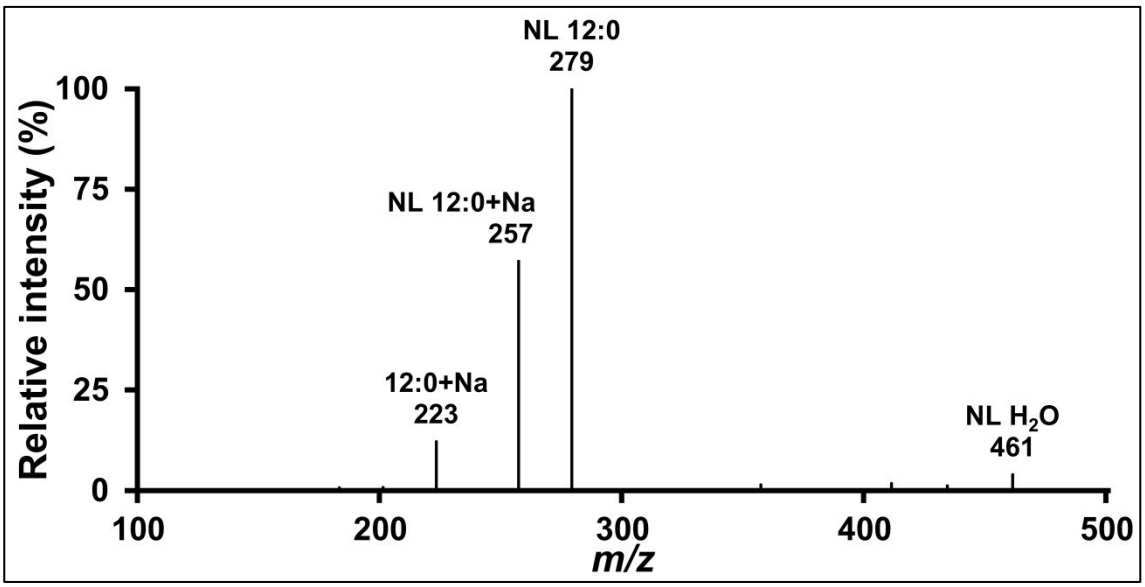

Figure 10: Tandem mass spectrum of [DG 12:0/12:0/0:0+Na]$^+$ (*m/z* 479.37070).

However, in contrast to TGs, the ammoniated adducts seldom deliver informative spectra (as do the ethylamine adducts), indicating that they are not sufficiently stable under the conditions employed. Sodium adducts (Figure 10) are dominated by fragments generated by loss of one fatty acyl, either as a neutral fatty acid, or a neutral fatty acid plus sodium. Additional fragment ions of smaller intensity correspond to protonated or sodiated fatty acids.

As is also the case with TGs, positional assignment is very difficult for DGs, with 1,2-DG and 1,3-DG differing only minutely in the relative intensities of neutral loss fragments.

4.3.3.4 PC, LPC and plasmalogen-PC

Derivatives of phosphatidylcholine, which contain a quaternary nitrogen atom carrying a permanent positive charge in the head group, are readily ionisable as protonated or

sodiated molecules in positive ion mode. In negative ion mode, they form formate adducts (or acetate adducts, depending on the type of solvent additive), as well as demethylated ions ($[M\text{-}CH_3]^-$). Sodium adducts in positive ion mode can be particularly misleading, since they have only a minute difference in *m/z* from the protonated form of another lipid of the same class (e.g. $[PC\ 36:1+Na]^+$ and $[PC\ 38:4+H]^+$ have a difference of only 2.4 mDa, which cannot be baseline separated at the mass resolution used.

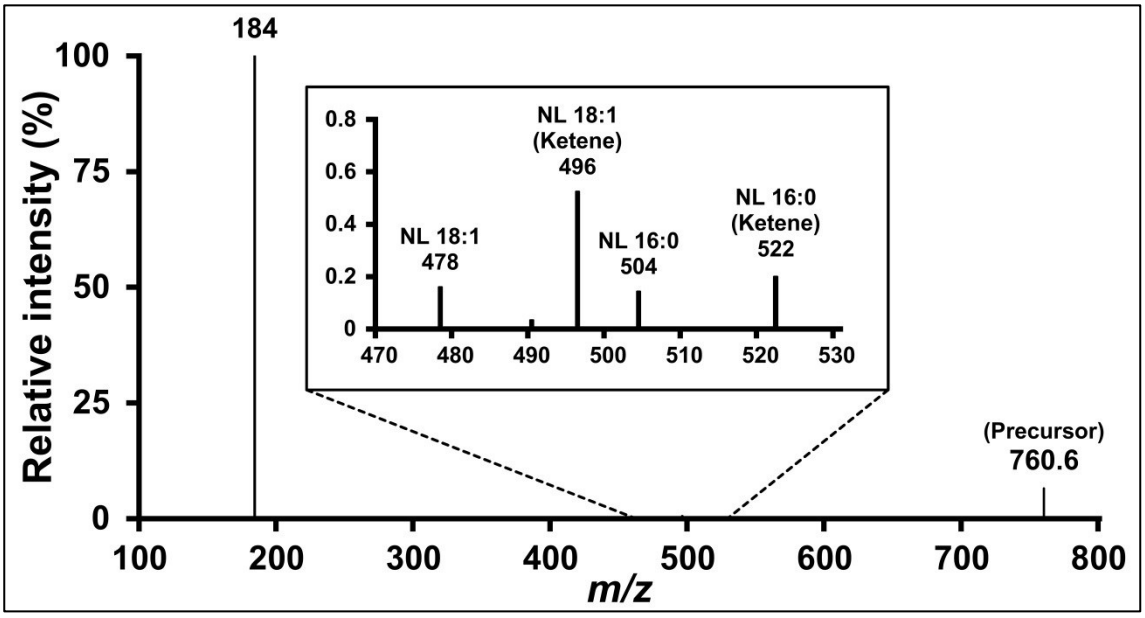

Figure 11: Tandem mass spectrum of $[PC\ 16:0/18:1+H]^+$ (*m/z* 760.58508).

Tandem mass spectra of protonated choline phospholipids (PC, LPC, and PC plasmalogens) are dominated by an ion at *m/z* 184, corresponding to the phosphocholine head group (Figure 11). Collisional activation with higher energy leads to the occurrence of two smaller head group ions at *m/z* 125 and *m/z* 104 (corresponding to further dissociation of the phosphocholine ion with the respective losses of trimethylamine and monometaphosphoric acid). Fatty acyls are usually lost as neutral fatty acids, or as ketenes. In the case of diacyl PC, the relative intensities of the fatty acid neutral losses are indicative of their *sn*-positions, with cleavage of the *sn*-2 fatty acyl being the preferred reaction.

Sodiated choline phospholipids have distinctly different fragmentation behaviour and can therefore easily be distinguished from other PC adducts (Figure 12). Usually, the most prominent fragment ions correspond to loss of trimethylamine (-59 Da) and neutral phosphocholine (-183 Da), while the neutral loss of sodiated phosphocholine (-205 Da) is also observed. Another distinct fragment for all sodiated choline phospholipids is *m/z* 147,

corresponding to the sodium salt of O,O'-dimethylenephosphoric acid. This fragment is usually not observable in ion traps due to low mass cut-off. The fatty acyls may be cleaved as neutral fatty acids, as neutral fatty acids plus sodium, or these two fragments may additionally lose trimethylamine. In contrast to protonated PC, the loss of the *sn*-1 fatty acyl is preferred.

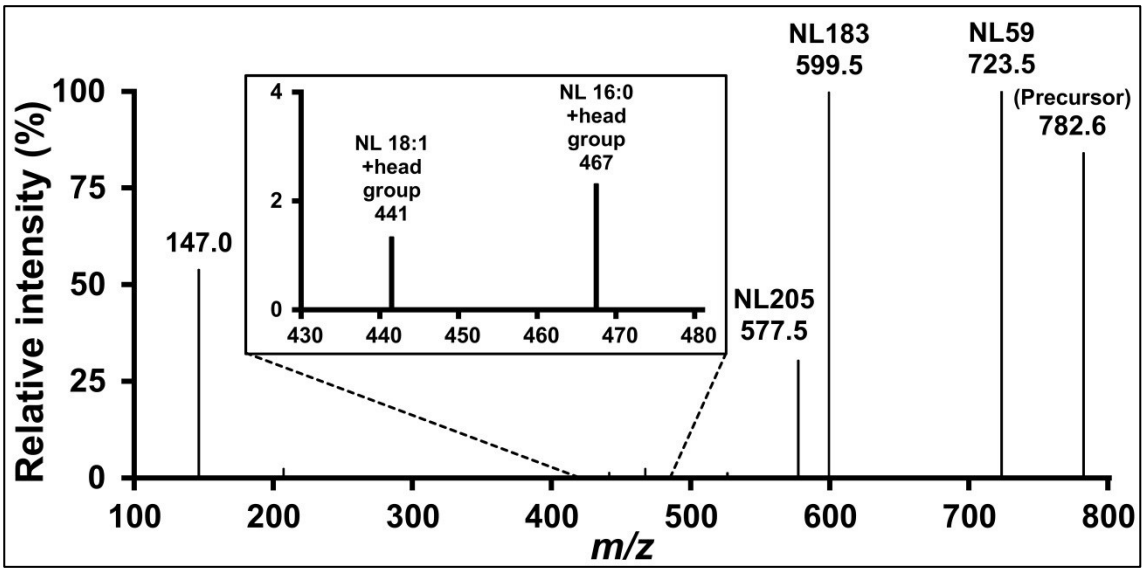

Figure 12: Tandem mass spectrum of $[PC\ 16:0/18:1+Na]^+$ (*m/z* 782.56703).

In negative ion mode, formate, acetate adducts, and also demethylated forms of PC generally follow the same fragmentation patterns (Figure 13). Small head group ions are glycerophosphocholine (*m/z* 242), the corresponding water loss (*m/z* 224), and demethylated phosphocholine (*m/z* 168). However, these ions are observed mostly at higher collision energies, if they are not lost to low mass cut-off. Fatty acyl ions are carboxylate anions, and neutral losses as fatty acids or as ketenes, either alone or together with formic acid. Positional assignment is easy, as both the carboxylates and the neutral losses predominantly originate from the fatty acyl at the *sn*-2 position. Tandem mass spectra of plasmalogen species show the corresponding anions of the enolate, but only at a minute fraction compared to the fatty acyl carboxylate (most likely due to resonance stabilisation of the carboxylate).

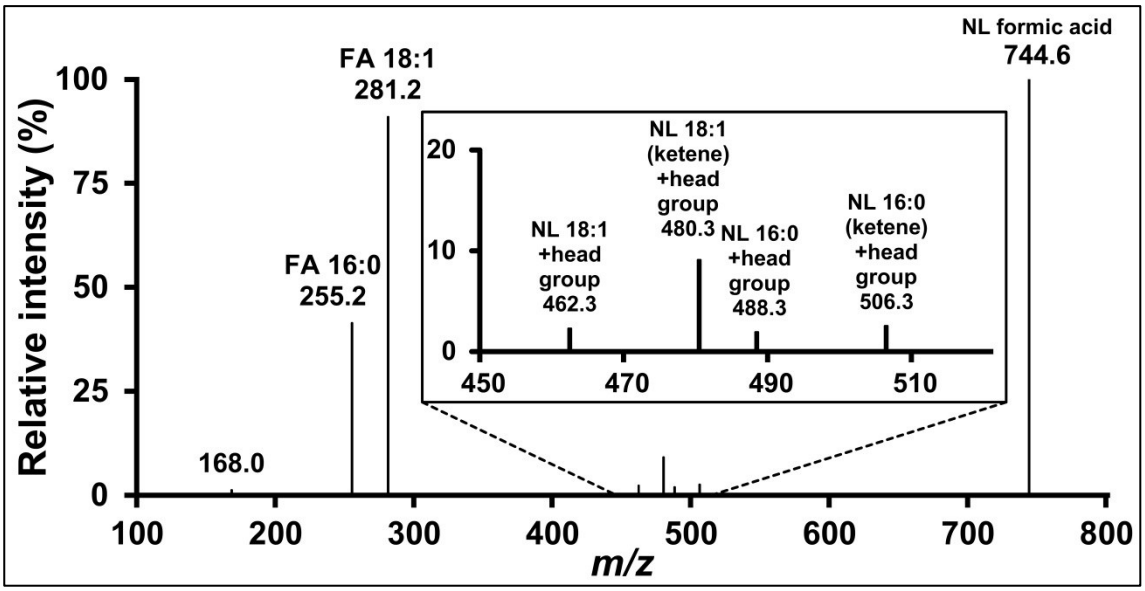

Figure 13: Tandem mass spectrum of $[PC\ 16:0/18:1+HCOO]^-$ (*m/z* 804.57601).

4.3.3.5 PE, LPE and plasmalogen-PE

Ethanolamine phospholipids ionize readily in both polarities, in positive ion mode as protonated molecules and sodium adducts, and as deprotonated molecules in negative ion mode.

Their protonated forms (Figure 14) usually yield a single prominent ion corresponding to the neutral loss of phosphoethanolamine (-141 Da). Small neutral losses of the fatty acyls, either as fatty acids, as ketenes, or as ketenes together with phosphoethanolamine, may also be visible, with cleavage of the *sn*-2 fatty acyl preferred over *sn*-1.

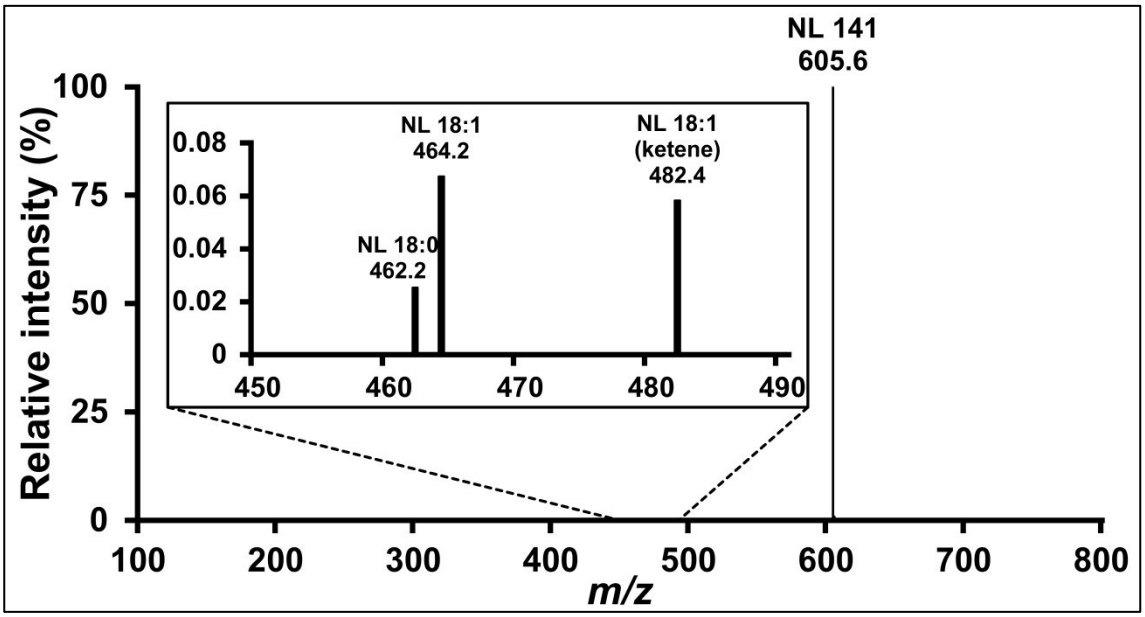

Figure 14: Tandem mass spectrum of $[PE\ 18:1/18:1+H]^+$ (*m/z* 746.56943).

Interestingly, PE plasmalogens do not show the typical PE head group neutral loss of -141 Da, but instead show prominent fragment ions derived from cleavage of the 1*Z*-alkenyl linked fatty alcohol at the *sn*-1 position and the esterified fatty acyl at the *sn*-2 position (Figure 15). Since this fragmentation behaviour is specific to the *sn*-1 1*Z*-alkenyl linkage and does not occur for other acyl/alkenyl PE species, the position of the alkenyl and the acyl chain can be deduced from the mere occurrence of the fragment ions (listed in Table 1 for the most common fatty acyl and alkenyl chains).

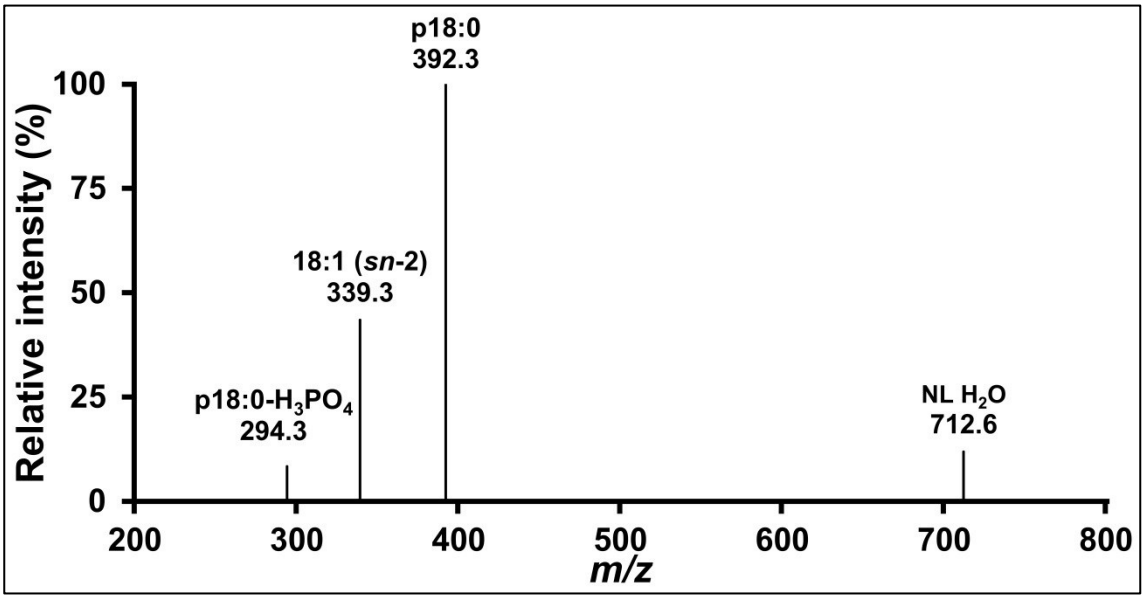

Figure 15: Tandem mass spectrum of $[PE\ P\text{-}18:0/18:1+H]^+$ (*m/z* 730.57452).

Sodiated forms of ethanolamine phospholipids (Figure 16) show typical neutral losses of ethanolamine (-61 Da) and the corresponding water loss (-43 Da), neutral loss of phosphoethanolamine (-141 Da) and the corresponding water loss (-123 Da), and of sodiated phosphoethanolamine (-163 Da). The characteristic small head group ions are sodiated phosphoethanolamine (*m/z* 164) and the corresponding water loss (*m/z* 146), and phosphate associated with sodium (*m/z* 121). Sodiated forms of plasmalogen PEs additionally show a class-specific fragment ion at *m/z* 307, while the same fragments derived from chain cleavage as for protonated plasmalogen PEs may also be observed.

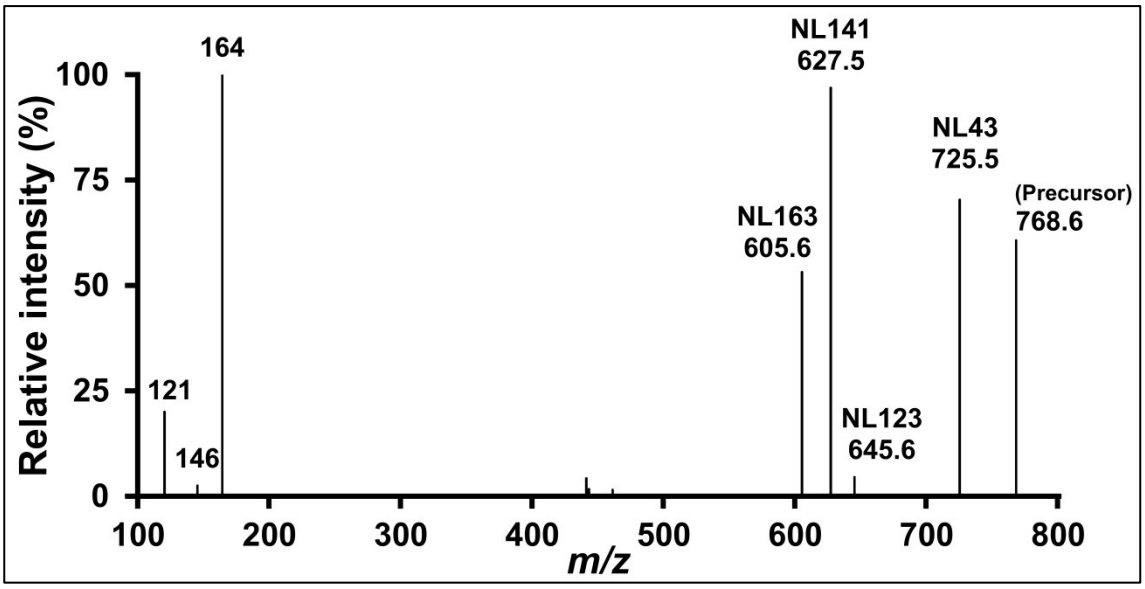

Figure 16: Tandem mass spectrum of [PE 18:1/18:1+Na]$^+$ (*m/z* 768.55138).

Deprotonated PE phospholipids (Figure 17) show intense carboxylate anions and also neutral losses of fatty acids and ketenes upon collisional activation, all preferably from the fatty acyl at the *sn*-2 position. Head group fragments (ethanolamine and glycerophosphoethanolamine at *m/z* 140 and *m/z* 214 with the corresponding water losses at *m/z* 122 and *m/z* 196) also occur, but are of extremely low abundance. Tandem mass spectra of deprotonated plasmalogen species show an abundant *sn*-2 carboxylate, while the *sn*-1 enolate is barely observable.

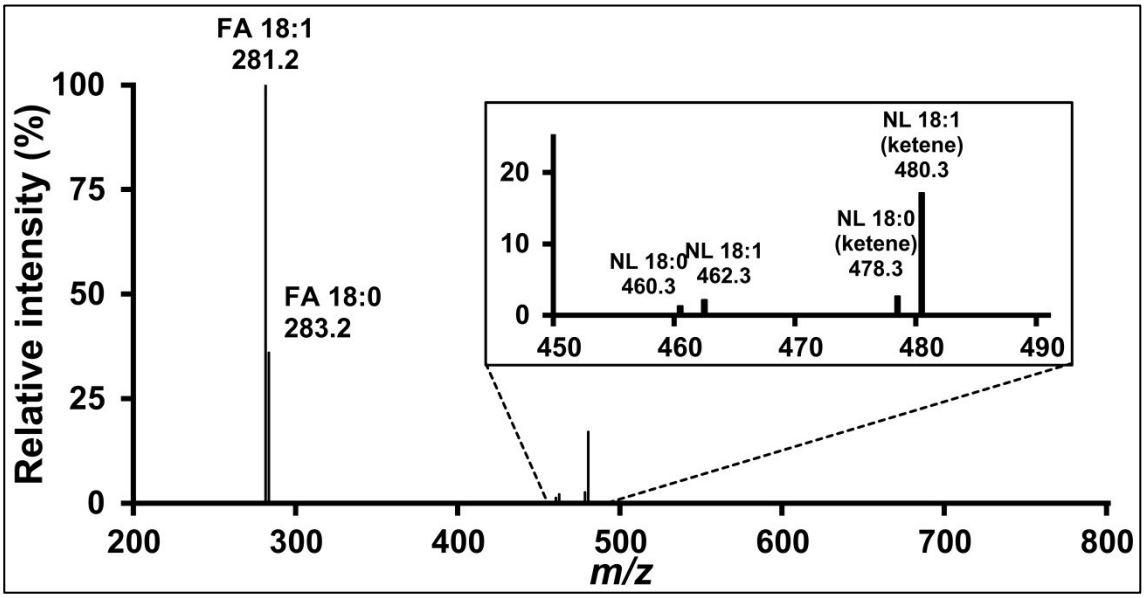

Figure 17: Tandem mass spectrum of [PE 18:0/18:1–H]$^-$ (*m/z* 744.55488).

Table 1: PE plasmalogen fragment ions. The identities and positions of the 1*Z*-alkenyl chain at the *sn*-1 position and the acyl chain at the *sn*-2 position can be deduced from the observable fragment ions. Note that the common nomenclature for plasmalogens already implies the *sn*-1 1*Z*-double bond. The double bond in the *sn*-1 alkenyl chain of PE P-16:0/20:4 is therefore not mentioned in the shorthand nomenclature. Note also that an additional fragment ion corresponding to the loss of phosphate (-98 Da) from the 1*Z*-alkenyl fragment is often also observed.

	1*Z*-alkenyl fragment	**acyl fragment**
	***sn*-1**	***sn*-2**
16 : 0	364	327
16 : 1	362	325
16 : 2	360	323
18 : 0	392	341
18 : 1	390	339
18 : 2	388	337
18 : 3	386	335
18 : 4	384	333
20 : 0	420	369
20 : 1	418	367
20 : 2	416	365
20 : 3	414	363
20 : 4	412	361
20 : 5	410	359
20 : 6	408	357
22 : 0	448	397
22 : 1	446	395
22 : 2	444	393
22 : 3	442	391
22 : 4	440	389
22 : 5	438	387
22 : 6	436	385
22 : 7	434	383

4.3.3.6 PS and LPS

The major ions for serine phospholipids are protonated molecules in positive ion mode, and deprotonated molecules in negative ion mode.

In positive ion mode (Figure 18), collisional activation results in a single prominent fragment ion corresponding to the neutral loss of phosphoserine (-185 Da), while neutral losses of the fatty acyls as fatty acids or ketenes, alone or together with phosphoserine, are barely, if at all, visible. The neutral loss of the fatty acyl at the *sn*-2 position is preferred.

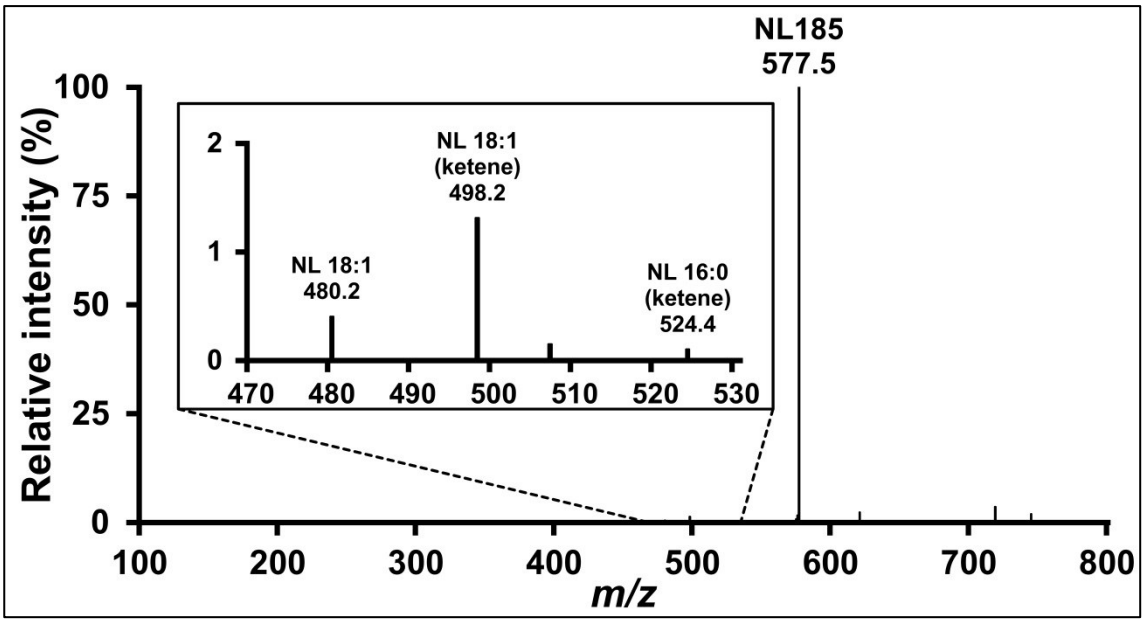

Figure 18: Tandem mass spectrum of $[PS\ 16:0/18:1+H]^+$ (*m/z* 762.57491).

Tandem mass spectrometry of the deprotonated ion of PS (Figure 19) or of LPS shows the neutral loss of serine (-87 Da) as the only characteristic head group fragment. Cleavage of the fatty acyls leads to neutral losses of fatty acids as carboxylates and as ketenes, both with and without the serine moiety. While the carboxylate anions predominantly originate from the *sn*-1 position, the neutral losses of the *sn*-2 fatty acyl are preferred.

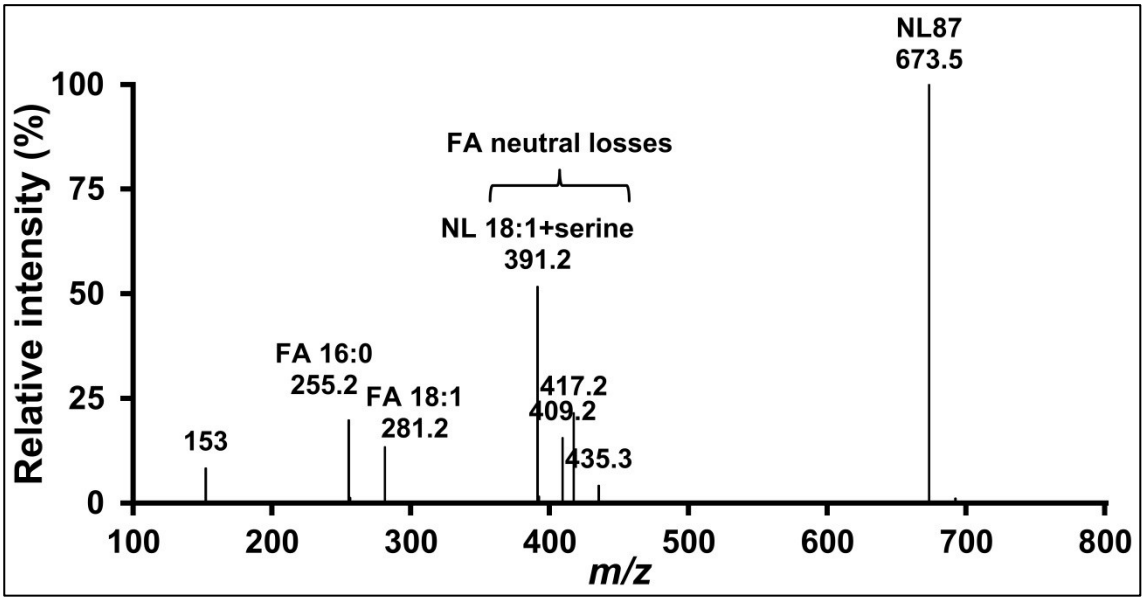

Figure 19: Tandem mass spectrum of $[PS\ 16:0/18:1–H]^-$ (*m/z* 760.51341)

Interestingly, serine phospholipids also form sodiated adducts in negative ion mode (as $[M\text{-}2*H^+\text{+}Na^+]^-$). However, the sodium adducts essentially lead to comparable tandem mass spectra as the deprotonated ions, with the only differences being a decrease in the

relative intensity of the serine neutral loss, and the additional occurrence of a fragment corresponding to the neutral loss of a fatty acid or of a ketene, together with serine and sodium.

4.3.3.7 PG

Phosphatidylglycerol species form protonated, sodiated, and ammoniated adducts in positive ion mode, while almost exclusively deprotonated ions occur in negative ion mode.

Protonated and ammoniated forms of PG do not generate useful tandem mass spectra; the fragmentation behaviour seems random and not reproducible across different molecular species. Sodiated PG (Figure 20) in contrast, forms multiple fragment ions indicative of the head group. These are the neutral losses of glycerol phosphate (-172 Da), the corresponding water loss (-154 Da), and loss of glycerol phosphate together with sodium (-194 Da). Sodiated glyerol phosphate (*m/z* 195) and its water loss (*m/z* 177) are also observable. The fatty acyls are lost as neutral fatty acids, and as ketenes, both alone and together with glycerol, with the loss of the neutral fatty acid at the *sn*-1 position preferred over *sn*-2.

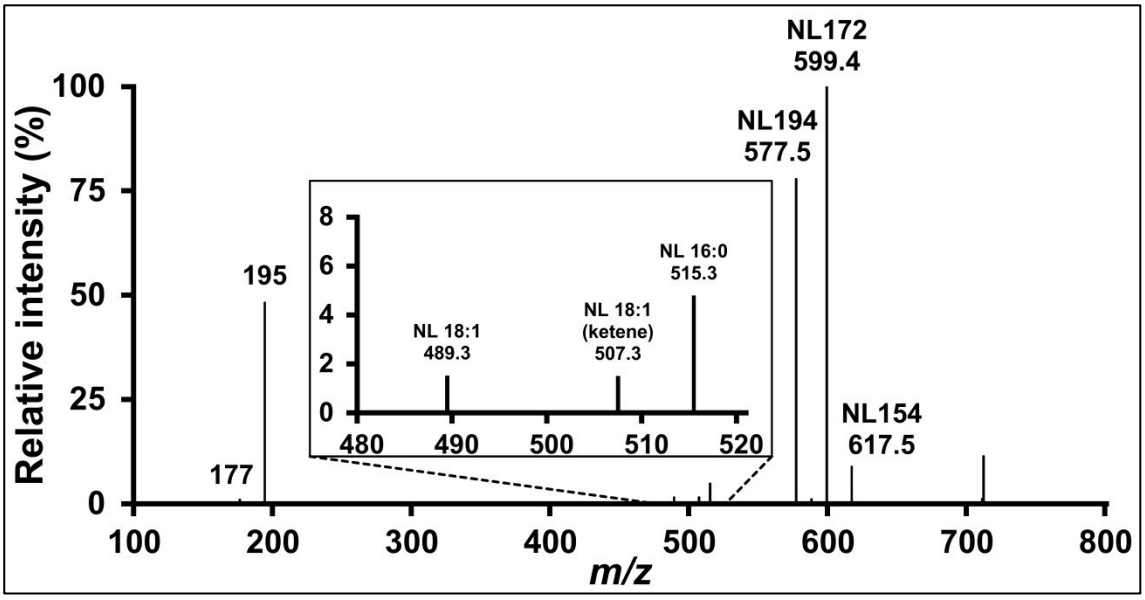

Figure 20: Tandem mass spectrum of $[PG\ 16:0/18:1+Na]^+$ (*m/z* 771.51466.

Tandem mass spectrometry of deprotonated PG (Figure 21) leads to major carboxylate anions, and ions corresponding to neutral losses of the fatty acyls (as neutral fatty acids, ketenes or together with the glycerol head group). The loss of the *sn*-2 fatty acyl is preferential for all ions indicative of the fatty acyls. Small head group fragments with *m/z* 209 and *m/z* 227 correspond to the charged phosphate group with two glycerol

moieties as well as the corresponding water loss, while a neutral loss of glycerol (-74 Da) may also be observed.

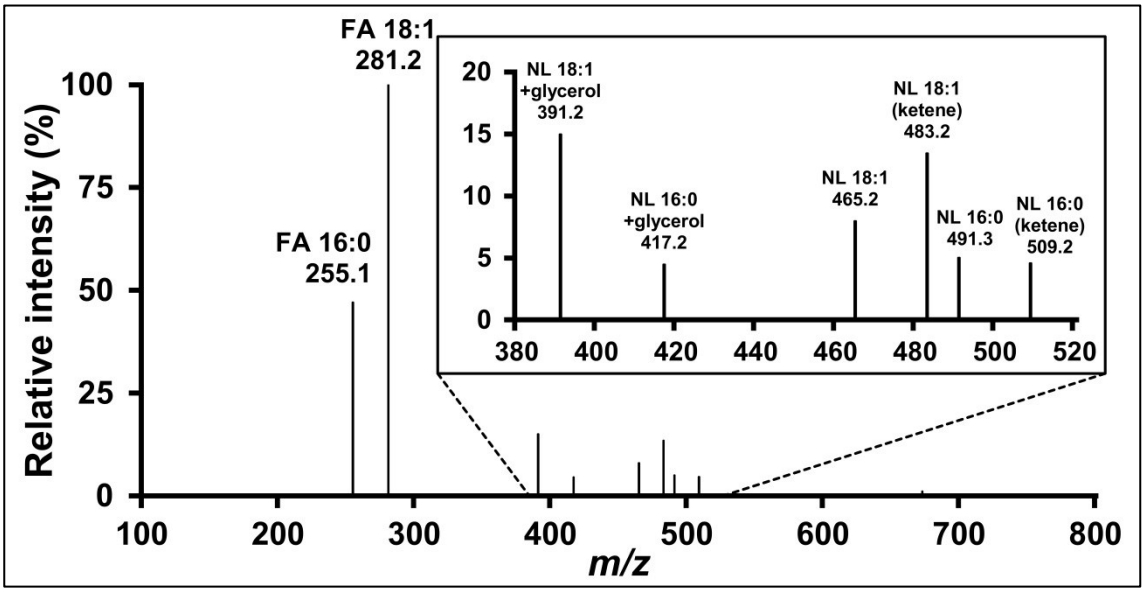

Figure 21: Tandem mass spectrum of $[PG\ 16:0/18:1–H]^-$ (*m/z* 747.51816).

4.3.3.8 PI

The hydroxyl groups of the inositol moiety make PI ideal for negative ionization, forming $[M–H]^-$ ions through abstraction of a proton. In positive ion mode, PI forms protonated, sodiated, and ammoniated adduct ions.

Under the experimental conditions employed, collisional activation of PI adducts in positive mode leads to unreproducible spectra varying greatly between molecular species differing in chain length and degree of unsaturation. Tandem mass spectra of protonated molecules show an abundant loss of inositolphosphate (-260 Da) as the only major head group fragment. The fatty acyls are lost as neutral fatty acids or ketenes, alone or together with inositolphosphate, with the neutral losses from the *sn*-2 position preferred over *sn*-1. Fatty acyls are also visible as dehydroxylated ions, and these ions originate more abundantly from the *sn*-1 position. Collisional activation of the sodiated adduct creates multiple fragment ions indicative of the head group. These correspond to neutral losses of the head group (phosphoinositol and its water loss, -260 Da and -242 Da; and of phosphoinositol together with sodium, -282 Da), and sodiated inositolphosphate at *m/z* 283. Neutral losses of the fatty acyls (as fatty acids, alone or together with inositolphosphate) are of extremely low abundance. The ammoniated adduct shows only

one major fragment, corresponding to the neutral loss of the inositolphosphate head group together with ammonia.

Tandem mass spectra of deprotonated PI (Figure 22) show abundant ions indicative of the head group as well as of the identities and positions of the fatty acyls. Numerous head group ions are visible; *m/z* 259, *m/z* 241, and *m/z* 223, correspond to phosphoinositol, and one or two water losses, while the larger ions at *m/z* 297 and *m/z* 315 derive from glycerophosphoinositol. Usually, *m/z* 241 is the most abundant head group ion and therefore often used in class-specific precursor scans. The fatty acyls are observable as carboxylate anions and as neutral losses (neutral fatty acids and ketenes, both alone or together with inositol). The stereospecific position of the fatty acyls can easily be derived from the relative intensity of the fragment ions; the carboxylates preferably originate from the *sn*-1 position, while the neutral losses of the *sn*-2 fatty acyls are more abundant than those from the *sn*-1 position.

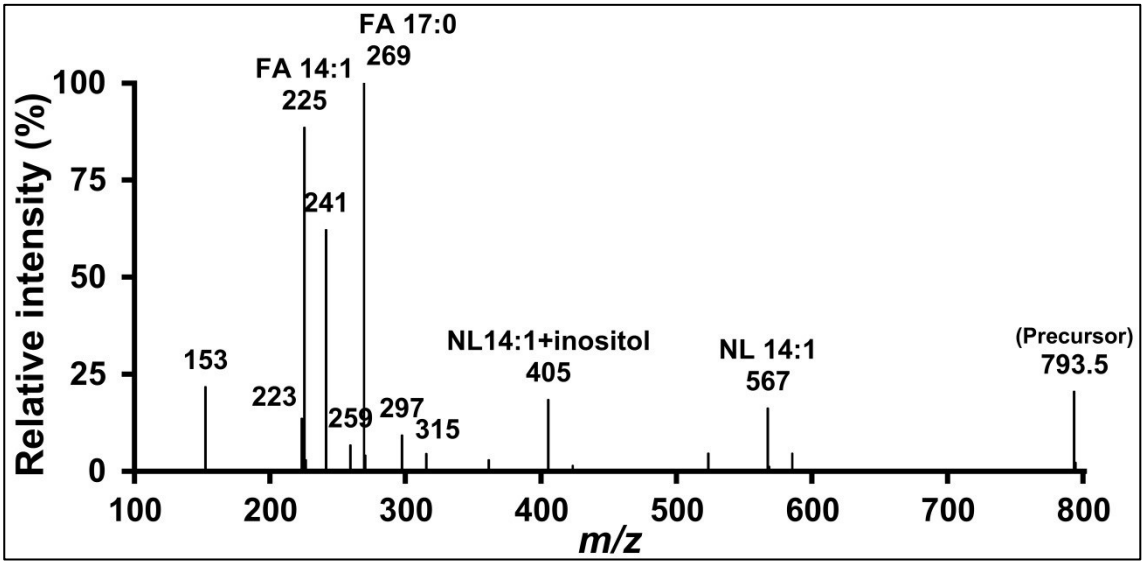

Figure 22: Tandem mass spectrum of $[PI\ 17:0/14:1–H]^-$ (*m/z* 793.48725).

4.3.3.9 SM

Sphingomyelin, due to the phosphocholine head group, behaves similarly to PC concerning adduct formation and tandem mass spectrometric behaviour. It forms protonated and sodiated adducts in positive ion mode, and formate adducts in negative ion mode.

Upon collisional activation, the protonated molecule forms only one major ion at *m/z* 184, corresponding to phosphocholine (Figure 23).

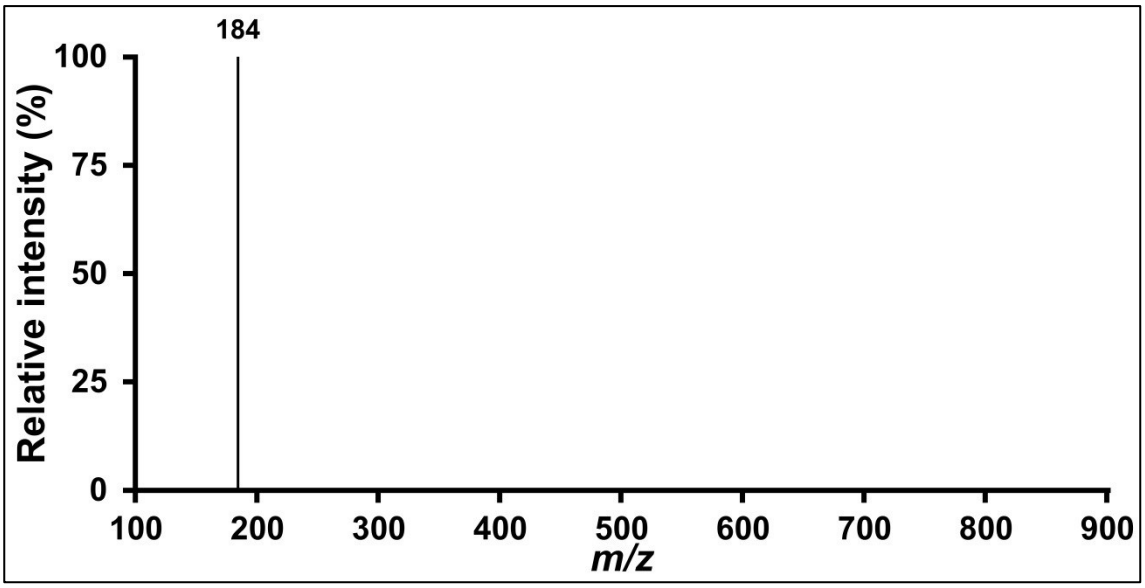

Figure 23: Tandem mass spectrum of $[SM\ 18:0+H]^+$ (*m/z* 731.60615).

Tandem mass spectrometry of the sodiated adduct (Figure 24) shows neutral losses of trimethylamine (-59 Da), phosphocholine (-183 Da), and sodiated phospohocholine (-205 Da), as well as *m/z* 147 (sodium salt of O,O'-dimethylenephosphoric acid).

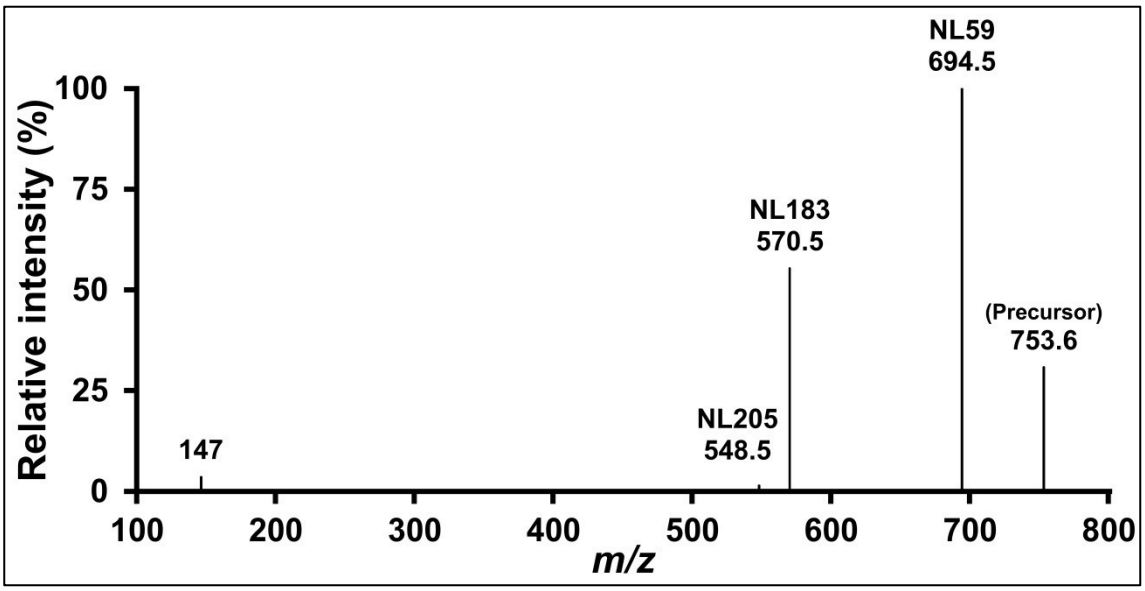

Figure 24: Tandem mass spectrum of $[SM\ 18:0+Na]^+$ (*m/z* 753.58810).

Formate adducts of SM in negative ion mode (Figure 25) show an unspecific neutral loss of formic acid next to demethylated phosphocholine at *m/z* 168, as well as very small fragment ions at *m/z* 123 (phosphoric acid ethyl ester), and sometimes *m/z* 449 (loss of two methyl groups of choline together with the N-linked fatty acyl.

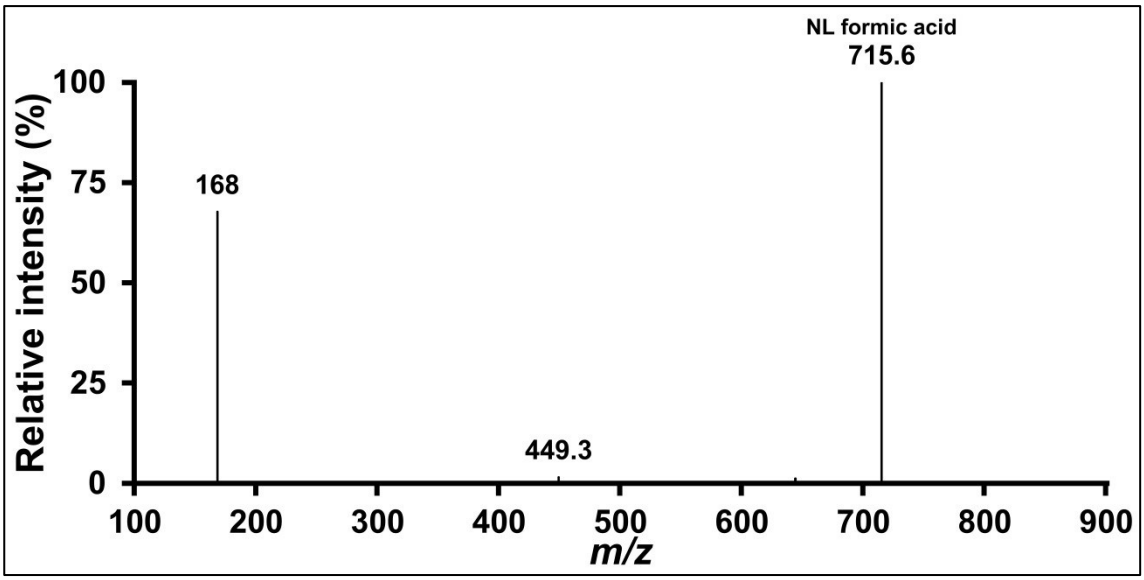

Figure 25: Tandem mass spectrum of $[SM\ 18:0+HCOO]^-$ (*m/z* 775.59708).

4.3.3.10 Cer

In positive ion mode, ceramides can be observed as protonated molecules or as sodium adducts. Around half of the protonated molecules spontaneously lose water, leading to dehydroxylated positive ions. In negative ion mode, Cer forms chloride adducts, formate adducts, or deprotonated molecules.

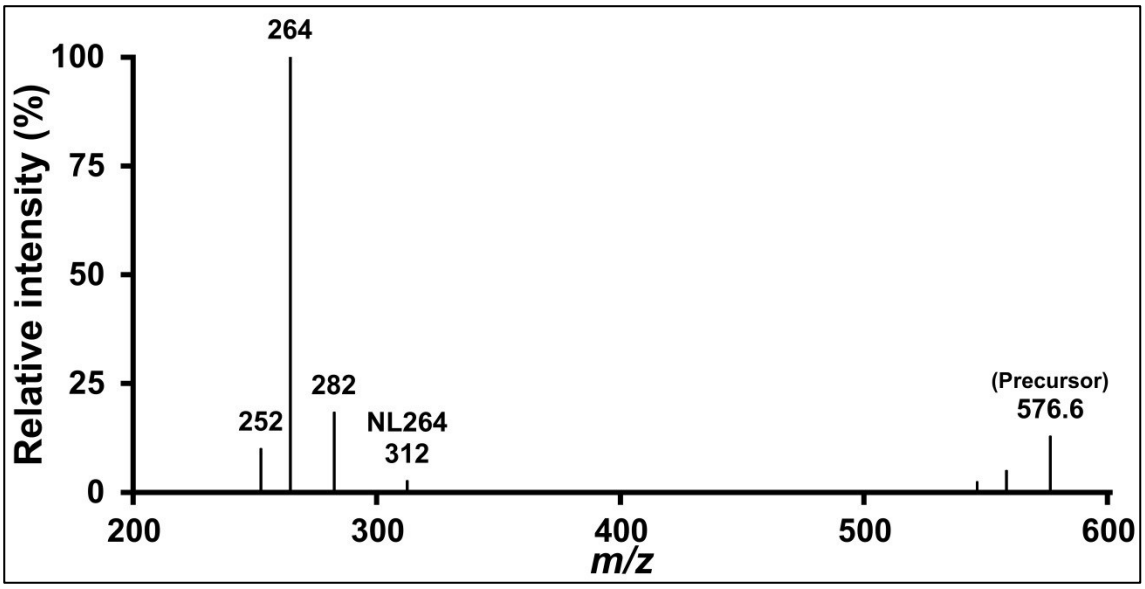

Figure 26: Tandem mass spectrum of $[Cer\ 20:0+H–H_2O]^+$ (*m/z* 576.57141).

The protonated molecule yields the "classical" ceramide fragments at *m/z* 282 and *m/z* 264 upon collisional activation, corresponding to cleavage of the amide bond and loss of one or two water molecules. The dehydroxylated positive ion (Figure 26) additionally shows an

ion at *m/z* 252 and a neutral loss of 264 Da (both indicative of the sphingoid backbone). The sodiated adduct yielded no indicative fragments under the experimental conditions employed.

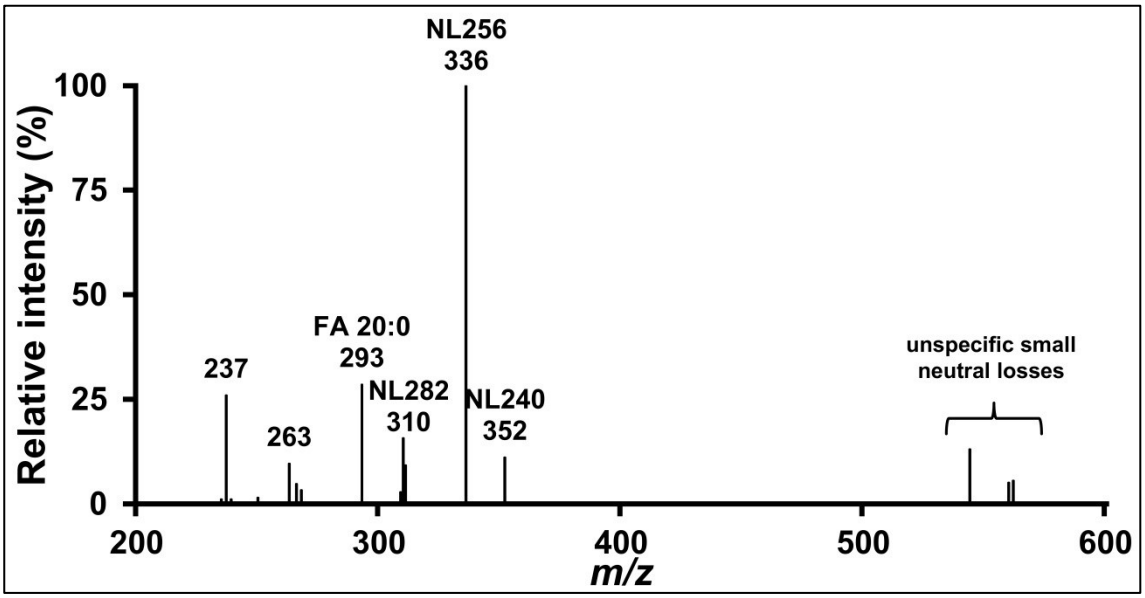

Figure 27: Tandem mass spectrum of $[Cer\ 20:0–H]^-$ (*m/z* 592.56742).

The chloride adduct in negative ion mode shows only an unspecific neutral loss of hydrochloric acid, and the MS^2 spectrum of the formate adduct is dominated by a loss of formic acid. Formate adducts and deprotonated molecules (Figure 27) additionally show multiple ions deriving from cleavages of both the sphingoid base and the amide-linked fatty acid. These are ions at *m/z* 237 and *m/z* 263 (charge remaining on the sphingoid part) and neutral losses of 240 Da, 256 Da, and 282 Da (charge remaining on the fatty acyl moiety). In the case of the formate adduct, formic acid is additionally lost as a neutral, yielding neutral losses of 286 Da, 302 Da, and 328 Da, respectively.

4.3.4 Identification

With this method, lipids are identified using three identification criteria. Firstly, high resolution mass spectrometry delivers the elemental composition of lipid molecular species with high confidence. Under the experimental conditions employed, mass resolution (FWHM) is routinely over 110 000 for lysophospholipids, over 80 000 for triacylglycerols, and over 70 000 for cardiolipins. Mass accuracy is usually well below 2 ppm, and far below 10 ppm even for low-abundance analytes. Retention time is another essential parameter for correct identification, as already explained in chapter 4.3.2, p. 31f. Since exactly the same chromatographic conditions are employed for positive and negative ion

mode, retention times for each lipid must be identical in both polarities. With the exception of glycerolipids (which do not form detectable ions in negative ion mode), all lipid classes investigated are detectable in both polarities. For additional selectivity and identification certainty, positive and negative chromatograms may be aligned (Figure 28) to exclude false positive results. Finally, tandem mass spectra, generated in parallel in the ion trap, may be inspected to obtain structural information, as detailed in chapter 4.3.3, p. 33ff.

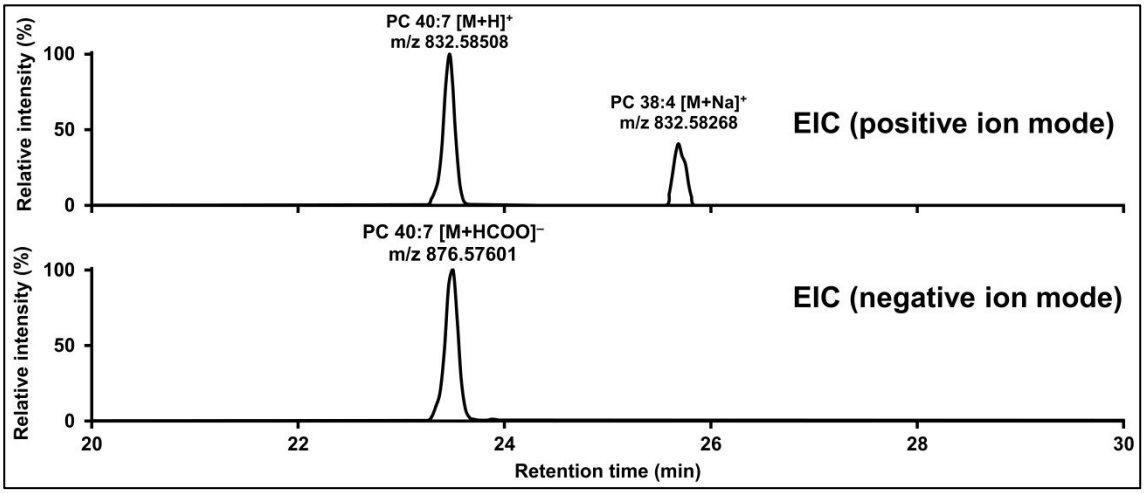

Figure 28: Extracted ion chromatograms (EIC) of PC 40:7 in positive and negative ion mode. The interference of the sodium adduct of PC 38:4 in positive ion mode cannot be mass separated due to minimal difference in *m/z* of only 0.0024 Da. EIC in negative ion mode confirms the retention time of PC 40:7.

Using the approach presented, literally hundreds of lipid molecular species can be identified from a single lipidomic sample. It is necessary to limit oneself concerning the number of lipid species for several reasons: Firstly, for almost all lipid classes, a small number of molecular species constitute the bulk of the total class amount. An in-depth analysis of TG in murine liver reveals that out of 375 candidate molecular species, the 18 most abundant species already represent over 90 % of the total TG amount, and 128 species represent over 99.9 % (Figure 29). The other molecular species, while numerous, contribute only negligibly to the total amount. For the class of PI this is even more pronounced, and only five out of 161 candidate molecular species represent over 95 % of total PI amount. This principle, termed the Pareto principle (Erridge 2006), can be found in many other fields of life (e.g. when writing a thesis, and 80 % of time invested is spent writing 20 % of the text). Another reason, why analysis of extremely low-abundance analytes in a global method is not recommended, is that accuracy often suffers at low

concentration levels. For targeted analysis of low-abundance components, specialized methods (such as for NAPEs, chapter 5) should be employed.

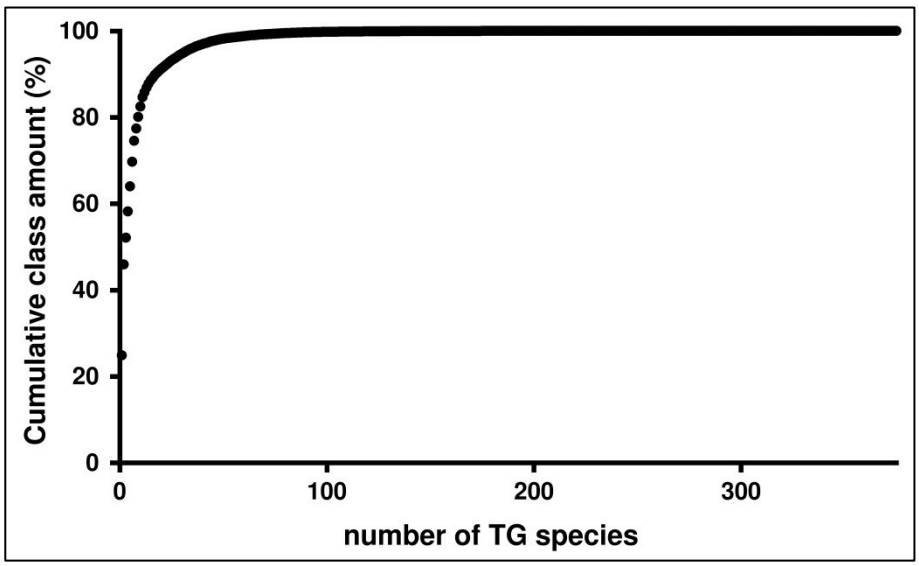

Figure 29: TG species and their contribution to total TG amount. Of 375 candidate TG species identified in murine liver, 18 species represent over 90 % of the total class amount. Most other lipid classes behave similarly, with a few molecular species constituting the major portion of the class.

For these reasons, a class-specific cut-off value of 1 % was chosen. For each lipid class, molecular species contributing a sum of less than 1 % to total class amount, were omitted from the analysis. For a global approach, this is a good compromise between comprehensiveness and time required for data analysis.

In total, 195 lipid species were identified in murine liver (58 glycerophospholipids, 106 glycerolipids, and 31 sphingolipids), while a total of around 350 lipid species were identified in *C. elegans* (see Figure 30 for overview and Supplementary Table 3, p. vii, Supplementary Table 4, p. xii, and Supplementary Table 5, p. xvii for complete results). This seemingly enormous difference in the number of species found is simply due to the fact that liver contains in its lipids predominantly fatty acyls with an even number of carbon atoms whereas lower organisms such as *C. elegans* contain a large amount of fatty acyls with an odd number of carbon atoms, thereby drastically increasing the number of lipid species by sheer combinatorial power.

The method presented is with its selectivity criteria strongly suited for lipidomic analyses at this level of complexity. Even for *C. elegans*, an enormously complex matrix, structural information including the identities and positions of fatty acyls about hundreds of lipids

can be gained in a single one-hour run. The only drawback is that the tandem mass spectra must be manually inspected as suitable automated solutions are not yet available.

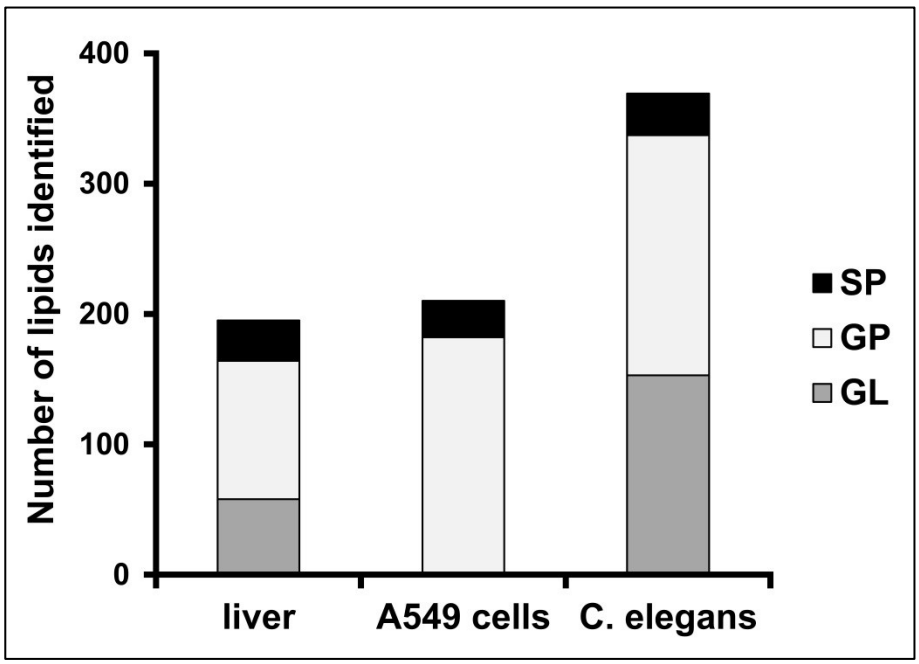

Figure 30: Number of lipid molecular species detected in murine liver, A549 cells and *C. elegans* embryos. GL: glycerolipids, GP: glycerophospholipids, SP: sphingolipids.

4.3.4.1 Structural isomers

One particular advantage of the chromatographic performance is the potential to separate structural isomers of lipids. Even-carbon PC are structural isomers of odd-carbon PE and vice versa, e.g. the internal standard PC 31:1 is a structural isomer of PE 34:1. Both have an elemental composition of $C_{38}H_{78}O_8NP$ and a molecular mass of 719.54651 Da, but differ in the chemical structure of the head groups and fatty acyl chains. While they cannot be separated based solely on their *m/z* value, chromatography causes these two phospholipids to elute at different times. Following the ECN model, PE 34:1 (ECN 32) elutes later than PC 31:1 (ECN 29) (Figure 31). Analogously, structural isomers of LPC and LPE (e.g. LPE 18:0 and LPC 15:0) are also chromatographically separated, with LPC 15:0 eluting well before LPE 18:0.

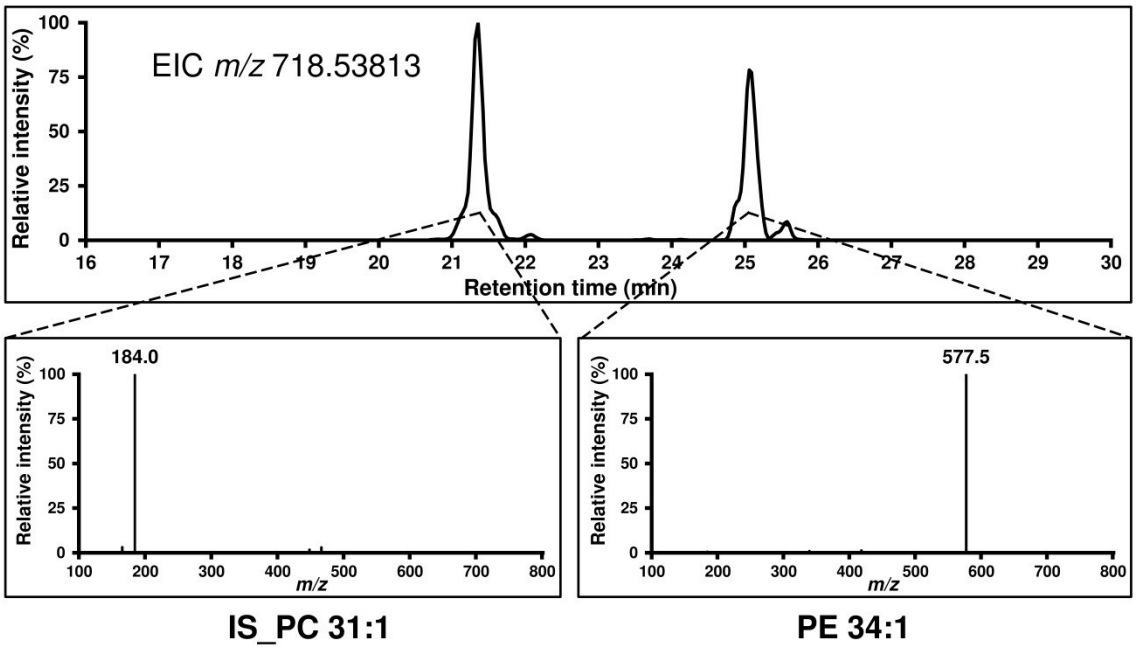

Figure 31: Separation of structural isomers belonging to different phospholipid classes. The internal standard PC 31:1 and the analyte PE 34:1 have identical molecular formula and therefore cannot be mass separated, but differ in retention time.

While chromatographic separation of structural isomers belonging to different lipid classes can be easily achieved, separation of isomers belonging to the same lipid class is a completely different and much more complex problem. The most relevant structural isomers within one phospholipid class are those with different fatty acyl constituents. The potential for complexity increases with the total length and number of double bonds in the lipid. For example, a phospholipid with 36 carbon atoms and four double bonds could consist of two 18:2 fatty acyls, one 18:1 and one 18:3 fatty acyl, or one 16:0 and one 20:4 fatty acyl chain – with all three of these combinations well within the expected range of biologically relevant fatty acyls. PE P-38:5 (Figure 32) shows three peaks which are clearly chromatographically separated (at 24.6, 24.9 and 25.3 min, respectively), as well as the peak originating from the second isotope of PE P-38:6 at 24.1 min.

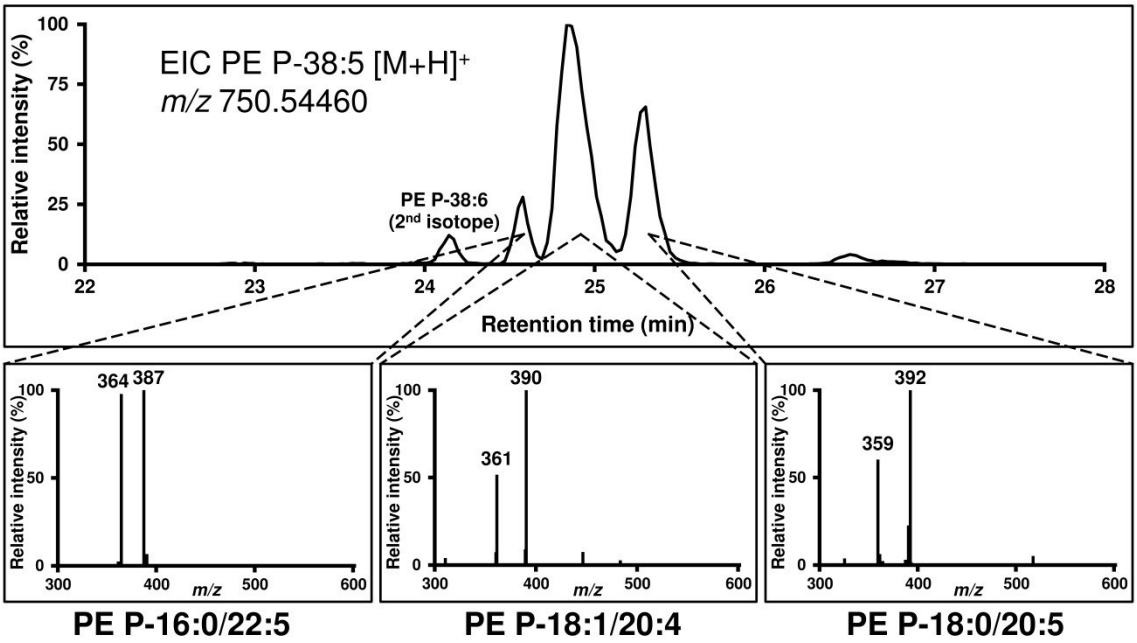

Figure 32: Structural isomers of PE plasmalogen species separated by chromatography. PE P-38:5 shows three chromatographic peaks corresponding to structural isomers differing in the alkenyl and acyl chains, as well as interference from the second isotope of PE P-38:6.

Manual inspection of the tandem mass spectra, described in detail in chapter 4.3.3.5, p. 42, and Table 1, p. 44, reveals that the three peaks belong to three different structural isomers, PE P-16:0/22:5, PE P-18:1/20:4, and PE P-18:0/20:5. Chromatographic separation of these peaks allows for separate analysis and quantitation, if necessary. Many other phospholipids and glycerolipids also show structural isomers that are either partially or completely chromatographically separated. However, not all structural isomers are baseline separated by chromatography and often one peak consists of multiple underlying structural isomers differing in fatty acyl composition.

It is noteworthy that structural isomers of phospholipids possess characteristic retention behaviour. In many cases, fatty acyl structural isomers are split into either two fatty acyls of similar length and degree of unsaturation (e.g. 18:2/18:2) or two fatty acyls differing distinctly in length and degree of unsaturation (e.g. 16:0/20:4). Figure 33 shows retention behaviour of PC molecular species with 36 carbon atoms and 1-5 double bonds. Fatty acyl structural isomers with two similar fatty acyls generally elute before those with different fatty acyls, with the extent of the chromatographic separation increasing with the number of double bonds.

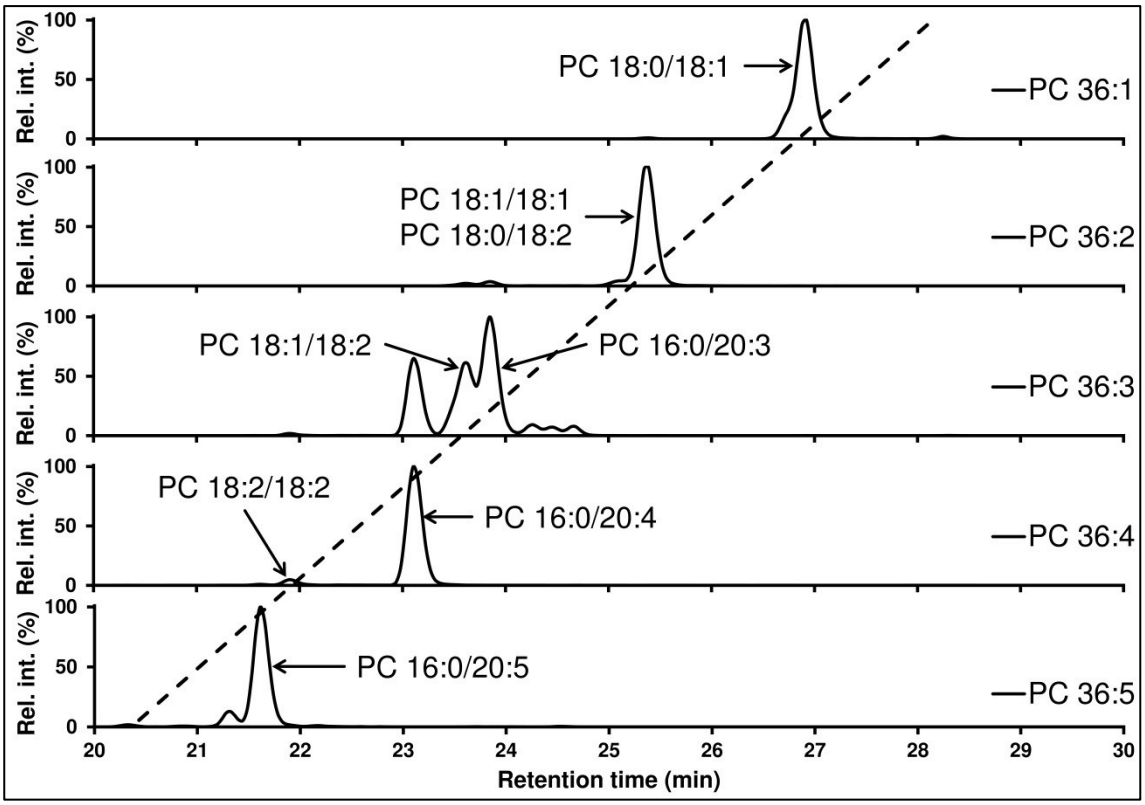

Figure 33: Retention behaviour of PC structural isomers. Homologous molecular species with two fatty acyls with 18 carbon atoms elute predictably along the dashed line, whereas the molecular species with fatty acyls containing 16 and 20 carbon atoms are clearly separated chromatographically and elute later.

4.3.4.2 Positional isomers

Many lysophospholipids show double peaks (Figure 34) These are most likely positional isomers or regioisomers, an observation consistent with published observations (Creer & Gross 1985; Murph et al. 2007; Lee et al. 2011; Koistinen et al. 2015). While the tandem mass spectra of both peaks show the same fragment ions (*m/z* 184 corresponding to protonated phosphocholine, and the water loss from the protonated parent ion), the intensity relationships of these two fragments are distinctly different. While the tandem mass spectra at the retention time of the first, smaller peak show a higher signal of *m/z* 184 compared to the neutral loss of water, the second peak shows the same fragment ions but with opposite intensity relationships – the neutral loss of water is of higher relative intensity than *m/z* 184. As previously shown (Lee et al. 2011), this indicates that the first peak belongs to the positional isomer with the acyl group at the *sn*-2 position (LPC 0:0/17:1, and LPC 0:0/18:1, respectively), while the second chromatographic peak belongs to the positional isomer with an *sn*-1 acyl chain (LPC 17:1/0:0, and LPC 18:1/0:0, respectively). In negative ion mode, there is also a clear difference between the tandem

mass spectra of the two peaks. While the tandem mass spectra of both peaks are dominated by the neutral loss of formic acid, the fatty acyl carboxylate anion (*m/z* 267 and *m/z* 283, respectively) gives a higher signal for the proposed *sn*-1 species.

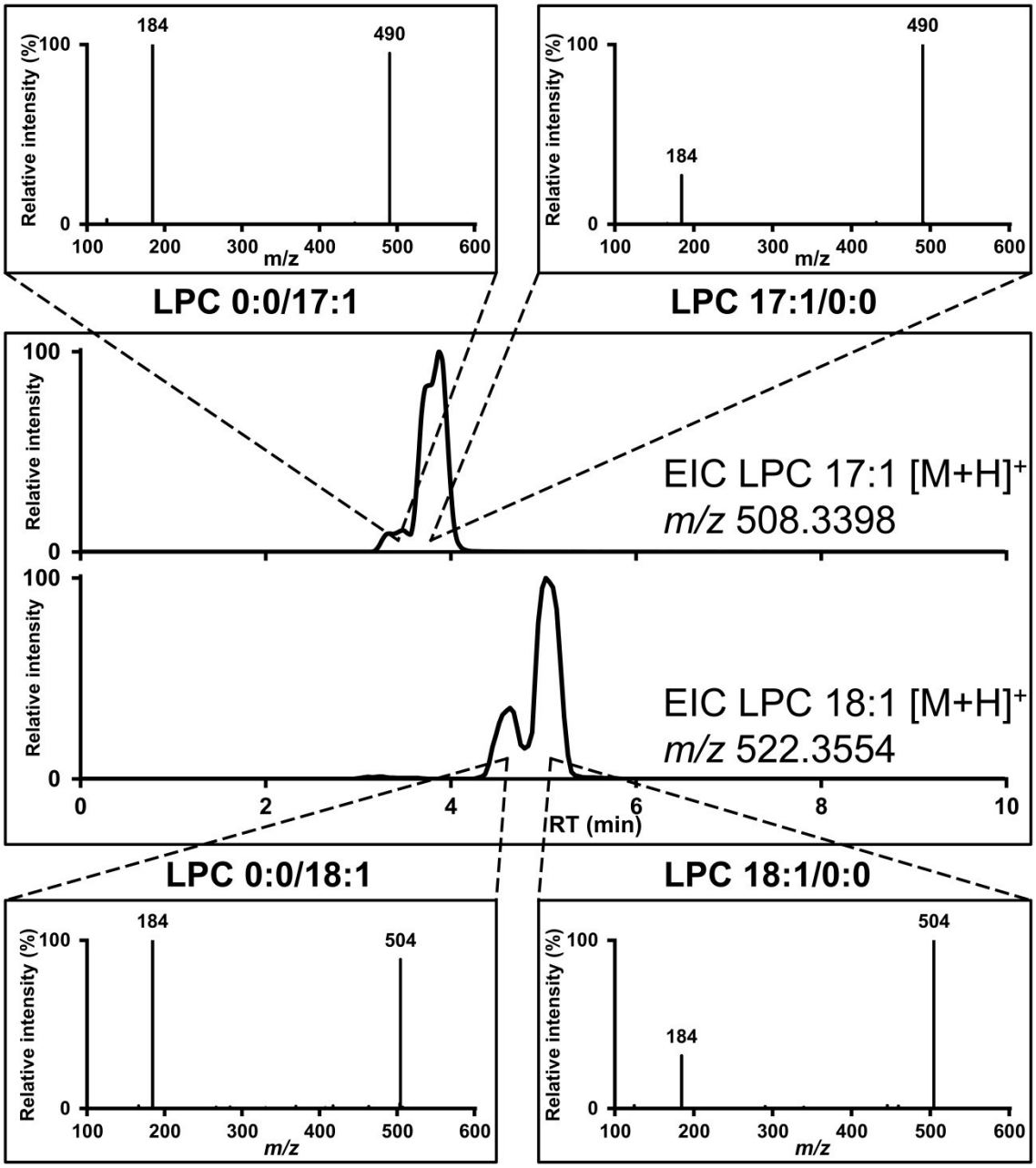

Figure 34: LPC regioisomers. Both internal standard LPC 17:1 and analyte LPC 18:1 show two chromatographically separated peaks as well as differences in the relative intensities of the two major fragment ions. Both tandem mass spectrometric and retention behavior conform to existing literature concerning lysophospholipid regioisomers.

The identification of LPC positional isomers is confirmed by the fact that the internal standard LPC 17:1 is certified to be a mixture of regioisomers (Avanti Polar Lipids n.d.).

The exact relative amount varies with batch number, but LPC 17:1/0:0 is generally more abundant than LPC 0:0/17:1, which is consistent with the positional assignment of the regioisomers based on retention behaviour and tandem mass spectra.

These putative positional isomers are also observable for LPE, with the tandem mass spectrum of the first, smaller peak most likely corresponding to the *sn*-1 regioisomer, showing a stronger head group fragment ion (neutral loss of 141 Da), while the tandem mass spectrum of the second, larger peak is dominated by the water loss from the protonated molecule.

It should be noted however, that lysophospholipid regioisomers are known to undergo spontaneous non-enzymatic intramolecular acyl migration, depending on exact storage conditions (Okudaira et al. 2014), a chemical phenomenon also encountered during synthesis of enantiomerically pure standards (D'Arrigo & Servi 2010). The regioisomers with the acyl chain at the *sn*-1 position have been found to be much more stable in solution, and thus, great care should be taken when identifying and quantifying lysophospholipid regioisomers to avoid that findings are results of artefacts.

Some positional isomers of diacyl phospholipids may also be minimally separated, but for all cases studied, the separation is by no means sufficient for separate analysis. E.g. PC 18:0/18:1 and PC 18:1/18:0 have a difference in RT of 0.1 min, but the individual peaks have a width of 0.8 min (controlled experiment performed with regioisomerically pure standards and a brand new chromatographic column), and they are not sufficiently separated chromatographically. It is also extremely difficult, if not impossible, to distinguish a mixture of regioisomers based solely on tandem mass spectra, since the relative abundance of the fatty acyl-derived fragment ions is always subject to some variation. Analysis of positional isomers of diacyl phospholipids and glycerolipids is therefore not possible with the presented method and remains a problem tackled only by specialized separation methods, such as silver-ion chromatography or ion mobility (Lisa et al. 2009; Groessl et al. 2015).

4.3.5 Method validation

The method was validated for murine liver, a representative sample matrix for lipidomic measurements. While the method has not specifically been validated for other sample matrices, it is reasonable to assume that attributes such as linear range or limits of quantitation are comparable. For each lipid subclass, one molecular species (occurring

non-naturally or only in small amounts) was chosen for validation purposes and the corresponding lipid standard was added. Obviously this is a compromise, as parameters such as ionization efficiency, matrix effect, etc., may still be different for other molecular species of the same lipid class. Table 2 lists validation parameters for all lipid classes evaluated.

Table 2: Validation data for lipids in positive and negative mode, determined for one molecular species per lipid class. The lower limit of quantitation (LLOQ) was conservatively determined because of the minimal but detectable natural abundance of the measured analytes. n=5; Accuracy (Acc.) and precision (Prec.) were determined at concentrations of 1 µM.

Lipid species	type of ion	LLOQ (fmol on column)	Linear range (µM)	R^2	Acc. (%)	Prec. (%RSD)
TG 51:0	$[M+NH_4]^+$	100	0.05–7.5	0.9874	-5	1.9
DG 24:0	$[M+NH_4]^+$	100	0.05–10	0.9918	-99	5.2
PC 24:0	$[M+H]^+$	10	0.005–25	0.9981	15	1.7
	$[M+HCOO]^-$	10	0.005–25	0.9886	13	0.9
PE 24:0	$[M+H]^+$	10	0.005–100	0.9957	-9	2.1
	$[M-H]^-$	10	0.005–10	0.9955	21	3.6
PS 24:0	$[M+H]^+$	10	0.005–100	0.9981	20	1.7
	$[M-H]^-$	10	0.005–100	0.9976	26	1.6
PG 24:0	$[M+H]^+$	100	0.05–100	0.9982	-10	1.6
	$[M-H]^-$	10	0.005–100	0.9945	22	0.8
LPC 15:0	$[M+H]^+$	10	0.005–25	0.9954	19	1.6
	$[M+HCOO]^-$	20	0.01–100	0.9939	2	1.0
Cer 17:0	$[M-OH]^+$	10	0.005–10	0.9867	12	2.8
	$[M-H]^-$	100	0.05–10	0.9940	-20	2.1
SM 17:0	$[M+H]^+$	20	0.01–50	0.9968	21	2.4
	$[M+HCOO]^-$	100	0.05–10	0.9940	-10	1.8

4.3.5.1 Linearity

The upper limit of the linear range of electrospray ionization is frequently cited as 10 µM (Cech & Enke 2001; Zook & Bruins 1997; Tang et al. 2004), although this clearly is not a constant, but rather depends on the exact parameters and the analytes measured. Linearity was evaluated for nine lipid classes (TG, DG, PC, PE, PS, PG, LPC, SM, Cer), using one representative molecular species per lipid class by spiking a liver extract to concentrations ranging from 1 nM to 100 µM. While multiple adduct ions per class in both polarities were monitored (except for glycerolipids, which do not form detectable negative ions), only one type of ion, usually the most abundant ion (see also Table 2), was chosen for quantitation in each polarity.

Linearity was conservatively estimated for each analyte, chosen as the broadest concentration range giving a coefficient of determination (R^2) of 0.99 or higher. Many analytes investigated exhibit some sort of saturation effects at higher concentrations, with the gravity of this effect differing hugely between classes: While TGs show drastic saturation effects above medium concentrations (above 7.5 µM), the saturation effects for PC (observed for concentrations above 25 µM) are almost negligible (Figure 35), and protonated and deprotonated forms of PG show excellent linearity over the whole concentration range investigated ($[M+H]^+$, R^2=0.9989; $[M–H]^–$, R^2=0.9945). For most analytes, sodiated adducts show saturation effects above medium concentrations, in contrast to protonated or deprotonated forms. This may be explained by the fact that the sodium ions, present as ubiquitous impurities, are only available for adduct formation in limited numbers, so that only a certain number of sodium adducts can be formed, while protons (for formation of protonated molecules) are of far greater abundance.

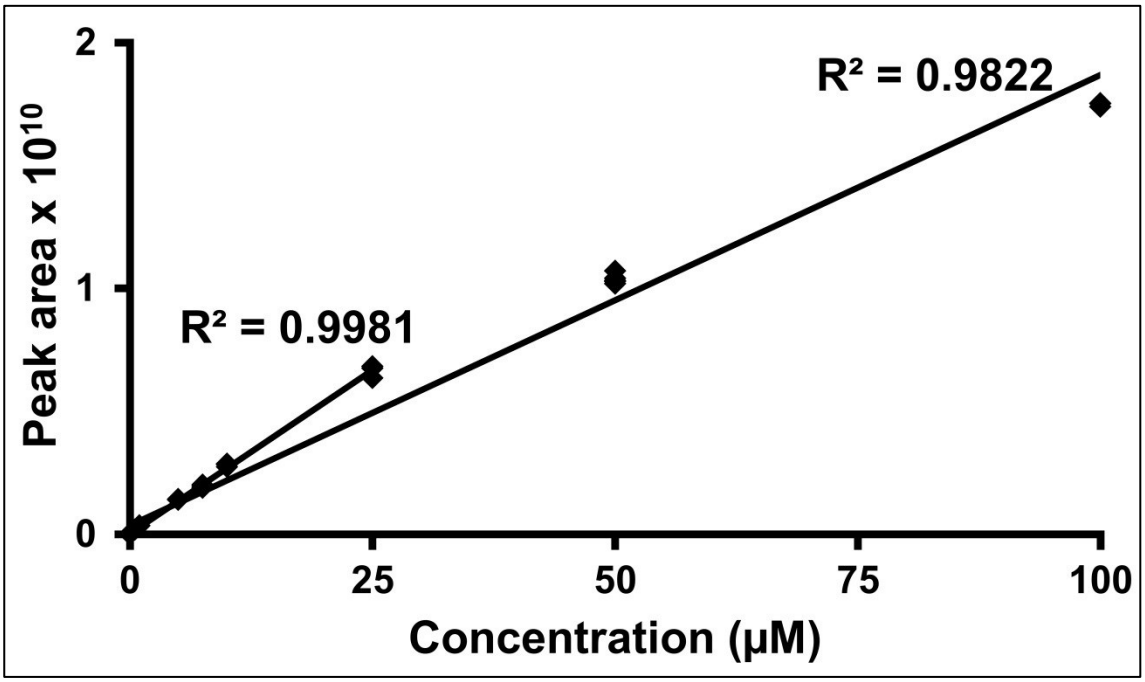

Figure 35: Linearity of PC 24:0 $[M+H]^+$. Linear regression is calculated for the linear range, given as 0.005-25 µM (R^2=0.9981), and over the whole concentration range investigated (R^2=0.9822). The saturation effect at higher concentrations is observable, but not drastic. Graph shows data from three replicates per concentration point.

Whenever absolute quantitation is performed, it is essential to be aware of the limitations in linear range, and analytes should not be quantified if their concentrations are well outside the proven linear range. However, in cases such as for protonated PC (Figure 35),

while the linear range is given as 0.005-25 µM, quantitation up to a concentration of 100 µM would still be justified.

4.3.5.1.1 TG

Triacylglycerols (detected as ammonium and sodium adducts) show a very strong saturation effect at concentrations above 7.5 µM. Indeed, the responses at concentrations of 7.5 µM, 50 µM, and 100 µM differ only by 20 %. This saturation effect may be explained to a certain degree by the limited amount of both ammonium or sodium ions necessary for adduct formation (which can be viewed as a form of ion suppression, since the TG 51:0 standard used for validation elutes approximately at the same retention time as other major TGs).

4.3.5.1.2 DG

The drastic saturation effects found for TGs could not be observed for DGs, which show acceptable linearity over the whole concentration range. However, the reason for DG exhibiting better linearity than TG may still be due to the fact that the DG standard used for validation (DG 24:0) is chromatographically separated from all other major compounds, and therefore does not suffer from matrix effect as much as TG; i.e., more sodium and ammonium ions may be available for adduct formation at the retention time of DG than of TG.

4.3.5.1.3 PC

Phosphatidylcholines, detected as protonated molecules and formate adducts in positive and negative ion mode respectively, show overall good linearity from the low nanomolar range to medium micromolar range (5 nM-25 µM). At higher concentrations (25-100 µM), both adducts show only mild saturation effects and quantitation in this range would still be well justifiable. Sodium adducts in positive ion mode show distinct saturation effects at concentrations over 25 µM.

4.3.5.1.4 PE

The protonated form of phosphatidylethanolamine was found to be linear over the whole concentration range investigated, while the deprotonated molecule shows mild saturation effects above 10 µM. Sodium adducts in positive ion mode show strong saturation effects at concentrations over 10 µM.

4.3.5.1.5 PS

Phosphatidylserine exhibits almost perfect linearity in both polarities over the whole range investigated.

4.3.5.1.6 PG

Protonated and deprotonated forms of phosphatidylglycerol, as well as the sodium adduct show excellent linearity over the whole concentration range in both polarities.

4.3.5.1.7 LPC

Lysophosphatidylcholine is comparable to the diacyl form concerning linearity, with only mild saturation effects over 25 µM for the protonated molecule. In negative mode, both the formate adduct and demethylated LPC show very good linearity over the whole concentration range investigated.

4.3.5.1.8 Cer

Ceramides were investigated in positive mode as their protonated, dehydroxylated and sodiated forms. In negative mode deprotonated molecules as well as chloride and formate adducts were observed. All types of ions show saturation effects above medium concentration levels, but the highest abundant adducts ($[M–OH]^+$, $[M–H]^–$) exhibit very good linearity up to 10 µM.

4.3.5.1.9 SM

Sphingomyelin shows good linearity up to medium concentrations for both the protonated molecule in positive ion mode and the formate adduct in negative ion mode. Some saturation effects are observable at concentrations above 50 and 10 µM in positive and negative ion mode respectively.

4.3.5.2 Limits of quantitation

While the upper limit of quantitation (ULOQ) is easily determined as the upper limit of the linear range, determination of the lower limit of quantitation (LLOQ) proved to be more difficult. This is due to the fact that practically all of the lipid molecular species employed for method validation can be found in a non-spiked sample. The short-chain or odd chain lipid molecular species investigated (e.g. 12:0/12:0 diacyl phospholipids or 17:0/17:0/17:0 TG) obviously occur in very small, but clearly detectable amounts in biological systems (while carry-over, contamination from the injection system, can be

ruled out). Therefore, the LLOQ for each lipid subclass was determined as the concentration level for which the response more than doubled when compared to the next-lower concentration level (For an example, see Figure 36).

For most lipid classes investigated, this approach results in values for LLOQ of around 5 nM, underlining the sensitivity of the method. The limit of detection (LOD) is much lower, but cannot be determined.

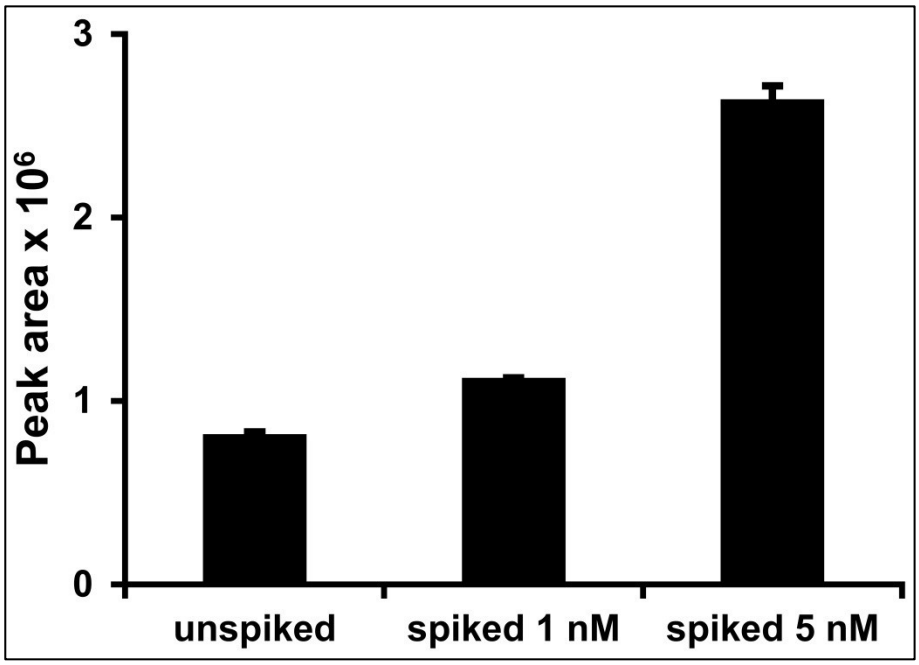

Figure 36: Determination of LLOQ for $[PC+H]^+$. LLOQ was determined as the concentration level for which the response was higher by a factor of >2 than the previous concentration level. Here, the LLOQ is 5 nM. Data shows means +/- SD from triplicate measurements.

4.3.5.3 Matrix effect

The matrix effect is a well-known phenomenon in LC-ESI-MS. Generally, it is the change in response when an analyte is measured within a matrix context, as opposed to the analyte being measured alone. A matrix is the plethora of small molecules, electrolytes and all other compounds present in a biological fluid, tissue, etc. The matrix effect may manifest itself as either an increase or a decrease in the response of analytes – signifying either ion enhancement or ion suppression (Cappiello et al. 2008). While there are many suggested explanations for ion suppression, most of them are closely related to the physicochemical properties of electrospray ionization, such as competition for available charges, change of surface tension and viscosity of the electrospray droplets, ion-pairing with sample

components, etc. (Annesley 2003), ion enhancement is not fully understood, but nevertheless an undeniable fact (Trufelli et al. 2011).

Many ways to overcome or at least minimize the matrix effect have been proposed. This includes improving sample preparation to eliminate as many interfering compounds as possible, e.g. via SPE, chromatographic separation prior to ESI-MS detection, optimization of ESI conditions, standard addition, or the internal standard approach (Trufelli et al. 2011). See also the next chapter for details about the difficulties in selecting suitable internal standards for lipidomic analyses.

For this method, the matrix effect was evaluated by analysing the internal standard mixture alone and additionally spiked into the three biological matrices (murine liver, A549 cells, and *C. elegans* lipid extracts, respectively). Figure 37 shows an example of graphical evaluation of the matrix effect for PE and PS internal standards in liver. While the responses of the PE internal standards are not substantially altered by presence of the liver matrix, the signal of the PS internal standards is drastically decreased due to ion suppression by matrix components.

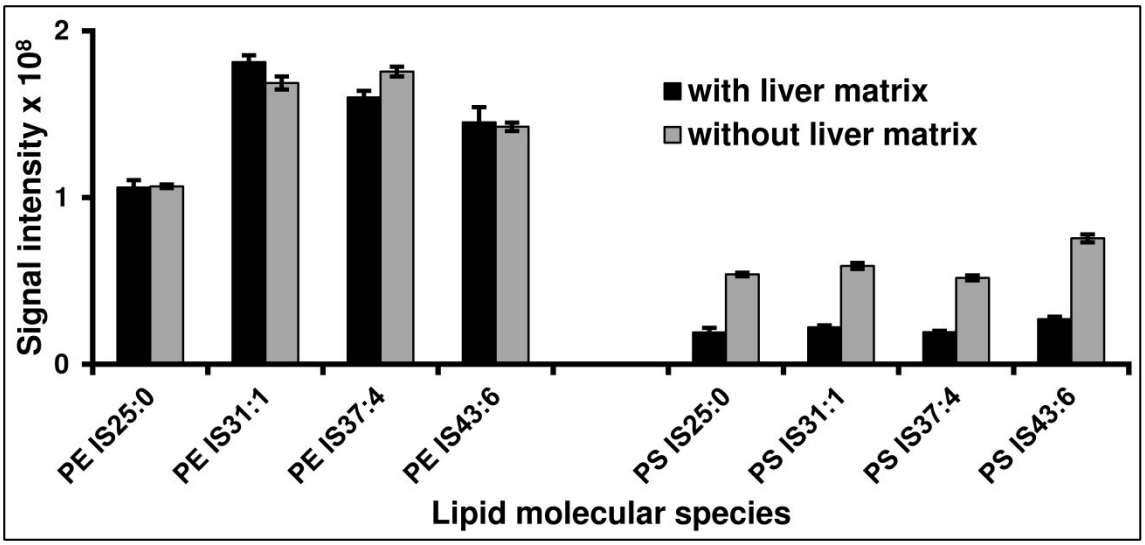

Figure 37: Matrix effect. While the response of PE molecular species barely decreases when analysed together with matrix, the signal of PS molecular species decreases substantially due to ion suppression.

For many lipid classes evaluated, the matrix effect is within an acceptable range (below 20 %), with only PS, PI, PG, and DG showing drastic ion suppression effects.

Another point to be considered is the difference in response between different molecular species of the same lipid class. It has been shown that this can be caused merely by differences in chain length and number of double bonds (Koivusalo et al. 2001). This

effect is particularly drastic for DGs: The 9 deuterated DG internal standards differ in their response by as much as 98 % (Figure 38). Different ionization efficiency due to varying chain length and number of double bonds is not the only evident reason for this. Solvent composition, which has a major influence on electrospray ionization behaviour, also changes substantially during elution of diacylglycerols, which alone can cause differences in response.

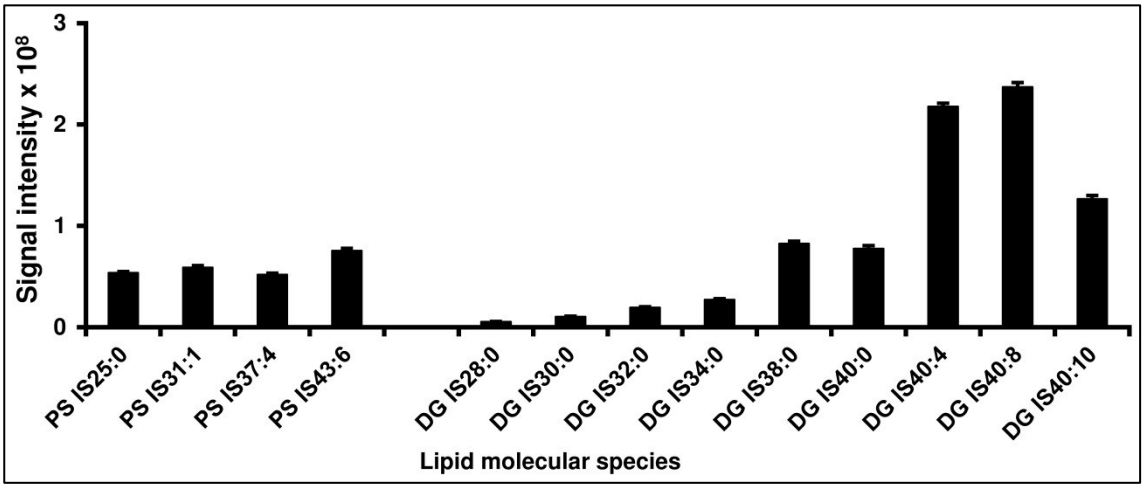

Figure 38: Differences in response for lipid molecular species of varying chain length and number of double bonds. While the response of PS molecular species is fairly constant, DG molecular species exhibit grave differences in response, although all compounds were analysed at the same concentration (5 µM).

Together, these two effects result in grave differences in response of the DG internal standards, despite identical concentration. However, this is a problem strictly limited to the class of DG. The difference in response between different molecular species of one lipid class is much less pronounced for TG and almost non-existent for PS and other phospholipid classes.

4.3.5.4 Accuracy and precision

Accuracy is the ability of an analytical method to correctly determine the measured value, while precision is the ability to perform these measurements reproducibly and with only minor deviation between replicate measurements. Both are essential parameters of an analytical method (Kromidas 2011).

Accuracy and precision were determined at a concentration of 1 µM. Despite the previously mentioned difficulties caused by matrix effect and varying ionization efficiency, the method generally delivers very good values for accuracy, with only DG

showing an error of more than 25 %. Precision, expressed as relative standard deviation of the calculated values, is excellent throughout, with an overall average RSD of only 3.4 %.

4.3.6 Common difficulties in lipidomic quantitation

Classical quantitative analysis, widespread in other fields such as pharmacological analysis, is not possible in the field of lipidomics as it calls for a calibration curve by spiking known amounts of an analyte to a matrix containing all sample components except for the analyte to be quantified (Kromidas 2011). While this approach may work well for exogenous compounds such as drugs, it is obvious that it is not possible when endogenous substances of detectable natural abundance are to be measured. Surrogate matrices (e.g. protein/electrolyte solutions mimicking body fluids) are only a mild compromise, since the complexity of the plethora of metabolites found in serum, cells or tissues is difficult, if not impossible, to imitate. External calibration without matrix is also error-prone, since all matrix effects are simply ignored. For these reasons, almost all quantitation in lipidomic measurements is performed using internal standards.

Generally, the prerequisites for internal standards are that they are undetectable in the sample to be measured, that they can be measured independently of the analyte, and that their chemical behaviour is similar to the analyte. They should also be added in the same concentration range as the analyte. The optimum choice for internal standards is almost always a stable isotope marked isotopologue of the analyte (usually deuterated or ^{13}C-labeled). However, in lipidomics, this would require a stable isotope labeled lipid species for every analyte. It is clear that this is simply not feasible if dozens or even hundreds of lipids are to be quantified.

For reasons of availability and economics, internal standards in lipidomics are usually lipid molecular species which do not occur in the biological matrix, or occur only in very small amounts,. These are often lipids with very short or very long fatty acyl chains, e.g. 12:0/12:0 or 24:0/24:0 diacyl phospholipid species. Since mammalian biological samples contain almost exclusively fatty acyl chains with an even number of carbon atoms, odd-carbon numbered fatty acyl chain lipid species (e.g. 37:4 diacyl phospholipids) are a good choice as internal standards. In this work, lipids were quantified using LIPID MAPS quantitative internal standards (Supplementary Table 2, p. vi). It should however be noted that mammals do contain odd-carbon fatty acyls within lipids (see detailed results in Supplementary Table 3, p. vii, and (Jenkins et al. 2015)), although these occur only in very low amounts. While this does not falsify quantitative results, as the internal standards are

added at concentrations much higher than the natural abundance, it does preclude these molecular species from quantitation.

While the use of quantitative internal standards containing odd-carbon fatty acyl chains is a reasonable approach for eukaryotic systems, it fails when the organism of interest contains high amounts of odd-carbon fatty acyls – as is the case for *C. elegans*. Indeed, for some lipid classes, even the most abundant molecular species is an odd-carbon species in *C. elegans* (Matyash et al. 2008). The "usual" internal standards used for quantitation (e.g. 17:1 LPC, 37:4 diacyl phospholipids etc.) cannot be used, as they already occur as highly abundant analytes. As a compromise, 25:0 diacyl phospholipid species were used for quantitation of diacyl- as well as for lysophospholipids. To evaluate the feasibility of this approach, the *C. elegans* sample was measured with and without addition of the internal standards. The addition of the internal standards covers the natural abundance by a factor of over 100, and thus, the natural abundance does not negatively influence the results.

Appropriate quantitative internal standards are also not available for all lipid subclasses. E.g., there are no suitable LIPID MAPS internal standards for LPE, LPS, and ether phospholipids. The only solution here is to quantify lysophospholipids with short chain diacyl species (25:0 diacyl phospholipids) and ether lipids with diacyl species. Indeed, the response of ether lipids does not differ substantially from that of diacyl lipids. This was tested for PE P-36:1 and PC P-36:1, which were found to be within 20 % of the respective 36:1 and 36:2 diacyl species in both polarities.

Quantitation in lipidomics therefore relies heavily on the selection of a suitable internal standard which it is almost always a compromise. Therefore it is essential to be aware of the pitfalls of lipidomic quantitation. Great care should be taken when comparing results generated through different measurement or quantitation methods. If quantitation is performed using external calibration, the results may differ strongly from results obtained through an odd-carbon internal standard, or a stable isotope-marked internal – even when quantifying the same analyte in the same sample. Therefore, even when absolute amounts are reported, quantitation in the field of lipidomics is at best considered semi-quantitative, and its value and significance lies in comparing multiple groups, such as physiological/developmental states, wild-type vs. knockout, treatment vs. control, etc., all measured with the same method. Additionally, the use of quality control samples is strongly encouraged.

4.4 Conclusion

A method for global and comprehensive analysis of the lipidome is the cornerstone of every laboratory dedicated to lipidomics, since untargeted lipidomic analysis is always a first step toward elucidating the role of lipids in health and disease. Therefore, such a method needs to be readily adaptable and applicable to the wide range of lipidomic model organisms and sample matrices, as well as being able to analyse the majority of all lipids present in biological systems. The method presented fulfils these criteria, making it a prime choice for untargeted lipidomic analysis.

An easy sample preparation procedure, based on liquid-liquid extraction, is able to separate lipids from proteins, salts and other sample components. It has been applied, with only minor modifications, to a wide variety of tissues and fluids of human and animal origin, as well as to other, more exotic samples, such as cell culture. The extraction method substitutes cancerogenic chloroform with methyl-*tert*-butyl ether, which has the additional benefit of simplified sample handling, as the organic phase forms the upper of two phases.

The chromatographic method used is able of impressive performance. It separates lipid species based on their overall hydrophobicity, determined mainly by the number of carbon atoms and double bonds in the fatty acyl chains. Additionally and very importantly, it is able to chromatographically separate structural isomers of phospholipids and glycerolipids differing in fatty acyl composition, as well as positional isomers of lysophospholipids, allowing for separate quantitation if necessary.

While lipid species are identified and quantified using information from high resolution accurate mass full scans, additional structural information is obtained from tandem mass spectra automatically generated in parallel. To gain deeper insight into the tandem mass spectrometric behaviour of lipids, a multitude of synthetic standards were subjected to fragmentation in controlled experiments and the resulting fragment ions were analysed. Using this knowledge, in-depth structural information, such as the fatty acyl constituents and even their *sn*-positions within lipids can be obtained for literally hundreds of phospholipids, sphingolipids, and glycerolipids in a single one hour run.

Method validation showed good values for linearity and for accuracy and precision in the biologically relevant concentration ranges. Knowledge of the matrix effect and the importance of selecting suitable internal standards additionally aid in avoiding the pitfalls of lipidomic quantitation.

Taken together, this method is suitable for large-scale untargeted lipidomic analysis of a variety of sample matrices relevant to lipidomic research. It is capable of delivering quantitative performance, as well as in-depth structural information about lipids thus fostering further advances in the lipidomic field.

5 ANALYSIS OF N-ACYLPHOSPHATIDYLETHANOLAMINES

5.1 Introduction

N-acylphosphatidylethanolamines (NAPEs) are triacylated phospholipids (Figure 39), generated by N-acylation of a PE molecule (Wellner et al. 2013). This reaction is catalysed by N-acyltransferase, which transfers a fatty acyl chain from a PC molecule onto the amino group of a PE molecule. NAPEs are primarily degraded by NAPE-PLD, a Ca^{2+}-dependent enzyme with phospholipase D activity, generating N-acylethanolamine (NAE). Alternative catabolic pathways are via a NAPE-selective hydrolase with phospholipase 1/2 activity, or generation of diacylglycerol (DG) and phospho-NAE by an enzyme with phospholipase C activity (Wang & Ueda 2009; Ueda et al. 2013).

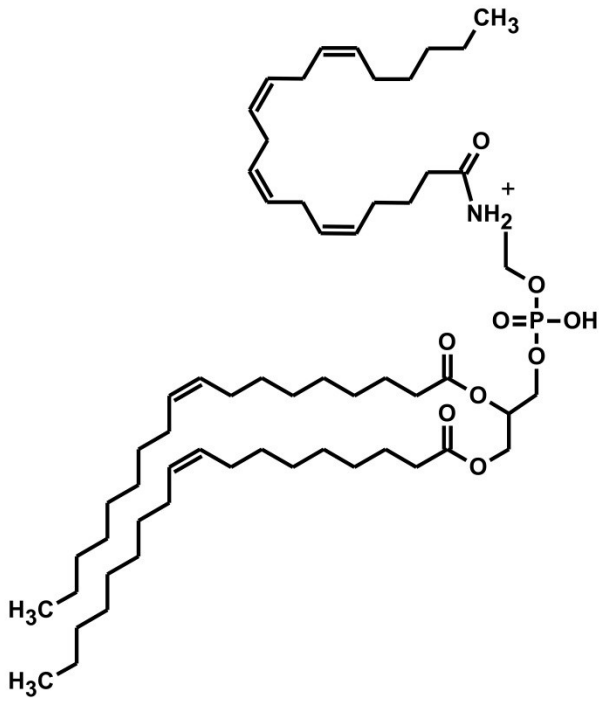

Figure 39: N-acylphosphatidylethanolamine (NAPE). Shown here is protonated PE 18:1/18:1-N-20:4. An additional fatty acyl is linked to a PE molecule via the head group nitrogen.

The degradation products of NAPEs, NAEs, exert a wide variety of biological effects. Among them are control of food intake, inflammation, pain sensation and neuroprotection (Hansen & Diep 2009). NAPEs themselves are speculated to have multiple biological functions themselves. Increase of NAPEs after neuronal damage may indicate a neuroprotective function (Hansen et al. 2008; Janfelt et al. 2012; Guan et al. 2006; H. S.

Hansen et al. 2000; H. H. Hansen et al. 2000), while postprandial increase of NAPE levels suggests an anorectic role (Gillum et al. 2008; Wellner et al. 2011).

Tissue levels of NAPEs are extremely low, in the range of a few nmol/g (Wellner et al. 2013), and analysis of NAPEs requires specialized approaches concerning sample preparation and LC/MS analysis, as they are usually not covered by "comprehensive" lipidomic approaches (Fauland et al. 2011; Kim & Hoppel 2013; Lísa & Holčapek 2015; Almeida et al. 2015). Hence, NAPEs are usually analysed by specialized sample preparation and mass spectrometric methods: After hydrolysis of the ether-bound fatty acyls at the *sn*-1 and *sn*-2 position, the resulting glycerophospho-NAE species may be measured, either by LC/MS, GC/MS or HPLC coupled to fluorescence detection (H. H. Hansen et al. 2000; Guo et al. 2010; Cadas et al. 1997; Schmid et al. 1997; T Sugiura et al. 1996). The drawback of these methods is that they group all NAPE species with one N-acyl chain together without the potential to analyse individual molecular species. Full scan approaches or SIM-based methods (Janfelt et al. 2012; Guan et al. 2006) are only able to deliver the elemental composition with no possibility to identify any of the acyl chains.

Here we present an approach for selective quantification of NAPE species, using a combination of LLE and SPE for sample purification. Reversed phase chromatography and detection with two SRM transitions per analyte ensure routine identification of both the N-acyl chain and the PE moiety with highest selectivity and sensitivity.

5.2 Materials and methods

5.2.1 Synthesis of NAPE

Due to the very limited commercial availability of NAPE molecular species, we synthesized our own range of NAPE standards for sample preparation and chromatographic method development. Synthesis of NAPE standards was performed as described by Guo et al. (Guo et al. 2010) modified after Höfle et al. (Höfle et al. 1978), thereby creating the corresponding palmitoyl-, heptadecanoyl-, steaoryl- and arachidonoyl-NAPEs from a natural PE mixture: 0.25 µmol L-α-phosphatidylethanolamine was dissolved in 1 mL dichloromethane and 25 µL of pyridine, diluted 1:25 (v/v) with dichloromethane, were added and the mixture was vortexed for 10 s. 6.25 µmol of the catalyst 4-dimethylaminopyridine and 6.5 µmol of acyl chloride (palmitoyl, heptadecanoyl, stearoyl or arachidonoyl chloride) were added, and the reaction was allowed to take place

for 18 h at room temperature. The reaction products were transferred to a glass tube and the reaction was quenched with 1 mL of saturated NH_4HCO_3. Phase separation was induced by centrifugation (3 min, 1250 g, 21 °C) and the upper aqueous phase was discarded. The lower, NAPE-containing phase was re-extracted and purified by LLE and SPE as described below.

5.2.2 Liquid-liquid extraction

LLE was performed according to Matyash et al. (Matyash et al. 2008), with some modifications. To 100 mg rat brain homogenate in a glass tube were added 50 pmol of commercially available PE 18:1/18:1-N-19:0 as internal standard. 1.5 mL methanol and 5 mL MTBE were added and the mixture was homogenized with a rotor-stator homogenizer. After 10 min of overhead shaking, 1.25 mL deionized water were added to induce phase separation. The mixture was shaken again for 10 min and centrifuged (3 min, 1250 g, 21 °C). The organic upper phase was transferred to a new glass tube while the lower aqueous phase was re-extracted with 2 mL of the upper phase of the mixture MTBE/methanol/water 10:3:2.5 (v/v/v). The combined upper phases were evaporated in a vacuum centrifuge and the lipid film was resuspended in 1 mL of SPE loading solvent (MTBE/chloroform/acetic acid 98:2:0.2 (v/v/v)).

5.2.3 Solid-phase extraction

SPE was performed on Strata SI-1 silica (55 µm, 70 Å), 500 mg/3 mL tubes, eight of which were processed simultaneously in a Varian VacElut 20 Manifold as described (H. H. Hansen et al. 2000) with minor modifications (Table 3). To increase sample throughput and ensure reproducible results, a constant negative pressure of 810 mbar was maintained. The NAPE containing fraction was collected, evaporated in a vacuum centrifuge and resuspended in 200 µL of 2-propanol/chloroform/methanol 90:5:5 (v/v/v).

Table 3: SPE method for NAPE purification

step	solvent composition (v/v/v)	volume (mL)
conditioning	MTBE/chloroform/acetic acid 98/2/0.2	7.5
sample loading	MTBE/chloroform/acetic acid 98/2/0.2	1.0
wash I	MTBE/chloroform/acetic acid 98/2/0.2	7.5
wash II	MTBE	5.0
NAPE elution	MTBE/chloroform/methanol 50/20/30	9.0

5.2.4 Chromatography

Chromatography was performed on a Bruker Advance UHPLC system using an Acquity UHPLC BEH C_8 (1.7 µm, 1 mm x 100 mm) column. Solvent A was deionized water with 1 vol% of 1 M aqueous ammonium formate and 0.1 vol% formic acid. Solvent B was acetonitrile/2-propanol 5:2 (v/v) with the same additives. Gradient elution started at 85 % solvent B and increased to 100 % B over 15 min. 100 % B were held for 3 min and the column was reequilibrated with 85 % B for another 12 min. Flow rate was 100 µL/min. 2 µL of sample were injected, the autosampler tray was kept at 10 °C and the column oven was thermostatted to 50 °C.

5.2.5 Mass spectrometry

NAPEs were detected on a Bruker Evoq Elite ER triple mass spectrometer, operating in SRM mode in positive polarity. Two transitions per analyte were monitored. Retention time windows were set ±1.5 min around the expected retention time, resulting in a median scan time of 25 ms per transition. Q1 and Q3 mass windows were 2 *m/z,* and collision gas was argon with a pressure of 1.5 mtorr (see Supplementary Table 6, p. xxv, for detailed SRM parameters for each analyte). Source parameters were as follows: Spray voltage, 4800 V; cone temperature, 300 °C; cone gas flow, 20 arbitrary units; heated probe temperature, 125 °C; heated probe gas flow, 15 arbitrary units; nebulizer gas flow, 20 arbitrary units; exhaust gas, on.

5.2.6 Data processing

Chromatograms were integrated using MS Data Review v. 8.2 and data were further processed using Microsoft Excel 2010. Quantification of naturally occurring NAPE species was performed by means of a one-point calibration using the synthetic internal standard PE 18:1/18:1-N-19:0.

5.2.7 Method validation

The method was validated for rat brain. Five rat brains were homogenized and the homogenate partitioned into aliquots of 100 mg. The aliquots were spiked with nonendogenous synthetic heptadecanoyl NAPEs to tissue concentrations from 10 to 2300 pmol/g. Accuracy was determined at three concentration points (low, 50 pmol/g; medium, 400 pmol/g; and high, 1400 pmol/g) by fitting the three concentration points into

the linear equation. All concentration points underwent the whole sample preparation procedure and analysis in triplicates.

5.3 Results and discussion

5.3.1 NAPE nomenclature

The first inconsistency in publications concerning NAPE analysis is nomenclature. The LIPID MAPS nomenclature, the "gold standard" in lipidomics currently does not include NAPEs (Fahy et al. 2005; Fahy et al. 2009), and neither do existing shorthand nomenclature systems (Liebisch et al. 2013). The following nomenclature system is therefore proposed, which defines NAPEs as deriving from N-acylation of a PE molecule, with an example for each level shown in Table 4. As the molecular structure is described in increasing detail, the effort required for identification rises dramatically. While the first two levels (lipid class mass and lipid species) are still possible using full scan approaches, identifying fatty acyls or N-acyl chains already requires tandem mass spectrometry. Identifying the location and orientation of the double bonds in fatty acyls is only possible using most advanced mass spectrometric methods (e.g. ozonolysis).

Table 4: Proposed NAPE nomenclature.

identification level	example
lipid class mass	NAPE (983)
lipid species	NAPE 52:1
N-acyl chain identified	**PE 36:1-N-16:0**
fatty acyl/alkyl	PE 18:0_18:1-N-16:0
fatty acyl/alkyl position	PE 18:0/18:1-N-16:0
LIPID MAPS Fatty Acyl/ Alkyl Structure	PE 18:0/18:1(9*Z*)-N-16:0

The approach described here identifies NAPE species on the N-acyl level (example in bold), but the fatty acyl constituents of the PE moiety are not elucidated. Identification at the fatty acyl level would be possible using advanced methods incorporating polarity switching and data dependent acquisition. While the N-acyl chain can easily be determined in positive polarity, the identities of the fatty acyls can only be elucidated in negative polarity (see also chapter 5.3.4, p. 77f). The required method therefore would incorporate N-acyl-specific neutral loss or precursor scans in positive ion mode for identification at the N-acyl level, and trigger product ion scans in negative ion mode which may be inspected to identify every species on the fatty acyl level.

5.3.2 Synthesis of NAPE standards

Since commercial availability of NAPE standards for development of sample preparation as well as for optimisation of chromatographic and mass spectrometric parameters is strongly limited, standards were synthesised from a natural PE mixture using palmitoyl, heptadecanoyl, steaoryl and arachidonoyl chloride. The palmitoyl, steaoryl, and arachidonoyl NAPEs were used for chromatographic and mass spectrometric method development. The heptadecanoyl NAPEs, due to their absence in biological tissues, were used to validate the method in terms of linearity, accuracy and precision, as well as in terms of efficiency of the sample preparation procedure.

5.3.3 Efficiency of sample preparation method

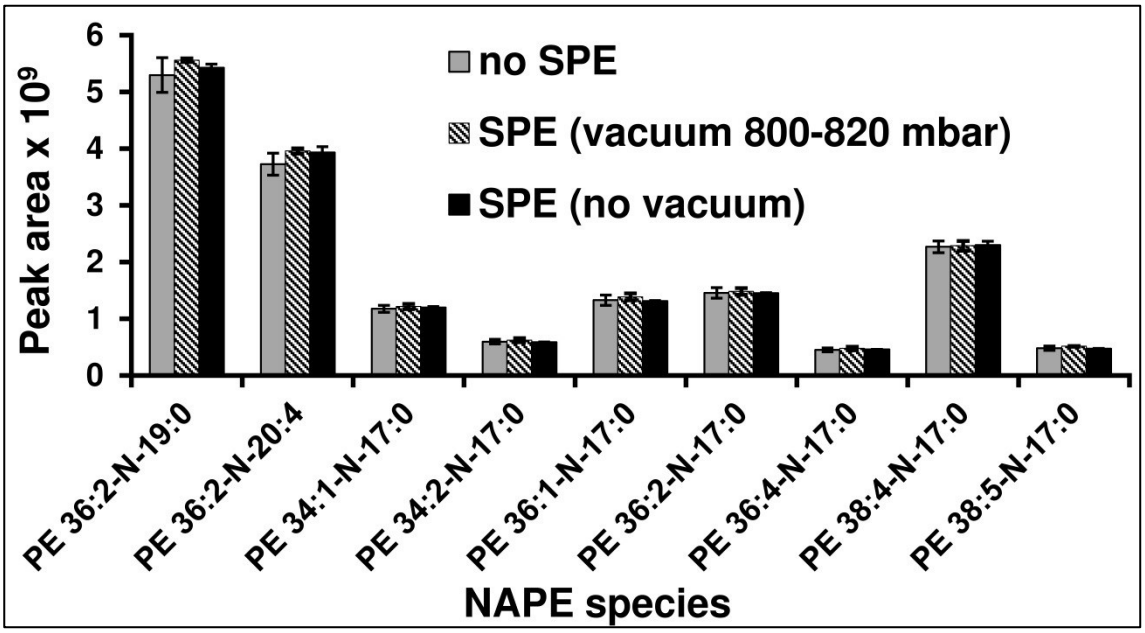

Figure 40: SPE efficiency for NAPE molecular species. No analyte loss caused by SPE sample preparation can be observed.

Low-abundance components such as NAPEs are notoriously difficult to analyse. Ion suppression effects may be exhibited by other sample components present in far greater amounts and the large concentration of other sample components may require the sample to be dissolved in a larger volume of solvent, effectively decreasing NAPE concentration. The presented sample preparation method, using a combination of LLE and SPE, is able to selectively isolate NAPE species, while eliminating other high-abundant lipid classes, such as triacylglycerols and phosphatidylcholines. The SPE sample preparation procedure neither causes analyte losses compared to unprocessed samples, nor is there a difference in

yield if SPE is performed under a negative pressure of 810 mbar compared to SPE performed under ambient pressure (Figure 40). However, performing SPE under constant negative pressure has significant advantages, as it leads to a constant dripping speed, and thereby increases both reproducibility and sample throughput.

5.3.4 NAPE detection and quantification

Collisional activation of the protonated or ammoniated adduct yields two prominent ions, both indicative of the N-acyl chain, caused by cleavages of the C-O bonds adjacent to the phosphate group (Figure 41A), similar to reported data on N-acylphosphatidylserine (Guan et al. 2008). Using CID in positive ion mode, the N-acyl chain of NAPEs can therefore be selectively identified. This would also enable selective precursor as well as neutral loss scans to screen for molecular species with a specific N-acyl chain.

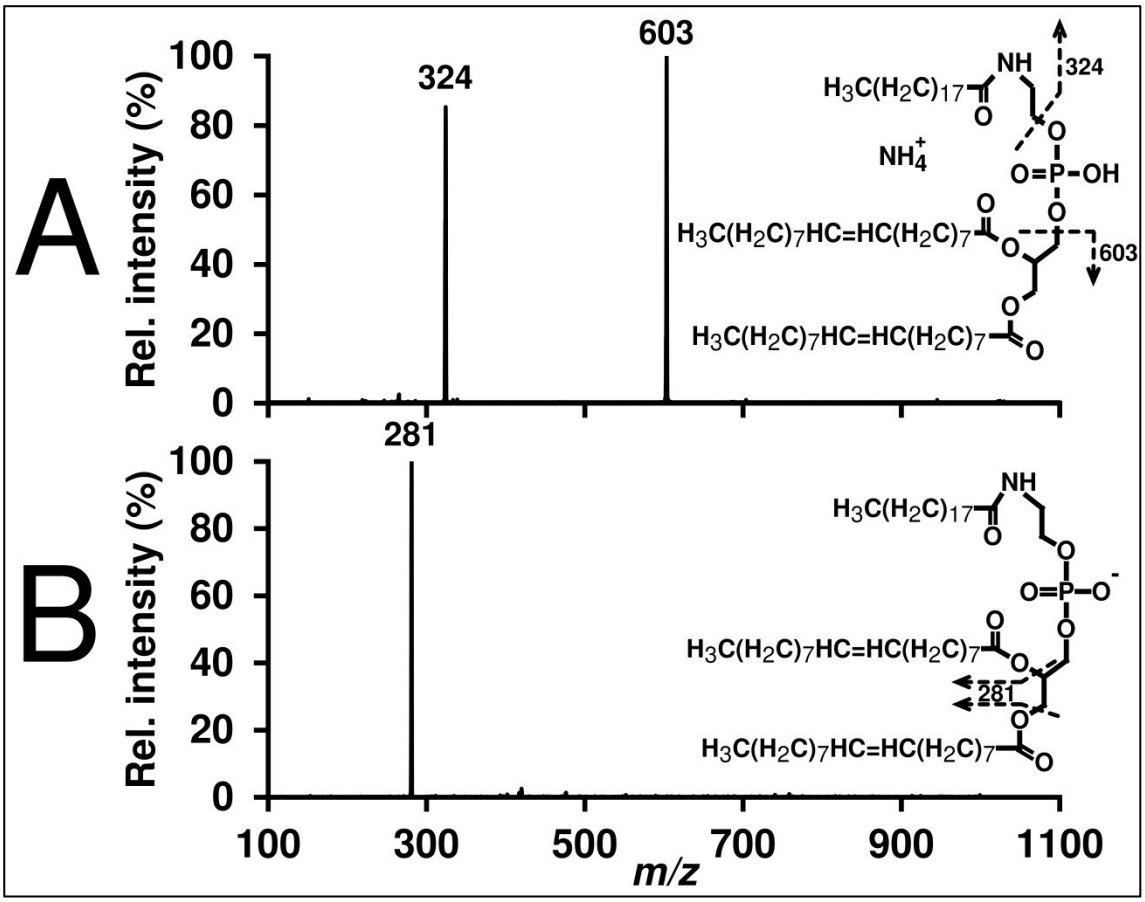

Figure 41: Tandem mass spectra of internal standard PE 18:1/18:1-N-19:0 in positive ion mode (A) and negative ion mode (B) at collision energies of 20 eV.

In contrast, CID of the deprotonated molecule in negative ESI yields only the carboxylate ions of the *sn*-1 and/or the *sn*-2 fatty acyl, but no fragment ion indicative of the N-acyl chain (Figure 41B). While fragment ions originating from the N-acyl chain have been

reported (Hansen et al. 1999), the corresponding data were generated with an ion trap. However, fragment spectra of phospholipids generated in ion traps are known to differ from those acquired in quadrupole-type instruments (Larsen et al. 2001). Under the conditions employed, negative polarity is therefore not suitable for identification of the N-acyl chain of NAPEs.

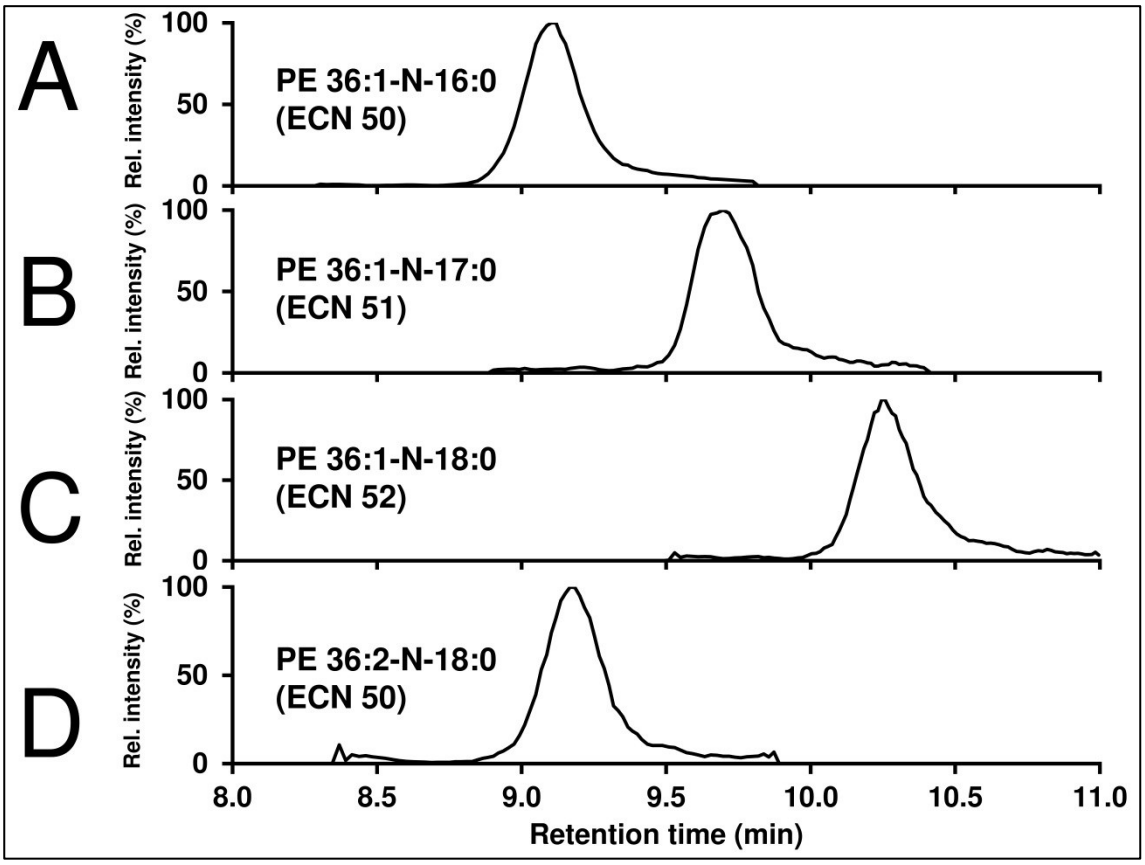

Figure 42: Extracted ion chromatograms of NAPE molecular species (A: PE 36:1-N-16:0, B: PE 36:1-N-17:0, C: PE 36:1-N-18:0, D: PE 36:2-N-18:0). Note the increase of retention time with increasing number of carbon atoms (A, B, C) and the decrease of retention time with increasing number of double bonds (C, D), consistent with the ECN model.

Retention time is an important aspect of correct identification in lipidomic data analysis. The retention behaviour in reversed-phase chromatography is well described by the effective/equivalent carbon number (ECN), calculated as ECN=[number of carbon atoms]–2*[number of double bonds] (Schwalbe-Herrmann et al. 2010; Lísa et al. 2011). Retention of lipids increases proportionally to ECN in reversed phase chromatography, a behaviour which allows for prediction of retention times. Figure 42 shows chromatograms of four NAPE species and illustrates how retention is influenced by the number of carbon atoms and number of double bonds.

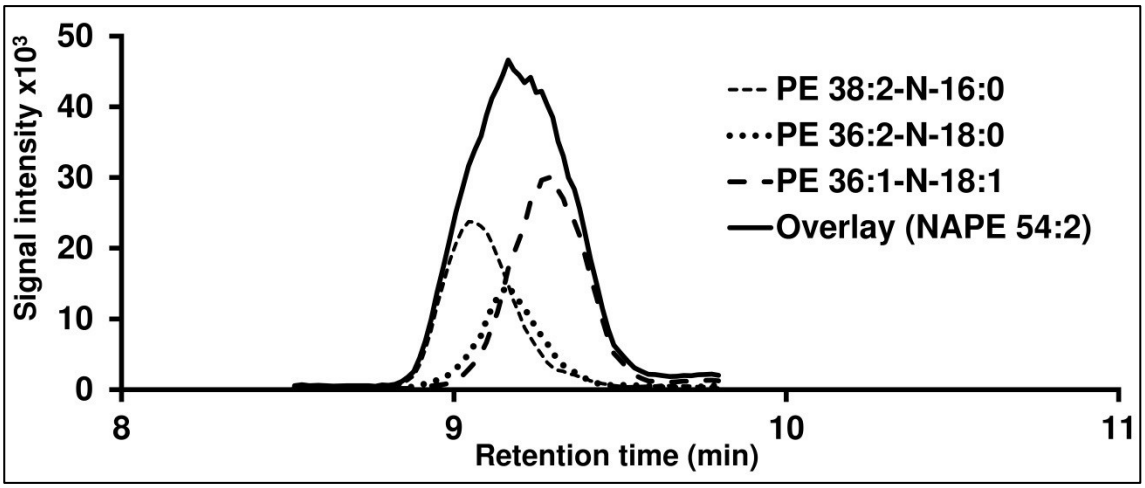

Figure 43: Extracted ion chromatograms of isobaric NAPE structural isomers. Selective detection is enabled by N-acyl chain specific selected reaction monitoring of PE 38:2-N-16:0 (small dashes), PE 36:2-N-18:0 (dots), and PE 36:1-N-18:1 (large dashes). Full scan approaches, even with high mass resolution, would only detect the sum of all structural isomers (continuous line).

Since NAPEs contain three fatty acyls, a number of structural isomers are possible for every species. PE 38:2-N-16:0, PE 36:2-N-18:0, and PE 36:1-N-18:1 are all structural isomers of NAPE 54:2. Their extracted ion chromatograms are shown in Figure 43, indicating that there still is some separation (despite all three having identical ECN). This also illustrates the importance of using N-acyl specific SRM transitions, since a full scan approach, even with high-resolution mass spectrometry, would only detect the sum of all three structural isomers, with no way of differentiating the three underlying compounds,. SRM in negative ion mode, using a fragment ion indicative of either the *sn*-1 or *sn*-2 acyl chain, also does not resolve ambiguity, since it does not identify the N-acyl chain. Using N-acyl specific scans in positive ion mode, as performed here, the N-acyl chain and the PE moiety are selectively identified.

The importance of using two complimentary SRM transitions per analyte to correctly identify NAPE molecular species is demonstrated in Figure 44. The dotted line shows the EIC of the charged N-acyl fragment of PE 36:2-N-18:1, while the dashed line shows EIC of the N-acyl neutral loss. At the correct retention time (6.8 min) both EICs show chromatographic peaks of comparable intensity. The peaks at 10.1 and 11.2 min show only the N-acyl fragment, but no N-acyl neutral loss. They therefore do not correspond to PE 36:2-N-18:1.

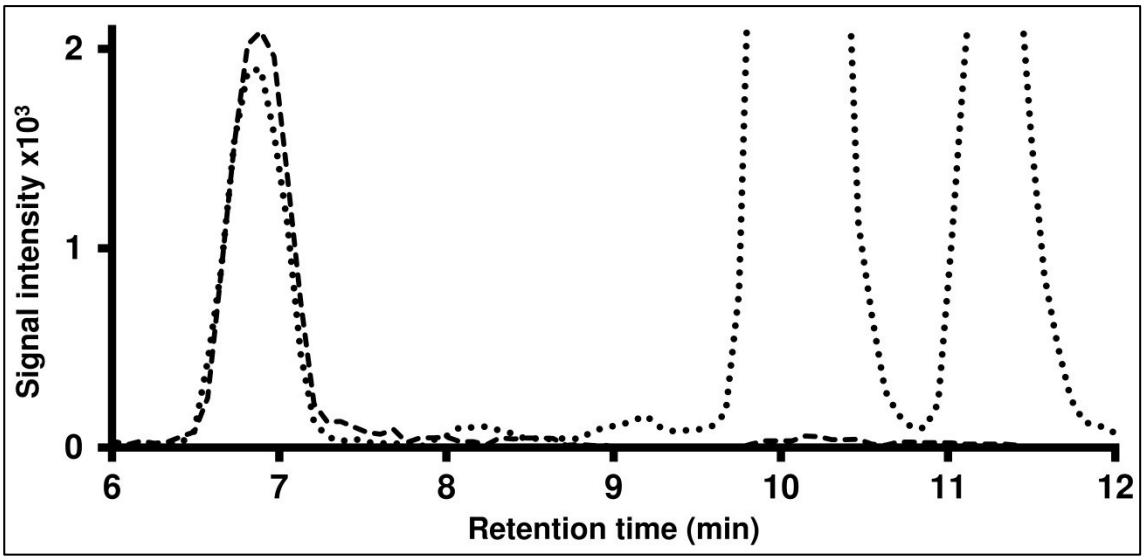

Figure 44: EICs of PE 36:2-N-18:1, y-axis zoomed to intensity of the correct peak. The dotted line shows the EIC of the N-acyl fragment while the dashed line shows the EIC of the N-acyl neutral loss. The correct peak at 6.8 min shows both EICs at the same retention time and comparable intensity.

5.3.5 Method validation

Linearity of the method was evaluated by addition of non-endogenous heptadecanoyl-NAPEs to rat brain samples in the concentration range of 10-2300 pmol/g. All five species investigated show excellent linearity over the whole concentration range, and values for accuracy and precision are usually well below 20 % (Table 5). Precision was additionally calculated for 41 biological NAPEs from 15 separately processed liver samples. While imprecision (expressed by % RSD) is generally higher at lower concentrations, it is under 20 % for all species over 25 pmol/g, which together account for more than 90 % of detected NAPE amount.

Table 5: Validation data for NAPEs. Linearity data (unweighted) is derived from three separately processed samples for each of the nine concentration points ranging from 10 to 2300 pmol/g.

Analyte	Slope	Intercept	R^2	Accuracy (%)			Precision (%)		
				low	medium	high	low	medium	high
PE 34:1-N-17:0	0.7351	2.2269	0.9919	22.9	8.6	13.4	24.3	7.7	16.9
PE 34:2-N-17:0	0.5178	0.7397	0.9901	13.0	10.4	20.6	17.5	13.3	18.3
PE 36:1-N-17:0	0.6628	4.1666	0.9944	17.3	6.3	14.6	18.0	1.2	5.8
PE 36:2-N-17:0	0.8528	3.6243	0.9942	13.0	8.5	12.0	6.9	2.8	8.9
PE 38:4-N-17:0	1.1342	15.414	0.9940	16.8	3.9	10.4	3.4	3.7	12.3

Sample preparation is usually the biggest source of error in the analytical workflow, which is underlined by the relatively high value for RSD of the internal standard (27 % RSD over 39 separately processed samples). This underlines its importance in correcting for different yields during the multi-step sample preparation and analysis procedure. The usual problems in lipidomic quantitation (chapter 4.3.6, p. 67f) occur: the lack of analyte-free matrices and stable-isotope labeled standards for each analyte precludes NAPEs from classical quantitation, leaving only a one-point calibration using a non-endogenous internal standard as a suitable quantitation method.

5.3.6 NAPEs detected in rat brain

The method was applied to rat brain, a complex matrix where many other phospholipids are present in very high concentrations. During preliminary experiments, 73 candidate NAPE species were identified. In the final method, SRM transitions for 5 heptadecanoyl-NAPEs and the internal standards were added, leading to a total number of 79 quantifiable analytes, each of which was monitored using two transitions (one for the charged N-acyl fragment, and one for the N-acyl neutral loss). See Supplementary Table 6, p. xxv, for detailed scan parameters and also for quantitative results.

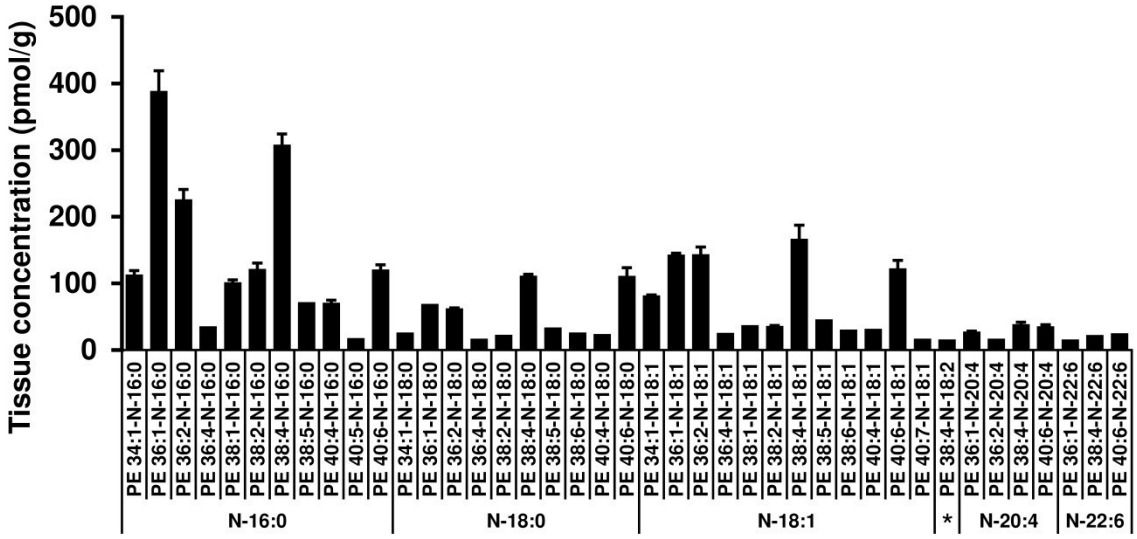

Figure 45: NAPE species quantified in rat brain. Values are means (n=3), error bars represent single standard deviation, asterisk annotates N-18:2 species.

Of the 73 NAPE species monitored, 21 were detected, but quantified below the LLOQ (corresponding to 10 pmol/g, the lowest concentration point for which linearity is proven). The remaining 41 NAPE molecular species are distributed among six N-acyl chains, of which palmitic acid, stearic acid, and oleic acid make out the bulk of 95 % (Figure 45). As

expected and conforming to existing literature (Wellner et al. 2013; Hansen et al. 2008; Cadas et al. 1997; Takayuki Sugiura et al. 1996; Berger et al. 2004), the concentrations of NAPE species is extremely low, totalling only 3 nmol/g, with the most abundant molecular species (PE 36:1-N-16:0) quantified at 383±36 pmol/g.

5.4 Conclusion

The method presented is able to selectively and sensitively identify intact NAPE molecular species from complex biological matrices. Sample preparation using a two-step process of liquid-liquid and solid-phase extraction efficiently eliminates many potentially interfering substances present in far greater abundance than the target analytes and improves identification certainty. The mass spectrometric method uses not one, but two N-acyl chain specific SRM transitions for each analyte, thereby routinely identifying both the N-acyl and the PE moiety.

The method is suitable for detection and quantification of NAPEs, which are physiologically highly relevant signalling precursors present only at minor concentrations. In rat brain, 41 intact NAPE species with six different N-acyl chains and totalling a tissue concentration of 3 nmol/g were quantified.

6 HIGH RESOLUTION TANDEM MASS SPECTROMETRY IN CANCER METABOLISM RESEARCH

6.1 Introduction

Glucose is the predominant carbon source for most cellular systems, through the pathway of glycolysis. Glycolysis produces energy (in the form of ATP and NADH), by converting glucose to pyruvate, and it is also the predominant pathway for glycerol biosynthesis (Löffler 2004). Cancer cells have an unusually high rate of glycolysis, followed by lactate fermentation, a phenomenon known as the Warburg effect (Koppenol et al. 2011). Tumour growth requires high rates of mitosis, which in turn requires synthesis of new cell membranes. Structural lipids such as sterols and phospholipids are essential constituents of cellular membranes; cancer cells therefore have high demand for newly synthesized phospholipids. Just as fatty acid synthesis is upregulated in many cancer cells, biosynthesis of the glycerol backbone of phospholipids is also required (Schulze & Harris 2012). Glycerol is usually obtained through glycolysis, provided that the substrate glucose is available. However, cancer cells and tumours are able to survive, perform mitosis, and grow, even under conditions of low glucose, indicating that they are able to utilize a glycerol source other than glucose (Leithner et al. 2014).

Amino acids are speculated to be a potential source of glycerol through the pathway of glyceroneogenesis. Using this pathway, glycolysis would essentially be reversed, and other precursors such as amino acids would be utilized to synthesize glycerol-3-phosphate for incorporation into lipids (Nye et al. 2008). However, the exact conditions under which cancer cells are able to synthesize glycerol *de novo* from amino acids have not been investigated and the extent and efficiency of this pathway is unclear and needs to be resolved.

6.2 Hypothesis and aim

To study the metabolism of lung cancer cells and to investigate whether they are able to produce glycerol from carbon sources other than glucose (in particular amino acids), the incorporation of ^{13}C from uniformly labelled $^{13}C_5$-glutamine into the glycerol backbone of phospholipids is to be quantified.

The challenges of this approach are precisely locating the ^{13}C label within phospholipids and determining whether the incorporation of the stable isotope label is specific to one

phospholipid class or occurs across multiple classes. It is also essential to quantify the enrichment of ^{13}C within the glycerol backbone of the phospholipid, whilst taking into account the natural abundance of ^{13}C.

6.3 Materials and methods

6.3.1 Sample preparation

A549 adenocarcinomic human alveolar basal epithelial cells were grown in standard medium for 24 h, then in deprivation medium containing 0.2 mM glucose and glutamine, and then in medium containing either 0.2 mM, 1 mM, or 10 mM glucose, with either monoisotopic glutamine or $^{13}C_5$-glutamine, and for varying periods of time (24 h, 48 h or 72 h). Lipid extraction was performed as described (Matyash et al. 2008), with minor alterations: One million A549 cells in a 12 mL glass tube with a Teflon-lined cap were homogenized in 1.5 mL methanol with a rotor-stator homogenizer to disrupt the cell membranes. 5 nmol of PC 24:0 were added as extraction control and after addition of 2.5 mL MTBE, the mixture was vortexed for 10 s and sonicated for 10 min. After further addition of 2.5 mL MTBE and 10 min overhead shaking, 1.25 mL of deionized water was added to induce phase separation. After further 10 min overhead shaking, the samples were centrifuged (3 min, 1350 g, 21 °C) and the upper organic phase was recovered. The lower aqueous phase was re-extracted with 2 mL of the upper phase of MTBE/methanol/water 10:3:2.5 (v/v/v). The upper phases were combined and evaporated in a vacuum centrifuge. The dried lipid film was resuspended in 1 mL of chloroform/methanol 1:1 (v/v) and stored at -20 °C prior to analysis.

6.3.2 Chromatography

Chromatography was modified after Triebl et al. (Triebl et al. 2014). Separation was performed on a Phenomenex Kinetex HILIC column (2.1 mm x 100 mm, 2.6 µm), thermostatted to 50 °C in a Thermo Accela 1250 HPLC system. Mobile phase A was deionized water containing 1 vol% 1 M aqueous ammonium formate and 0.1 vol% formic acid. Mobile phase B was acetonitrile/2-propanol (5/2, v/v) with the same additives. Gradient elution started at 95 % mobile phase B and changed to 75 % B over 10 minutes. The column was reequilibrated for 8 min with 95 % B. Flow rate was 250 µL/min and 2 µL of sample, thermostatted to 10 °C were injected using full loop injection mode.

6.3.3 Mass spectrometry

The Orbitrap Velos Pro mass spectrometer operated in negative ion mode in alternating full MS and tandem MS mode. Full scan spectra were acquired at a target resolution of 30 000 (FWHM at *m/z* 400). Tandem mass spectra were acquired at a target resolution of 7 500 (FWHM at *m/z* 400) and phospholipid classes were analysed using HCD activation (normalized collision energy, 75; activation time, 0.1 ms; FT first mass mode, fixed at *m/z* 100). For the first three minutes, PI molecular species were isolated (*m/z* 887.5±75), for the next three minutes diacyl-PE and plasmalogen-PE molecular species (*m/z* 745.5±75) and for the remainder of the gradient PC molecular species (*m/z* 804.5±100). To assess isolation efficiency, the experiments were performed once with a collision energy setting of 1.

6.3.4 Data processing

Xcalibur Quan Browser and Microsoft Excel were used for data processing. For each lipid class investigated (PI, PE and PC), two sets of fragment ions were monitored: One head group fragment ion containing glycerol and the other set not containing glycerol. For each set, the EICs of five isotopologues (containing zero, one, two, three and four ^{13}C atoms, respectively) were integrated. See Table 6 for chemical structures of target fragment ions and Supplementary Table 7, p. xxix, for exact *m/z* values and elemental compositions. Areas of the respective isotopologues were normalized to the monoisotopic ion. Control samples grown on $^{12}C_5$-Gln were used to correct for the natural abundance of ^{13}C.

Table 6: Structures of phospholipid head group fragment ions differing only in the glycerol moiety with elemental compositions and nominal *m/z*.

PC	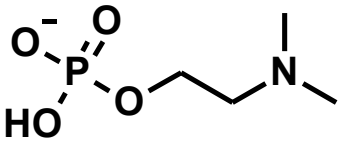	$C_4H_{11}O_4PN$ *m/z* 168
	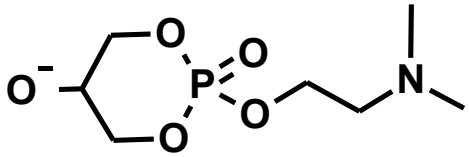	$C_7H_{15}O_5PN$ *m/z* 224
PE	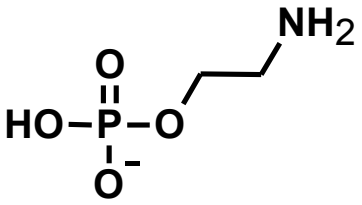	$C_2H_7O_4PN$ *m/z* 140
	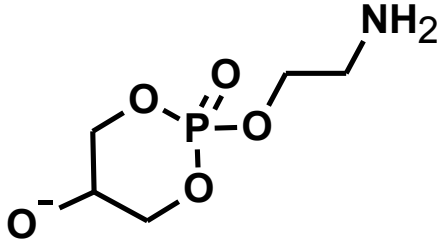	$C_5H_{11}O_5PN$ *m/z* 196
PI	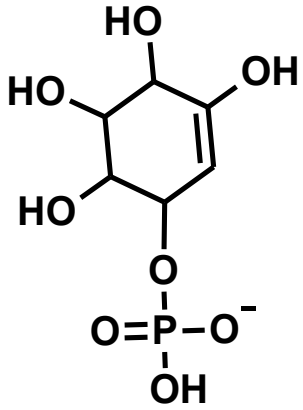	$C_6H_{10}O_8P$ *m/z* 241
	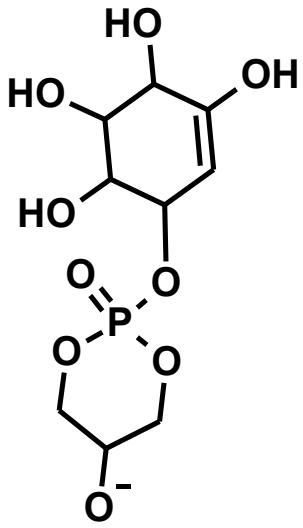	$C_9H_{14}O_9P$ *m/z* 297

6.4 Results and discussion

Figure 46A shows the TIC of a HILIC separation of an A549 cell extract. The major phospholipid classes PI, PE and PC are well separated, whereas there is little separation within phospholipid classes (Figure 46B). The samples contain a relatively high amount of ether-linked ethanolamine phospholipids (plasmalogen PE), which are not chromatographically separated from the diacyl species. Since all molecular species of one lipid class elute at the same time, the use of a broad isolation window prior to fragmentation enables analysis not only of single phospholipid molecular species, but of all species of one phospholipid class.

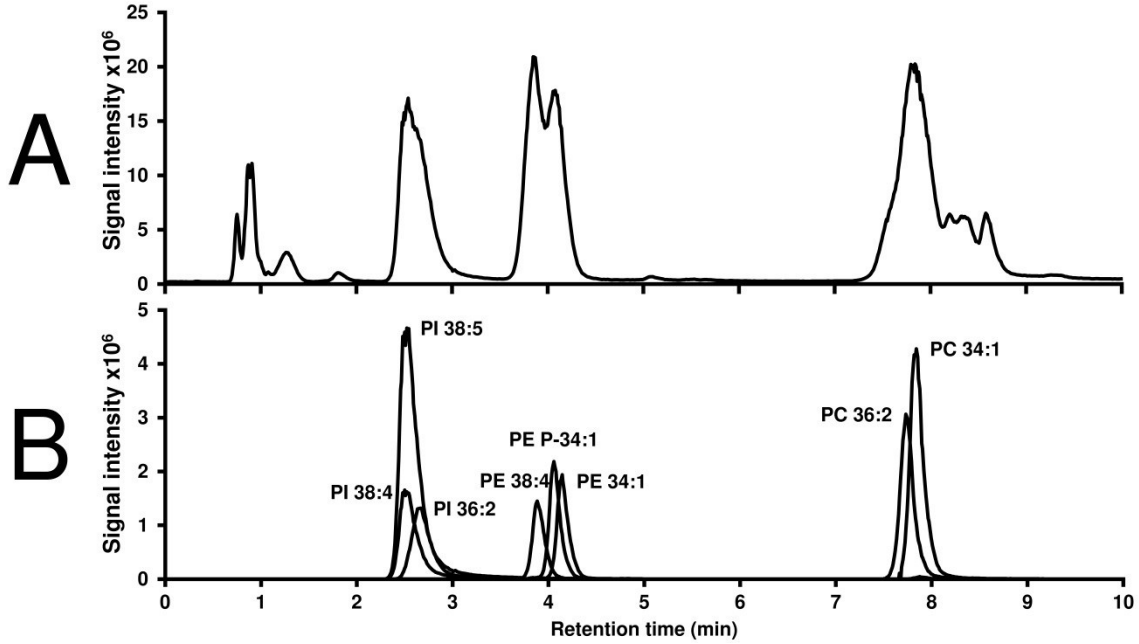

Figure 46: TIC of HILIC separation of an A549 cell extract (A) and EICs of selected phospholipids (B). While the major phospholipid classes PI, PE, and PC are well separated, there is little separation within classes.

The approach of using a very broad isolation window to fragment multiple ions simultaneously, in this case all molecular species from one lipid class, is unusual but effective (Figure 47). There is essentially no difference between a full scan spectrum (top panel) and a fragment spectrum recorded at a low collision energy setting (bottom panel), indicating that all target ions, i.e. all molecular species of one phospholipid class, are effectively isolated and the fragment spectra generated in this way result from not merely one, but all PC molecular species. Thus, the results obtained represent the whole phospholipid class.

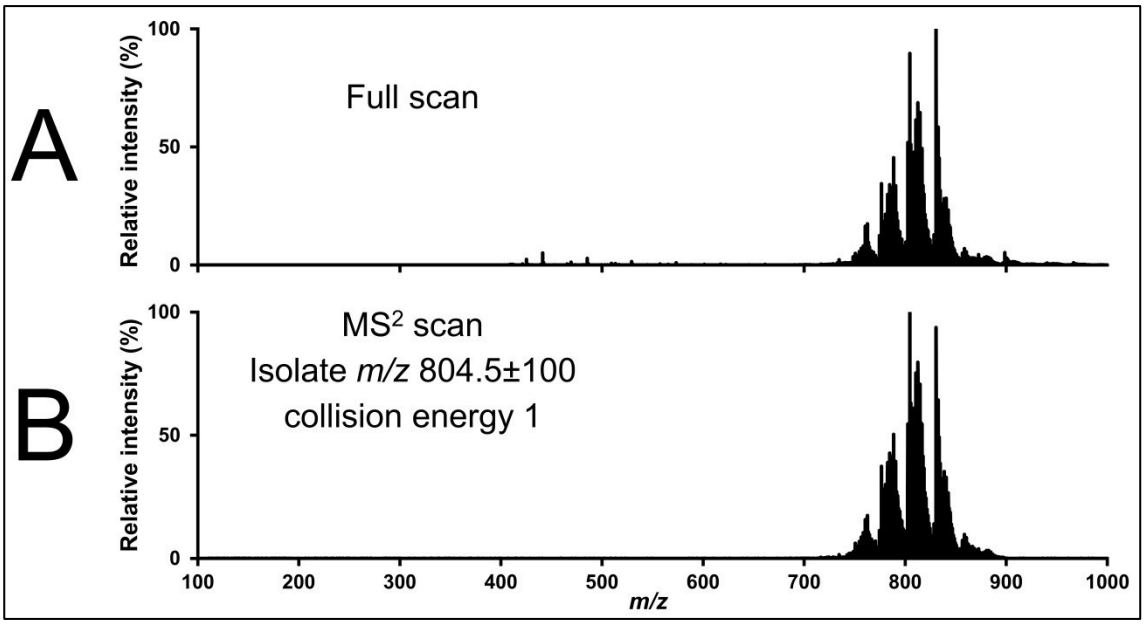

Figure 47: Full scan (A) and tandem MS scan recorded at low collision energy (B) at the retention time of PC illustrates the efficiency of the broad isolation window for MS^2 scans: All PC molecular species visible in the full scan are isolated, and appear in the tandem mass spectrum.

6.4.1 Determination of the location of the stable isotope label

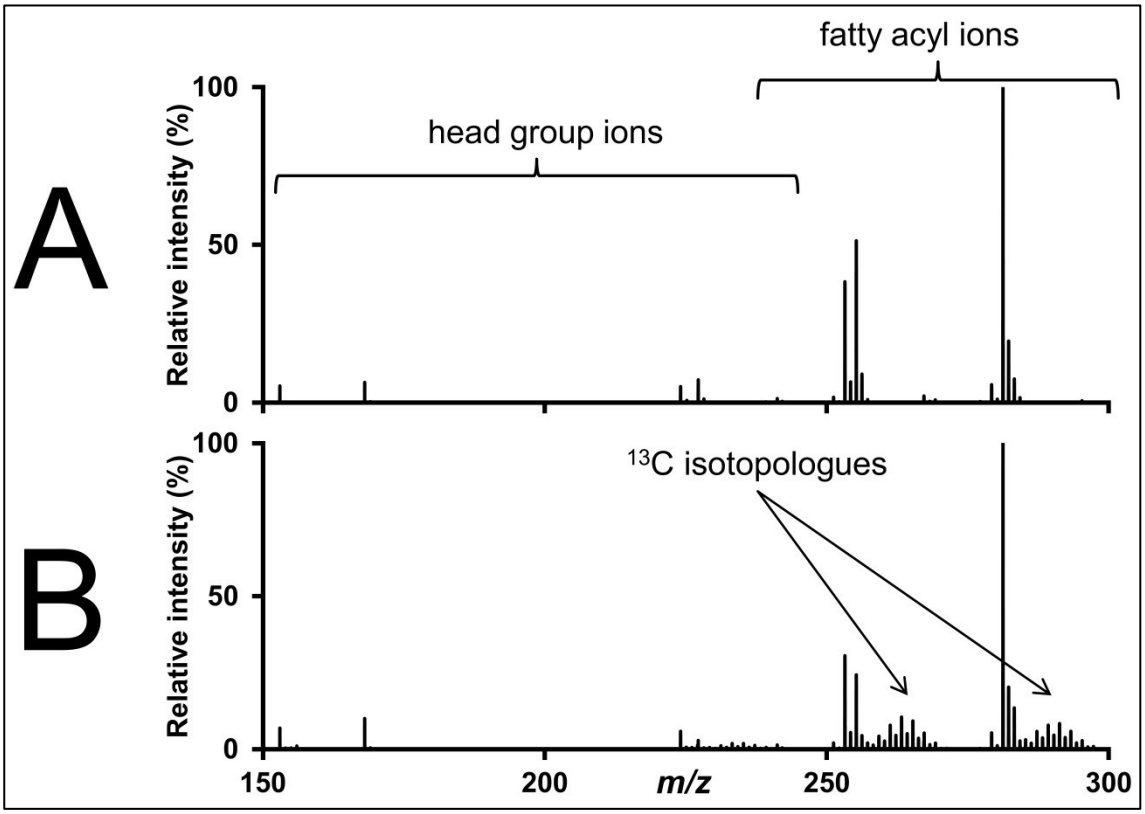

Figure 48: Tandem mass spectra of PC from control cells (A) and cells grown on $^{13}C_5$-Gln (B).

Figure 48 shows differences in the tandem mass spectra of PC species between control and treatment samples. Control samples already show some isotopologues of fatty acid carboxylate ions, but these are merely caused by the natural abundance of ^{13}C. Greater changes can be seen in the isotopic "envelope" of the treatment samples, indicating that at least some carbon atoms of fatty acid synthesis or elongation originate from the labelled glutamine. The spacing by 2 Da also indicates fatty acid elongation by a two-carbon unit, via acetyl-CoA. However, incorporation of the ^{13}C label into the fatty acyls is not the concern, but rather incorporation into the glycerol backbone.

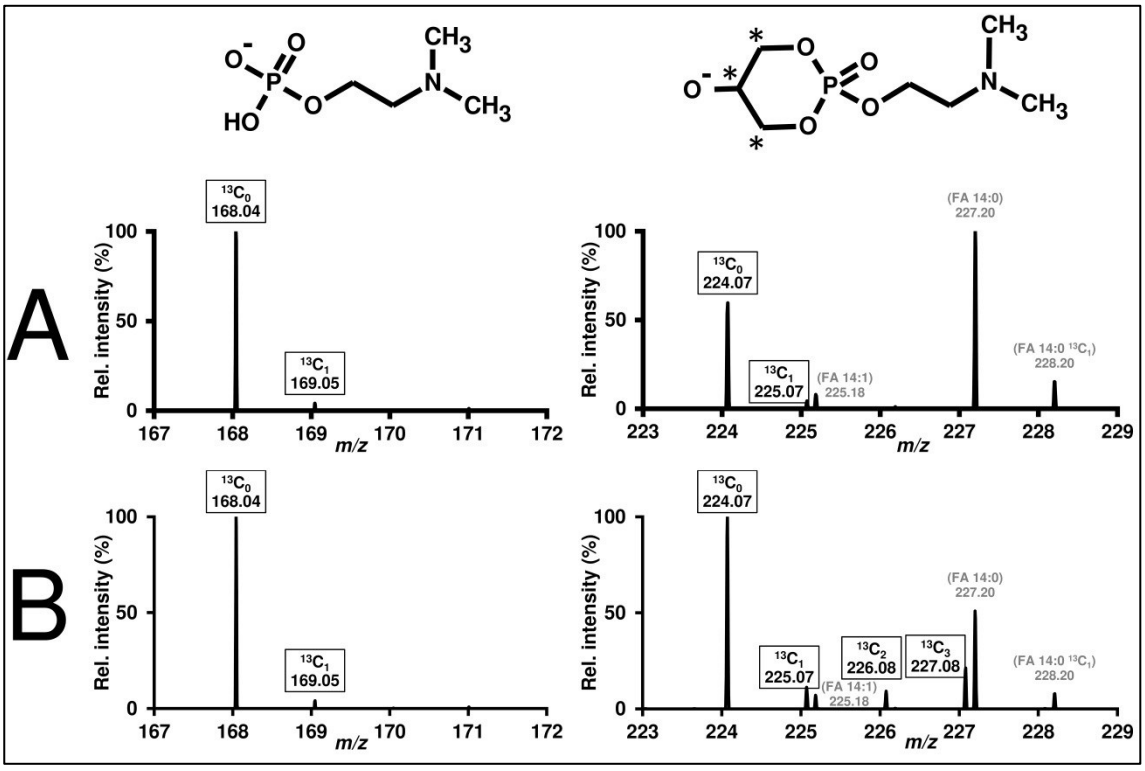

Figure 49: PC head group fragment ions from control cells grown on ^{12}C-glutamine (A) and cells grown on $^{13}C_5$-Glutamine (B), zoomed to ranges of the head group ion not containing glycerol (*m/z* 168) and containing glycerol (*m/z* 224). Asterisks indicate the glycerol carbon atoms; mass peaks labelled in grey correspond to fatty acyl ions.

The major head group fragment ions of choline phospholipids are *m/z* 153 (cyclic glycerophosphocholine), *m/z* 168 (demethylated phosphocholine) and *m/z* 224 (demethylated glycerophosphocholine) (Hsu et al. 2014). Figure 49 shows PC fragment spectra from control samples grown on ^{12}C-glutamine (panel A) and treatment samples grown on ^{13}C-glutamine (panel B) zoomed to the region of phosphocholine and glycerophosphocholine head group fragments (*m/z* 168 and *m/z* 224). The isotopologues of phosphocholine do not differ between control and treatment samples, with the

^{13}C-isotopologue at *m/z* 169 in both cases merely representing the natural abundance of ^{13}C of ~3 %. This indicates that there is no incorporation of ^{13}C from the growth medium into the choline moiety of PC.

In contrast, there are distinct changes within the isotopologues of glycerophosphocholine (*m/z* 224) between treatment and control samples. While control samples show only the $^{13}C_1$-isotopologue at *m/z* 225 (arising from the natural abundance of ^{13}C of ~7 %), treatment samples show prominent ions of $^{13}C_1$-, $^{13}C_2$- and $^{13}C_3$-glycerophosphocholine at *m/z* 225.07, *m/z* 226.08, and *m/z* 227.08, respectively. Note that the head group ions are clearly mass separated from the fatty acid carboxylate ions and their isotopologues (e.g. *m/z* 227.08, $^{13}C_3$-glycerophosphocholine and *m/z* 227.20, myristic acid). There is also no peak at *m/z* 228.08 which would correspond to $^{13}C_4$-glycerophosphocholine. This confirms the precise location of the ^{13}C-label as the glycerol portion of the glycerophosphocholine head group: If the choline moiety containing a total of five carbon atoms were also ^{13}C-labelled, this would result in fragment ions containing more than three ^{13}C isotopes. However, incorporation of ^{13}C from the growth medium into choline does not occur at all under the experimental conditions.

This approach illustrates how detailed analysis of characteristic fragment ions and their isotopologues enables the precise localization of the ^{13}C label within the phospholipid head group: While there is no incorporation of ^{13}C into the phosphocholine moiety, there clearly is incorporation of ^{13}C into the glycerophosphocholine moiety. The ^{13}C label must therefore be localized in the part of the molecule in which these two fragments differ – which is the glycerol moiety.

The method of using a pair of fragment ions differing only by the glycerol moiety is not limited to phosphatidylcholine – in fact, also ethanolamine phospholipids (diacyl PE and PE plasmalogens) as well as PI show suitable fragment ions analogous to PC (Table 6). The fragmentation pathways and mechanisms by which these fragment ions are generated have previously been discussed in great detail by Hsu and Turk (Hsu & Turk 2009) and Murphy (Murphy 2015). As illustrated by Figure 46, PI, PE and PC together constitute the bulk of the phospholipidome of A549 cells.

6.4.2 Quantitative analysis and enrichment

Quantitative analysis and graphical representation of data is possible using the peak area of the indicative fragments and their isotopologues. Experiments performed in triplicate

additionally allow for the results to be statistically treated. As proof of concept, the time-dependent incorporation of ^{13}C from the uniformly labelled amino acid glutamine into the glycerol moiety of three phospholipid classes under low glucose conditions is shown in Figure 50. Analogously to PC (as explained in the previous chapter), the label can be precisely localized for PE and PI by comparing a pair of fragment ions differing only in the glycerol moiety. While there is no enrichment of ^{13}C (or in the case of PE, only minor enrichment) in the fragment ion not containing glycerol (phosphocholine, phosphoethanolamine, and phosphoinositol, respectively; left panels in Figure 50), the fragment ions containing glycerol show a clear time-dependent enrichment of ^{13}C (right panels in Figure 50). This again confirms the location of the label at the glycerol for all three phospholipid classes.

After 72 h of growth in low glucose medium containing ^{13}C-glutamine, 15-20 % of the glycerol backbone of PC, PE, and PI is fully ^{13}C-labelled. This indicates that glutamine has been used to synthesize the glycerol portion of phospholipids.

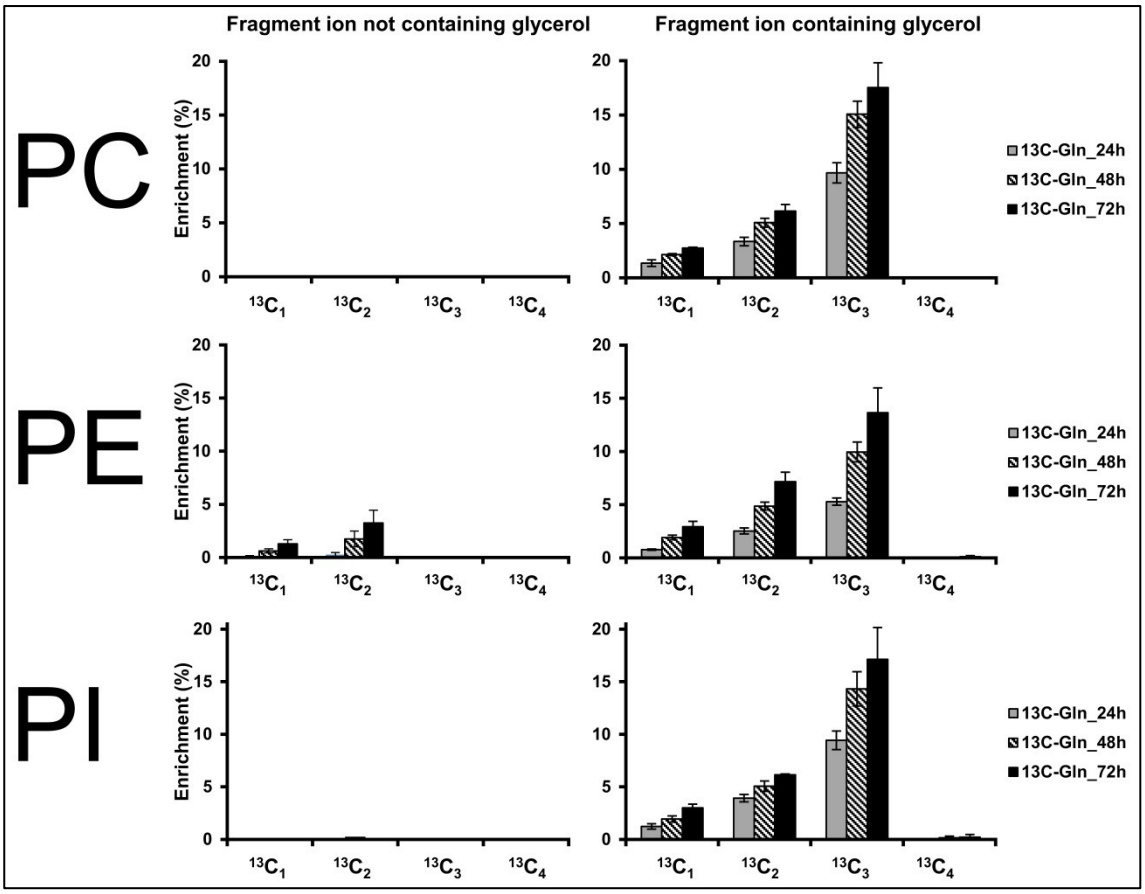

Figure 50: Time-dependent incorporation of ^{13}C from glutamine into the glycerol backbone of PE, PE and PI. Note minor enrichment in the ethanolamine, which only contains two carbon atoms.

Under the conditions employed, A549 lung cancer cells therefore clearly are able to use glutamine as a carbon source to synthesize the glycerol backbone of choline, ethanolamine and inositol phospholipids. The measurement method using isotope ratios is also very reliable, as illustrated by the barely visible error bars (denoting standard deviation from three biological replicates).

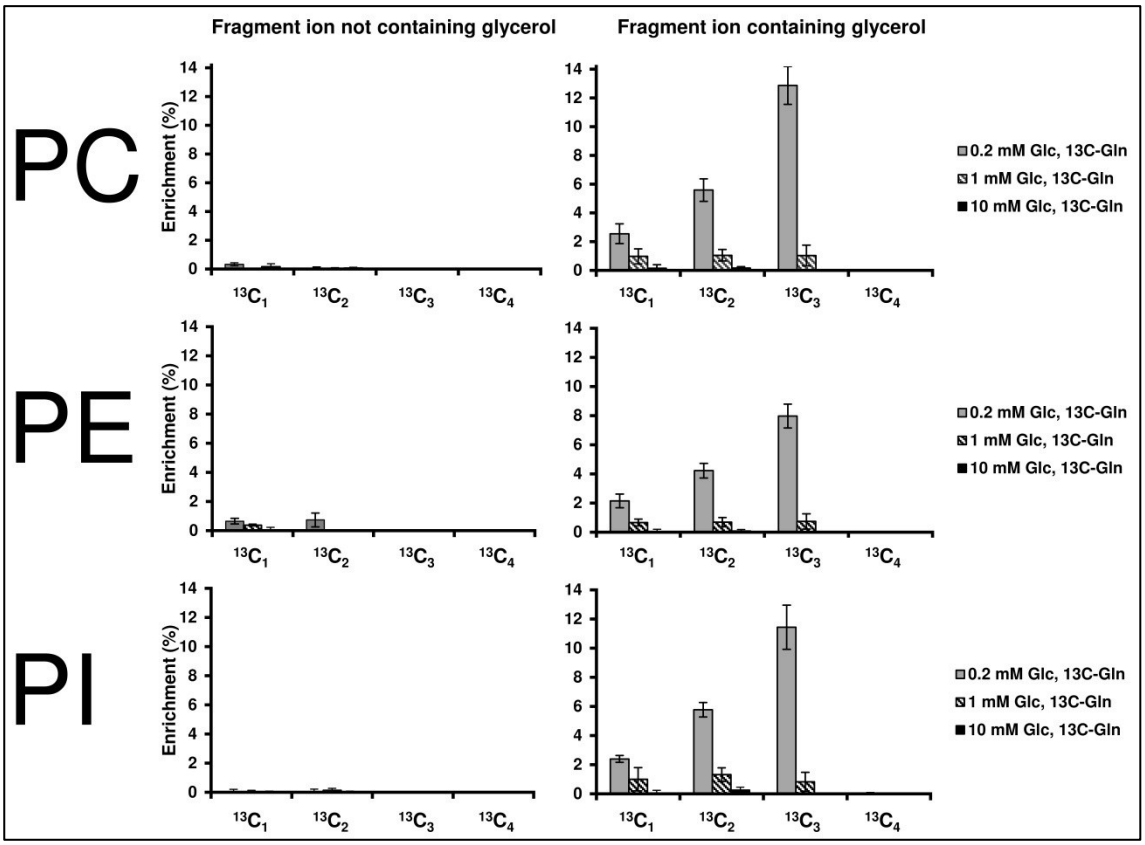

Figure 51: ^{13}C-enrichment in the glycerol backbone of phospholipids under various glucose concentrations. Glutamine is used to synthesize glycerol only at low glucose concentrations (0.2 mM). Values are corrected for natural abundance of ^{13}C; error bars denote one standard deviation from three replicate biological experiments.

So far, these results show that A549 cells are generally able to use glutamine as a carbon source for glycerol biosynthesis. This is expected to happen only if the demand for glycerol cannot be met by glycolysis. For further investigation, cells were grown in medium containing various concentrations of glucose (0.2 mM, 1 mM and 10 mM) and containing $^{13}C_5$-glutamine. The enrichment of ^{13}C in the head groups is shown in Figure 51. For all three classes investigated, the fragment ion not containing glycerol shows no enrichment (or only minimal enrichment in the case of PE) at all three glucose concentrations. In contrast, the head group fragment containing glycerol shows distinct ^{13}C enrichment at the lowest glucose concentration (0.2 mM), but only minimal or no

enrichment at higher glucose concentrations for all three phospholipid classes. This indicates that a glucose concentration of 0.2 mM is not sufficient to provide the necessary glycerol for phospholipid synthesis and the cells need to utilize another carbon source for biosynthesis of glycerol. They therefore shift biosynthesis of glycerol from glycolysis to glyceroneogenesis using glutamine as substrate.

6.5 Conclusion

A sophisticated approach to study the incorporation of a stable isotope label into phospholipids along with precise localisation of the label within three phospholipid classes and quantitative analysis is presented. HILIC separation of a lipid extract, together with targeted high-resolution/accurate mass tandem mass spectrometric detection provides all necessary data. The isotopologues of two pairs of fragment ions differing only in the glycerol moiety are used to identify the location of the stable isotope label and to calculate the enrichment of ^{13}C in the glycerol backbone of phospholipids.

Using this approach, it can be shown that while cancer cells preferentially use glucose to synthesize glycerol for incorporation into phospholipids, they are able to switch to a second metabolic pathway under conditions of glucose deprivation. Using this pathway, they use glutamine as a carbon source for glycerol biosynthesis.

7 DISCUSSION

Lipidomics is a diverse field of research encompassing both the demand for global and large-scale analysis of the lipidome, as well as for specialised targeted analysis methods for extremely low-abundance analytes. Furthermore, it is a field relevant to multiple other research areas such as that of cancer metabolism, where lipidomic analyses comprising highly sophisticated detection methods may aid in the investigation of metabolic pathways and their regulation. The presented work offers practical and highly relevant analytical solutions to a majority of potential demands in the lipidomic field.

Firstly, a method for global lipidomic analysis comprises the main part of this work. Global and comprehensive analysis of the lipidome is one of the most important core demands in the lipidomic field. Global lipidomic methods are often used for large-scale untargeted screening approaches, in order to gain a "first look" into the lipidome. A suitable global lipidomics method must therefore be applicable to a wide variety of sample materials, and encompass the potential to analyse as many lipids as possible. Automated data analysis is another prerequisite for such a method in order to cope with the enormous extent and complexity of the lipidome.

The presented method encompasses a simple but versatile lipid extraction method, powerful chromatography, and detection with high resolution accurate mass spectrometry together with automated parallel generation of tandem mass spectra. This combination results in the potential to quantitatively analyse hundreds of glycerolipids, glycerophospholipids and sphingolipids from a single sample in less than an hour. At the same time, the method enables structural analysis of lipids through inspection of tandem mass spectra. A variety of lipid standards belonging to over a dozen lipid classes were subjected to mass spectrometric fragmentation in a controlled experiment. The resulting fragment spectra were then analysed to expand the existing knowledge about the tandem mass spectrometric behaviour of lipids. Taking this knowledge into consideration, the method presented enables quantitative analysis of hundreds of lipids, together with the potential to separate and, in an untargeted manner, identify and quantify even structural isomers and in some cases positional isomers. Since quantitation is an essential requirement for lipidomic analysis, the method was validated in the biologically relevant concentration range for lipids and was found to be optimally suitable for untargeted

lipidomic analysis. Additionally, its applicability to even the most complex biological organisms relevant to lipidomic research has successfully been shown.

Secondly, the lipidomic demand for specialized analysis of selected lipid subclasses is exemplified by a method for quantitation of intact N-acylphosphatidylethanolamine species, which are biologically highly relevant signalling lipids, present at only minute concentrations. In a targeted approach such as this, specialized sample preparation methods, such as the combination of liquid-liquid extraction and solid-phase extraction, offer the potential to selectively isolate the analytes in question from a complex biological matrix. Analysis by highly selective selected reaction monitoring methodology, using two structurally specific transitions per analyte, together with chromatographic separation, results in a highly sensitive and selective detection method for these lipids together with routine determination of both the N-acyl and the phosphatidylethanolamine moiety. The method was also validated in the biologically relevant concentration range for N-acylphosphatidylethanolamine species and the results have been published.

Thirdly and finally, the importance and relevance of lipidomic mass spectrometric methods in the field of cancer metabolic research is shown. Using fairly standard lipidomic analysis methods such as lipid extraction, chromatographic separation, and detection by high resolution accurate mass spectrometry, but combining this with the in-depth acquired knowledge about tandem mass spectrometric behaviour of phospholipids, a complex problem can be tackled. In particular, the incorporation of a stable-isotope labelled amino acid precursor into phospholipids is shown, precisely locating the label at the glycerol portion. This reveals a pathway through which cancer cells are able to synthesize phospholipids in order to grow and proliferate even in the harsh conditions of glucose deprivation.

These three approaches show how the field of lipidomics, and in particular its preferred analytical methodology using liquid chromatography coupled to mass spectrometry, is used to aid in revealing not only the structures of lipids, but also their functions, regulatory mechanisms and metabolic pathways. Lipidomics is relevant to many other research fields, which in the future can all be expected to profit tremendously from the advances in lipidomic instrumentation and methodology.

8 REFERENCES

Almeida, R; Pauling, JK; Sokol, E; Hannibal-Bach, HK and Ejsing, CS: *Comprehensive lipidome analysis by shotgun lipidomics on a hybrid quadrupole-orbitrap-linear ion trap mass spectrometer.* Journal of the American Society for Mass Spectrometry, 26(1), pp.133–48. 2015.

Annesley, TM: *Ion Suppression in Mass Spectrometry*. Clinical Chemistry, 49(7), pp.1041–4. 2003.

Anon: *IUPAC-IUB Commission on Biochemical Nomenclature the nomenclature of lipids.* The Journal of biological chemistry, 242(21), pp.4845–9. 1967.

Anon: *IUPAC-IUB Commission on Biochemical Nomenclature. The nomenclature of lipids: notice of revisions.* The Journal of Biological Chemistry, 245(7), p.1511. 1970.

Asakawa, Y; Tokida, N; Ozawa, C; Ishiba, M; Tagaya, O and Asakawa, N: Suppression effects of carbonate on the interaction between stainless steel and phosphate groups of phosphate compounds in high-performance liquid chromatography and electrospray ionization mass spectrometry. Journal of Chromatography A, 1198-1199, pp.80–6. 2008.

Ashraf, MZ and Srivastav, S: *Oxidized Phospholipids: Introduction and Biological Significance*. In G. Kostner, ed. *Lipoproteins - Role in Health and Diseases*. InTech, pp. 409–430. 2012.

Avanti Polar Lipids, I: *LIPID MAPS Certificate of Analysis, Mass Spectrometry Reference Standard 1-(10Z-Heptadecenoyl)-2-Hydroxy-sn-Glycero-3-Phosphocholine*.

Avanti Polar Lipids, I: *Storage & Handling of Lipids*.

Baker, PRS; Armando, AM; Campbell, JL; Quehenberger, O and Dennis, E a: *Three-dimensional enhanced lipidomics analysis combining UPLC, differential ion mobility spectrometry, and mass spectrometric separation strategies.* Journal of Lipid Research, 55(11), pp.2432–42. 2014.

Bang, DY and Moon, MH: *On-line two-dimensional capillary strong anion exchange/reversed phase liquid chromatography–tandem mass spectrometry for comprehensive lipid analysis*. Journal of Chromatography A, 1310, pp.82–90. 2013.

Berger, C; Schmid, PC; Schabitz, W-R; Wolf, M; Schwab, S and Schmid, HHO: *Massive accumulation of N-acylethanolamines after stroke. Cell signalling in acute cerebral ischemia?* Journal of Neurochemistry, 88(5), pp.1159–1167. 2004.

Bligh, E and Dyer, W: *A rapid method of total lipid extraction and purification*. Canadian Journal of Biochemical Physiology, 37(52), p.1978. 1978.

Bochkov, VN; Oskolkova, O V; Birukov, KG; Levonen, A; Binder, CJ and Sto, J: *Generation and Biological Activities of Oxidized Phospholipids*. Antioxidants & Redox Signaling, 12(8), pp.1009–1059. 2010.

Bowden, J a.; Bangma, JT and Kucklick, JR: *Development of an Automated Multi-Injection Shotgun Lipidomics Approach Using a Triple Quadrupole Mass Spectrometer*. Lipids, 49(6), pp.609–619. 2014.

Bruins, AP: *Mass spectrometry with ion sources operating at atmospheric pressure*. Mass Spectrometry Reviews, 10(1), pp.53–77. 1991.

Buszewski, B and Noga, S: *Hydrophilic interaction liquid chromatography (HILIC) - a powerful separation technique*. Analytical and Bioanalytical Chemistry, 402(1), pp.231–47. 2012.

Cadas, H; di Tomaso, E and Piomelli, D: *Occurrence and biosynthesis of endogenous cannabinoid precursor, N-arachidonoyl phosphatidylethanolamine, in rat brain.* The Journal of Neuroscience, 17(4), pp.1226–42. 1997.

Cappiello, A; Famiglini, G; Palma, P; Pierini, E; Termopoli, V and Trufelli, H: *Overcoming Matrix Effects in Liquid Chromatography−Mass Spectrometry*. Analytical Chemistry, 80(23), pp.9343–9348. 2008.

Cappiello, A; Famiglini, G; Palma, P and Siviero, A: *Liquid chromatography-electron ionization mass spectrometry: Fields of application and evaluation of the performance of a direct-ei interface*. Mass Spectrometry Reviews, 24(6), pp.978–989. 2005.

Cech, NB and Enke, CG: *Practical implications of some recent studies in electrospray ionization fundamentals*. Mass Spectrometry Reviews, 20(6), pp.362–387. 2001.

Cífková, E; Holčapek, M; Lísa, M; Ovčačíková, M; Lyčka, A; Lynen, F and Sandra, P: *Nontargeted Quantitation of Lipid Classes Using Hydrophilic Interaction Liquid Chromatography-Electrospray Ionization Mass Spectrometry with Single Internal Standard and Response Factor Approach*. Analytical Chemistry, 84(22), pp.10064–70. 2012.

Cohen, E; Cvitas, T; Frey, J; Holmström, B; Kuchitsu, K; Marquardt, R; Mills, I; Pavese, F; Quack, M; Stohner, J; Strauss, H; Takami, M and Thor, A: *Quantities, Units and Symbols in Physical Chemistry, IUPAC Green Book, 3rd Edition*. Cambridge, UK: IUPAC & RSC Publishing. 2008.

Creer, MH and Gross, RW: *Separation of isomeric lysophospholipids by reverse phase HPLC.* Lipids, 20(12), pp.922–8. 1985.

Crick, FH: *On protein synthesis.* Symposia of the Society for Experimental Biology, 12, pp.138–63. 1958.

D'Arrigo, P and Servi, S: *Synthesis of lysophospholipids*. Molecules, 15, pp.1354–1377. 2010.

Dole, M: *Molecular Beams of Macroions*. The Journal of Chemical Physics, 49(5), p.2240. 1968.

Eberlin, LS; Ferreira, CR; Dill, AL; Ifa, DR and Cooks, RG: *Desorption electrospray ionization mass spectrometry for lipid characterization and biological tissue imaging*. Biochimica et Biophysica Acta, 1811(11), pp.946–60. 2011.

Ejsing, CS; Sampaio, JL; Surendranath, V; Duchoslav, E; Ekroos, K; Klemm, RW; Simons, K and Shevchenko, A: *Global analysis of the yeast lipidome by quantitative shotgun mass spectrometry*. Proceedings of the National Academy of Sciences of the United States of America, 106(7), pp.2136–41. 2009.

Ekroos, K ed.: *Lipidomics*. Wiley-VCH Verlag GmbH & Co. KGaA. 2012.

Eliuk, S and Makarov, A: *Evolution of Orbitrap Mass Spectrometry Instrumentation*. Annual Review of Analytical Chemistry, 8(1), pp.61–80. 2015.

Ellis, SR; Brown, SH; In Het Panhuis, M; Blanksby, SJ and Mitchell, TW: *Surface analysis of lipids by mass spectrometry: More than just imaging*. Progress in Lipid Research, 52(4), pp.329–353. 2013.

Erridge, P: *The Pareto principle*. British Dental Journal, 201(7), pp.419–419. 2006.

Fahy, E; Subramaniam, S; Brown, HA; Glass, CK; Merrill, AH; Murphy, RC; Raetz, CRH; Russell, DW; Seyama, Y; Shaw, W; Shimizu, T; Spener, F; van Meer, G; VanNieuwenhze, MS; White, SH; Witztum, JL and Dennis, E a: *A comprehensive classification system for lipids*. Journal of Lipid Research, 46(5), pp.839–61. 2005.

Fahy, E; Subramaniam, S; Murphy, RC; Nishijima, M; Raetz, CRH; Shimizu, T; Spener, F; van Meer, G; Wakelam, MJO and Dennis, EA: *Update of the LIPID MAPS comprehensive classification system for lipids*. Journal of Lipid Research, 50 Suppl, pp.S9–S14. 2009.

Fauland, A; Köfeler, H; Trötzmüller, M; Knopf, A; Hartler, J; Eberl, A; Chitraju, C; Lankmayr, E and Spener, F: *A comprehensive method for lipid profiling by liquid chromatography-ion cyclotron resonance mass spectrometry*. Journal of Lipid Research, 52(12), pp.2314–22. 2011.

Fauland, A; Trötzmüller, M; Eberl, A; Afiuni-Zadeh, S; Köfeler, H; Guo, X and Lankmayr, E: *An improved SPE method for fractionation and identification of phospholipids*. Journal of Separation Science, 36(4), pp.744–51. 2013.

Fenn, JB; Mann, M; Meng, CK; Wong, SF and Whitehouse, CM: *Electrospray Ionization for Mass Spectrometry of Large Biomolecules*. Science, 246(6), pp.64–71. 1989.

Folch, J; Lees, M and Sloane Stanley, GH: *A Simple Method for the Isolation and Purification of Total Lipides from Animal Tissues*. The Journal of Biological Chemistry, 226(1), pp.497–509. 1957.

Gibson, GTT; Mugo, SM and Oleschuk, RD: *Nanoelectrospray emitters: Trends and perspective*. Mass Spectrometry Reviews, 28(6), pp.918–936. 2009.

Gillum, MP; Zhang, D; Zhang, X; Erion, DM; Jamison, RA; Choi, C; Dong, J; Shanabrough, M; Duenas, HR; Frederick, DW; Hsiao, JJ; Horvath, TL; Lo, CM; Tso, P; Cline, GW and Shulman, GI: *N-acylphosphatidylethanolamine, a Gut-*

Derived Circulating Factor Induced by Fat Ingestion, Inhibits Food Intake. Cell, 135(5), pp.813–824. 2008.

Griffiths, WJ: *Tandem mass spectrometry in the study of fatty acids, bile acids, and steroids*. Mass Spectrometry Reviews, 22(2), pp.81–152. 2003.

Griffiths, WJ; Ogundare, M; Williams, CM and Wang, Y: *On the future of "omics": lipidomics*. Journal of Inherited Metabolic Disease, 34(3), pp.583–592. 2011.

Groessl, M; Graf, S and Knochenmuss, R: *High resolution ion mobility-mass spectrometry for separation and identification of isomeric lipids*. The Analyst, 140(20), pp.6904–6911. 2015.

Gross, JH: *Massenspektrometrie*. Berlin, Heidelberg: Springer Berlin Heidelberg. 2013.

Guan, XL; He, X; Ong, W-Y; Yeo, WK; Shui, G and Wenk, MR: *Non-targeted profiling of lipids during kainate-induced neuronal injury*. The FASEB Journal, 20(8), pp.1152–1161. 2006.

Guan, Z; Li, S; Smith, DC; Shaw, WA and Raetz, CRH: *Identification of N-Acyl Phosphatidylserine Molecules in Eukaryotic Cells*. Biochemistry, 46(50), pp.14500–14513. 2008.

Guo, L; Amarnath, V and Davies, SS: *A liquid chromatography-tandem mass spectrometry method for measurement of N-modified phosphatidylethanolamines*. Analytical Biochemistry, 405(2), pp.236–45. 2010.

Han, X; Yang, K and Gross, RW: *Multi-dimensional mass spectrometry-based shotgun lipidomics and novel strategies for lipidomic analyses*. Mass Spectrometry Reviews, 31, pp.134–178. 2012.

Han, X; Yang, K; Yang, J; Fikes, KN; Cheng, H and Gross, RW: *Factors influencing the electrospray intrasource separation and selective ionization of glycerophospholipids*. Journal of the American Society for Mass Spectrometry, 17(2), pp.264–274. 2006.

Hankin, J a.; Murphy, RC; Barkley, RM and Gijón, M a.: *Ion mobility and tandem mass spectrometry of phosphatidylglycerol and bis(monoacylglycerol) phosphate (BMP)*. International Journal of Mass Spectrometry, 378, pp.255–263. 2015.

Hansen, HH; Hansen, SH; Bjørnsdottir, I and Hansen, HS: *Electrospray ionization mass spectrometric method for the determination of cannabinoid precursors: N-acylethanolamine phospholipids (NAPEs)*. Journal of Mass Spectrometry, 34(7), pp.761–7. 1999.

Hansen, HH; Hansen, SH; Schousboe, A and Hansen, HS: *Determination of the phospholipid precursor of anandamide and other N- acylethanolamine phospholipids before and after sodium azide-induced toxicity in cultured neocortical neurons*. Journal of Neurochemistry, 75(2), pp.861–871. 2000.

Hansen, HH; Ikonomidou, C; Bittigau, P; Hansen, SH and Hansen, HS: *Accumulation of the anandamide precursor and other N-acylethanolamine phospholipids in infant rat*

models of in vivo necrotic and apoptotic neuronal death. Journal of Neurochemistry, 76(1), pp.39–46. 2008.

Hansen, HS and Diep, TA: *N-acylethanolamines, anandamide and food intake.* Biochemical Pharmacology, 78(6), pp.553–60. 2009.

Hansen, HS; Moesgaard, B; Hansen, HH and Petersen, G: *N-Acylethanolamines and precursor phospholipids - relation to cell injury.* Chemistry and Physics of Lipids, 108(1-2), pp.135–50. 2000.

Hartler, J; Trotzmuller, M; Chitraju, C; Spener, F; Kofeler, HC and Thallinger, GG: *Lipid Data Analyzer: unattended identification and quantitation of lipids in LC-MS data*. Bioinformatics, 27(4), pp.572–577. 2011.

Helle, N; Baden, M and Petersen, K: *Automated Solid Phase Extraction*. In pp. 93–129. 2011.

Hennion, M-C: *Solid-phase extraction: method development, sorbents, and coupling with liquid chromatography*. Journal of Chromatography A, 856(1-2), pp.3–54. 1999.

de Hoffmann, E: *Tandem mass spectrometry: A primer*. Journal of Mass Spectrometry, 31(2), pp.129–137. 1996.

Höfle, G; Steglich, W and Vorbrüggen, H: *4-Dialkylaminopyridines as Highly Active Acylation Catalysts. [New synthetic method (25)]*. Angewandte Chemie International Edition in English, 17(8), pp.569–583. 1978.

Holčapek, M; Jirásko, R and Lísa, M: *Recent developments in liquid chromatography-mass spectrometry and related techniques*. Journal of Chromatography A, 1259, pp.3–15. 2012.

Hsu, FF; Lodhi, IJ; Turk, J and Semenkovich, CF: *Structural distinction of diacyl-, alkylacyl, and alk-1-enylacyl glycerophosphocholines as [M-15]- ions by multiple-stage linear ion-trap mass spectrometry with electrospray ionization*. Journal of the American Society for Mass Spectrometry, 25(8), pp.1412–1420. 2014.

Hsu, F-F and Turk, J: *Electrospray ionization multiple-stage linear ion-trap mass spectrometry for structural elucidation of triacylglycerols: assignment of fatty acyl groups on the glycerol backbone and location of double bonds*. Journal of the American Society for Mass Spectrometry, 21(4), pp.657–69. 2010.

Hsu, F-F and Turk, J: *Electrospray ionization with low-energy collisionally activated dissociation tandem mass spectrometry of glycerophospholipids: Mechanisms of fragmentation and structural characterization*. Journal of Chromatography B, 877(26), pp.2673–2695. 2009.

Hsu, F-F; Turk, J; Rhoades, ER; Russell, DG; Shi, Y and Groisman, E a: *Structural characterization of cardiolipin by tandem quadrupole and multiple-stage quadrupole ion-trap mass spectrometry with electrospray ionization*. Journal of the American Society for Mass Spectrometry, 16(4), pp.491–504. 2005.

Hu, Q; Noll, RJ; Li, H; Makarov, A; Hardman, M and Graham Cooks, R: *The Orbitrap: a new mass spectrometer*. Journal of Mass Spectrometry, 40(4), pp.430–43. 2005.

Janfelt, C; Wellner, N; Leger, P-L; Kokesch-Himmelreich, J; Hansen, SH; Charriaut-Marlangue, C and Hansen, HS: *Visualization by mass spectrometry of 2-dimensional changes in rat brain lipids, including N-acylphosphatidylethanolamines, during neonatal brain ischemia*. The FASEB Journal, 26(6), pp.2667–2673. 2012.

Jenkins, B; West, J and Koulman, A: *A Review of Odd-Chain Fatty Acid Metabolism and the Role of Pentadecanoic Acid (C15:0) and Heptadecanoic Acid (C17:0) in Health and Disease*. Molecules, 20(2), pp.2425–2444. 2015.

Kalvodova, L; Sampaio, JL; Cordo, S; Ejsing, CS; Shevchenko, A and Simons, K: *The lipidomes of vesicular stomatitis virus, semliki forest virus, and the host plasma membrane analyzed by quantitative shotgun mass spectrometry.* Journal of Virology, 83(16), pp.7996–8003. 2009.

Kanu, AB; Dwivedi, P; Tam, M; Matz, L and Hill, HH: *Ion mobility-mass spectrometry.* Journal of Mass Spectrometry, 43(1), pp.1–22. 2008.

Kim, J and Hoppel, CL: *Comprehensive approach to the quantitative analysis of mitochondrial phospholipids by HPLC–MS*. Journal of Chromatography B, 912(6), pp.105–114. 2013.

Kingdon, KH: *A Method for the Neutralization of Electron Space Charge by Positive Ionization at Very Low Gas Pressures*. Physical Review, 21(4), pp.408–418. 1923.

Kliman, M; May, JC and McLean, J a: *Lipid analysis and lipidomics by structurally selective ion mobility-mass spectrometry*. Biochimica et Biophysica Acta (BBA) - Molecular and Cell Biology of Lipids, 1811(11), pp.935–945. 2011.

Knittelfelder, OL; Weberhofer, BP; Eichmann, TO; Kohlwein, SD and Rechberger, GN: *A versatile ultra-high performance LC-MS method for lipid profiling*. Journal of Chromatography B, 951-952, pp.119–28. 2014.

Knochenmuss, R: *Ion formation mechanisms in UV-MALDI*. The Analyst, 131(9), p.966. 2006.

Koistinen, KM; Suoniemi, M; Simolin, H and Ekroos, K: *Quantitative lysophospholipidomics in human plasma and skin by LC-MS/MS*. Analytical and bioanalytical chemistry, 407(17), pp.5091–5099. 2015.

Koivusalo, M; Haimi, P; Heikinheimo, L; Kostiainen, R and Somerharju, P: *Quantitative determination of phospholipid compositions by ESI-MS: effects of acyl chain length, unsaturation, and lipid concentration on instrument response*. Journal of Lipid Research, 42(4), pp.663–72. 2001.

Koppenol, WH; Bounds, PL and Dang, C V: *Otto Warburg's contributions to current concepts of cancer metabolism*. Nature Reviews Cancer, 11(5), pp.325–337. 2011.

Kromidas, S: *Handbuch Validierung in der Analytik* 2nd ed. S. Kromidas, ed. Weinheim: Wiley-VCH Verlag GmbH & Co. KGaA. 2011.

Larsen, A; Uran, S; Jacobsen, PB and Skotland, T: *Collision-induced dissociation of glycero phospholipids using electrospray ion-trap mass spectrometry*. Rapid Communications in Mass Spectrometry, 15(24), pp.2393–2398. 2001.

Lee, JY; Min, HK and Moon, MH: *Simultaneous profiling of lysophospholipids and phospholipids from human plasma by nanoflow liquid chromatography-tandem mass spectrometry*. Analytical and Bioanalytical Chemistry, 400(9), pp.2953–61. 2011.

Leithner, K; Hrzenjak, A; Trötzmüller, M; Moustafa, T; Köfeler, HC; Wohlkoenig, C; Stacher, E; Lindenmann, J; Harris, AL; Olschewski, A and Olschewski, H: *PCK2 activation mediates an adaptive response to glucose depletion in lung cancer*. Oncogene, (August 2013), pp.1–7. 2014.

Li, M; Yang, L; Bai, Y and Liu, H: *Analytical Methods in Lipidomics and Their Applications*. Analytical Chemistry, 86(1), pp.161–175. 2014.

Liebisch, G; Binder, M; Schifferer, R; Langmann, T; Schulz, B and Schmitz, G: *High throughput quantification of cholesterol and cholesteryl ester by electrospray ionization tandem mass spectrometry (ESI-MS/MS)*. Biochimica et Biophysica Acta (BBA) - Molecular and Cell Biology of Lipids, 1761(1), pp.121–128. 2006.

Liebisch, G; Ejsing, CS and Ekroos, K: *Identification and Annotation of Lipid Species in Metabolomics Studies Need Improvement*. Clinical Chemistry, 61(12), pp.1542–1544. 2015.

Liebisch, G; Lieser, B; Rathenberg, J; Drobnik, W and Schmitz, G: *High-throughput quantification of phosphatidylcholine and sphingomyelin by electrospray ionization tandem mass spectrometry coupled with isotope correction algorithm*. Biochimica et Biophysica Acta (BBA) - Molecular and Cell Biology of Lipids, 1686(1-2), pp.108–117. 2004.

Liebisch, G and Scherer, M: *Quantification of bioactive sphingo- and glycerophospholipid species by electrospray ionization tandem mass spectrometry in blood*. Journal of Chromatography B, 883-884, pp.141–6. 2012.

Liebisch, G; Vizcaíno, JA; Köfeler, H; Trötzmüller, M; Griffiths, WJ; Schmitz, G; Spener, F and Wakelam, MJO: *Shorthand notation for lipid structures derived from mass spectrometry.* Journal of Lipid Research, 54(6), pp.1523–30. 2013.

Lintonen, TPI; Baker, PRS; Suoniemi, M; Ubhi, BK; Koistinen, KM; Duchoslav, E; Campbell, JL and Ekroos, K: *Differential mobility spectrometry-driven shotgun lipidomics.* Analytical Chemistry, 86(19), pp.9662–9. 2014.

Lísa, M; Cífková, E and Holčapek, M: *Lipidomic profiling of biological tissues using off-line two-dimensional high-performance liquid chromatography-mass spectrometry*. Journal of Chromatography A, 1218(31), pp.5146–56. 2011.

Lísa, M and Holčapek, M: *Characterization of triacylglycerol enantiomers using chiral HPLC/APCI-MS and synthesis of enantiomeric triacylglycerols*. Analytical Chemistry, 85, pp.1852–1859. 2013.

Lísa, M and Holčapek, M: *High-Throughput and Comprehensive Lipidomic Analysis Using Ultrahigh-Performance Supercritical Fluid Chromatography–Mass Spectrometry*. Analytical Chemistry, 87(14), pp.7187–7195. 2015.

Lisa, M; Velinska, H and Holcapek, M: *Regioisomeric Characterization of Triacylglycerols Using Silver-Ion HPLC / MS and Randomization*. Analytical Chemistry, 81(10), pp.3903–3910. 2009.

Löffler, G: *Basiswissen Biochemie* 6. Auflage. Springer Medizin Verlag. 2004.

Lottspeich, F: *Bioanalytik* H. Zorbas, ed. Heidelberg: Spektrum Akademischer Verlag. 1998.

Lydic, T a; Busik, J V and Reid, GE: *A monophasic extraction strategy for the simultaneous lipidome analysis of polar and nonpolar retina lipids.* Journal of Lipid Research, 55, pp.1797–1809. 2014.

Maccarone, AT; Duldig, J; Mitchell, TW; Blanksby, SJ; Duchoslav, E and Campbell, JL: *Characterization of acyl chain position in unsaturated phosphatidylcholines using differential mobility-mass spectrometry.* Journal of Lipid Research, 55(8), pp.1668–1677. 2014.

Makarov, A: *Electrostatic Axially Harmonic Orbital Trapping: A High-Performance Technique of Mass Analysis*. Analytical Chemistry, 72(6), pp.1156–62. 2000.

Marshall, AG and Hendrickson, CL: *Fourier transform ion cyclotron resonance detection: principles and experimental configurations*. International Journal of Mass Spectrometry, 215(1-3), pp.59–75. 2002.

Matyash, V; Liebisch, G; Kurzchalia, T V; Shevchenko, A and Schwudke, D: *Lipid extraction by methyl-tert-butyl ether for high-throughput lipidomics*. Journal of Lipid Research, 49(5), pp.1137–46. 2008.

McDonnell, LA and Heeren, RMA: *Imaging mass spectrometry*. Mass Spectrometry Reviews, 26(4), pp.606–643. 2007.

McIntyre, TM; Zimmerman, G a. and Prescott, SM: *Biologically Active Oxidized Phospholipids*. Journal of Biological Chemistry, 274(36), pp.25189–25192. 1999.

McLafferty, FW; Stauffer, DA; Loh, SY and Wesdemiotis, C: *Unknown identification using reference mass spectra. Quality evaluation of databases.* Journal of the American Society for Mass Spectrometry, 10(12), pp.1229–40. 1999.

McLean, JA; Ridenour, WB and Caprioli, RM: *Profiling and imaging of tissues by imaging ion mobility-mass spectrometry*. Journal of Mass Spectrometry, 42(8), pp.1099–1105. 2007.

Mena-Bravo, A; Priego-Capote, F and Luque de Castro, MD: *Two-dimensional liquid chromatography coupled to tandem mass spectrometry for vitamin D metabolite profiling including the C3-epimer-25-monohydroxyvitamin D3*. Journal of Chromatography A, 1451, pp.50–57. 2016.

Meullemiestre, A; Breil, C; Abert-Vian, M and Chemat, F: *Microwave, ultrasound, thermal treatments, and bead milling as intensification techniques for extraction of lipids from oleaginous Yarrowia lipolytica yeast for a biojetfuel application*. Bioresource Technology, 211, pp.190–199. 2016.

Meyer, VR: *Practical high-performance liquid chromatography* 2nd ed. John Wiley & Sons, Ltd. 2010.

Moss, GP: *The nomenclature of lipids (Recommendations 1976) IUPAC-IUB Commission on Biochemical Nomenclature.* The Biochemical Journal, 171(1), pp.21–35. 1978.

Moss, GP; Smith, PAS and Tavernier, D: *Glossary of class names of organic compounds and reactivity intermediates based on structure (IUPAC Recommendations 1995)*. Pure and Applied Chemistry, 67(8-9). 1995.

Murph, M; Tanaka, T; Pang, J; Felix, E; Liu, S; Trost, R; Godwin, AK; Newman, R and Mills, G: *Liquid Chromatography Mass Spectrometry for Quantifying Plasma Lysophospholipids: Potential Biomarkers for Cancer Diagnosis*. In *Methods in Enzymology*. pp. 1–25. 2007.

Murphy, RC ed.: *Tandem Mass Spectrometry of Lipids: Molecular Analysis of Complex Lipids*. Cambridge, UK: The Royal Society of Chemistry. 2015.

Murphy, RC; Hankin, JA; Barkley, RM and Zemski Berry, KA: *MALDI imaging of lipids after matrix sublimation/deposition*. Biochimica et Biophysica Acta (BBA) - Molecular and Cell Biology of Lipids, 1811(11), pp.970–975. 2011.

Murphy, RC; James, PF; McAnoy, AM; Krank, J; Duchoslav, E and Barkley, RM: *Detection of the abundance of diacylglycerol and triacylglycerol molecular species in cells using neutral loss mass spectrometry.* Analytical Biochemistry, 366(1), pp.59–70. 2007.

Murray, KK; Seneviratne, CA and Ghorai, S: *High Resolution Laser Mass Spectrometry Bioimaging*. Methods, (March). 2016.

Nič, M; Jirát, J; Košata, B; Jenkins, A and McNaught, A eds.: *IUPAC Compendium of Chemical Terminology*. Research Triagle Park, NC: IUPAC. 2009.

Nye, CK; Hanson, RW and Kalhan, SC: *Glyceroneogenesis is the dominant pathway for triglyceride glycerol synthesis in vivo in the rat*. Journal of Biological Chemistry, 283(41), pp.27565–27574. 2008.

Okudaira, M; Inoue, A; Shuto, A; Nakanaga, K; Kano, K; Makide, K; Saigusa, D; Tomioka, Y and Aoki, J: *Separation and quantification of 2-acyl-1-lysophospholipids and 1-acyl-2-lysophospholipids in biological samples by LC-MS/MS*. Journal of Lipid Research, 55(10), pp.2178–2192. 2014.

Paglia, G; Kliman, M; Claude, E; Geromanos, S and Astarita, G: *Applications of ion-mobility mass spectrometry for lipid analysis*. Analytical and Bioanalytical Chemistry, 407(17), pp.4995–5007. 2015.

Passarelli, MK and Winograd, N: *Lipid imaging with time-of-flight secondary ion mass spectrometry (ToF-SIMS).* Biochimica et Biophysica Acta, 1811(11), pp.976–90. 2011.

Pellegrino, RM; Di Veroli, A; Valeri, A; Goracci, L and Cruciani, G: *LC/MS lipid profiling from human serum: a new method for global lipid extraction*. Analytical and Bioanalytical Chemistry, 406(30), pp.7937–7948. 2014.

Pizarro, C; Arenzana-Rámila, I; Pérez-del-Notario, N; Pérez-Matute, P and González-Sáiz, J-M: *Plasma Lipidomic Profiling Method Based on Ultrasound Extraction and Liquid Chromatography Mass Spectrometry*. Analytical Chemistry, 85(24), pp.12085–12092. 2013.

Prakash, C; Shaffer, CL and Nedderman, A: *Analytical Strategies for identifying drug metabolites*. Mass Spectrometry Reviews, 26, pp.340–369. 2007.

Pulfer, M and Murphy, RC: *Electrospray mass spectrometry of phospholipids*. Mass Spectrometry Reviews, 22(5), pp.332–64. 2003.

Quehenberger, O; Armando, AM; Brown, AH; Milne, SB; Myers, DS; Merrill, a. H; Bandyopadhyay, S; Jones, KN; Kelly, S; Shaner, RL; Sullards, CM; Wang, E; Murphy, RC; Barkley, RM; Leiker, TJ; Raetz, CRH; Guan, Z; Laird, GM; Six, D a.; et al.: *Lipidomics reveals a remarkable diversity of lipids in human plasma*. The Journal of Lipid Research, 51(11), pp.3299–3305. 2010.

Reis, A; Rudnitskaya, A; Blackburn, GJ; Mohd Fauzi, N; Pitt, AR and Spickett, CM: *A comparison of five lipid extraction solvent systems for lipidomic studies of human LDL*. Journal of Lipid Research, 54(7), pp.1812–24. 2013.

Rohner, TC; Staab, D and Stoeckli, M: *MALDI mass spectrometric imaging of biological tissue sections*. Mechanisms of Ageing and Development, 126(1), pp.177–185. 2005.

Sandra, K and Sandra, P: *Lipidomics from an analytical perspective*. Current Opinion in Chemical Biology, 17(5), pp.847–853. 2013.

Sarafian, MH; Gaudin, M; Lewis, MR; Martin, F; Holmes, E; Nicholson, JK and Dumas, M: *Objective Set of Criteria for Optimization of Sample Preparation Procedures for Ultra-High Throughput Untargeted Blood Plasma Lipid Profiling by Ultra Performance Liquid Chromatography–Mass Spectrometry*. Analytical Chemistry, 86(12), pp.5766–5774. 2014.

Schmid, PC; Kuwae, T; Krebsbach, RJ and Schmid, HHO: *Anandamide and other N-acylethanolamines in mouse peritoneal macrophages*. Chemistry and Physics of Lipids, 87(2), pp.103–110. 1997.

Schuhmann, K; Almeida, R; Baumert, M; Herzog, R; Bornstein, SR and Shevchenko, A: *Shotgun lipidomics on a LTQ Orbitrap mass spectrometer by successive switching between acquisition polarity modes*. Journal of Mass Spectrometry, 47(1), pp.96–104. 2012.

Schulze, A and Harris, AL: *How cancer metabolism is tuned for proliferation and vulnerable to disruption*. Nature, 491(7424), pp.364–373. 2012.

Schwalbe-Herrmann, M; Willmann, J and Leibfritz, D: *Separation of phospholipid classes by hydrophilic interaction chromatography detected by electrospray ionization mass spectrometry*. Journal of Chromatography A, 1217(32), pp.5179–83. 2010.

Scigelova, M; Hornshaw, M; Giannakopulos, A and Makarov, A: *Fourier Transform Mass Spectrometry*. Molecular & Cellular Proteomics, 10(7). 2011.

Shvartsburg, A a; Isaac, G; Leveque, N; Smith, RD and Metz, TO: *Separation and classification of lipids using differential ion mobility spectrometry.* Journal of the American Society for Mass Spectrometry, 22(7), pp.1146–55. 2011.

Sokol, E; Ulven, T; Faergeman, NJ and Ejsing, CS: *Comprehensive and quantitative profiling of lipid species in human milk, cow milk and a phospholipid-enriched milk formula by GC and MS/MS ALL*. European Journal of Lipid Science and Technology, 117(6), pp.751–759. 2015.

Sud, M; Fahy, E; Cotter, D; Brown, A; Dennis, EA; Glass, CK; Merrill, AH; Murphy, RC; Raetz, CRH; Russell, DW and Subramaniam, S: *LMSD: LIPID MAPS structure database*. Nucleic Acids Research, 35(Database), pp.D527–D532. 2007.

Sugiura, T; Kondo, S; Sukagawa, A; Tonegawa, T; Nakane, S; Yamashita, A; Ishima, Y and Waku, K: *Transacylase-Mediated and Phosphodiesterase-Mediated Synthesis of N -Arachidonoylethanolamine, an Endogenous Cannabinoid-Receptor Ligand, in Rat Brain Microsomes*. European Journal of Biochemistry, 240(1), pp.53–62. 1996.

Sugiura, T; Kondo, S; Sukagawa, A; Tonegawa, T; Nakane, S; Yamashita, A and Waku, K: *Enzymatic synthesis of anandamide, an endogenous cannabinoid receptor ligand, through N-acylphosphatidylethanolamine pathway in testis: involvement of Ca(2+)-dependent transacylase and phosphodiesterase activities*. Biochemical and Biophysical Research Communications, 218(1), pp.113–7. 1996.

Sun, C; Zhao, YY and Curtis, JM: *The direct determination of double bond positions in lipid mixtures by liquid chromatography/in-line ozonolysis/mass spectrometry*. Analytica Chimica Acta, 762, pp.68–75. 2013.

Tabb, DL; Shah, MB; Strader, MB; Connelly, HM; Hettich, RL and Hurst, GB: *Determination of peptide and protein ion charge states by fourier transformation of isotope-resolved mass spectra*. Journal of the American Society for Mass Spectrometry, 17(7), pp.903–915. 2006.

Takats, Z: *Mass Spectrometry Sampling Under Ambient Conditions with Desorption Electrospray Ionization*. Science, 306(5695), pp.471–473. 2004.

Tang, K; Page, JS and Smith, RD: *Charge competition and the linear dynamic range of detection in electrospray ionization mass spectrometry*. Journal of the American Society for Mass Spectrometry, 15(10), pp.1416–1423. 2004.

Taylor, G: *Disintegration of Water Drops in an Electric Field*. Proceedings of the Royal Society A: Mathematical, Physical and Engineering Sciences, 280(1382), pp.383–397. 1964.

Thermo Fisher Scientific Inc.: *Orbitrap Fusion™ Lumos™ Tribrid™ Mass Spectrometer*.

Todd, JFJ: *Recommendations for nomenclature and symbolism for mass spectroscopy (including an appendix of terms used in vacuum technology). (Recommendations 1991)*. Pure and Applied Chemistry, 63(10). 1991.

Triebl, A; Trötzmüller, M; Eberl, A; Hanel, P; Hartler, J and Köfeler, HC: *Quantitation of phosphatidic acid and lysophosphatidic acid molecular species using hydrophilic interaction liquid chromatography coupled to electrospray ionization high resolution mass spectrometry.* Journal of Chromatography A, 1347, pp.104–10. 2014.

Triebl, A; Weissengruber, S; Trötzmüller, M; Lankmayr, E and Köfeler, H: *Quantitative analysis of N -acylphosphatidylethanolamine molecular species in rat brain using solid-phase extraction combined with reversed-phase chromatography and tandem mass spectrometry*. Journal of Separation Science, 39(13), pp.2474–2480. 2016.

Trufelli, H; Palma, P; Famiglini, G and Cappiello, A: *An overview of matrix effects in liquid chromatography-mass spectrometry.* Mass Spectrometry Reviews, 30(3), pp.491–509. 2011.

Ueda, N; Tsuboi, K and Uyama, T: *Metabolism of endocannabinoids and related N-acylethanolamines: canonical and alternative pathways.* The FEBS journal, 280(9), pp.1874–94. 2013.

Urban, J; Afseth, NK and Štys, D: *Fundamental definitions and confusions in mass spectrometry about mass assignment, centroiding and resolution*. TrAC Trends in Analytical Chemistry, 53, pp.126–136. 2014.

Vas, G and Vékey, K: *Solid-phase microextraction: a powerful sample preparation tool prior to mass spectrometric analysis*. Journal of Mass Spectrometry, 39(3), pp.233–254. 2004.

Vaz, FM; Pras-Raves, M; Bootsma, AH and van Kampen, AHC: *Principles and practice of lipidomics*. Journal of Inherited Metabolic Disease, 38(1), pp.41–52. 2015.

Wakamatsu, A; Morimoto, K; Shimizu, M and Kudoh, S: *A severe peak tailing of phosphate compounds caused by interaction with stainless steel used for liquid chromatography and electrospray mass spectrometry*. Journal of Separation Science, 28(14), pp.1823–30. 2005.

Wakelam, MJO: *The uses and limitations of the analysis of cellular phosphoinositides by lipidomic and imaging methodologies*. Biochimica et Biophysica Acta (BBA) - Molecular and Cell Biology of Lipids, 1841(8), pp.1102–1107. 2014.

Wang, C; Wang, M and Han, X: *Comprehensive and Quantitative Analysis of Lysophospholipid Molecular Species Present in Obese Mouse Liver by Shotgun Lipidomics*. Analytical Chemistry, 87(9), pp.4879–4887. 2015.

Wang, J and Ueda, N: *Biology of endocannabinoid synthesis system*. Prostaglandins and Other Lipid Mediators, 89(3-4), pp.112–119. 2009.

Wellner, N; Diep, TA; Janfelt, C and Hansen, HS: *N-acylation of phosphatidylethanolamine and its biological functions in mammals*. Biochimica et Biophysica Acta (BBA) - Molecular and Cell Biology of Lipids, 1831(3), pp.652–662. 2013.

Wellner, N; Tsuboi, K; Madsen, AN; Holst, B; Diep, TA; Nakao, M; Tokumura, A; Burns, MP; Deutsch, DG; Ueda, N and Hansen, HS: *Studies on the anorectic effect of N-acylphosphatidylethanolamine and phosphatidylethanolamine in mice*. Biochimica et Biophysica Acta (BBA) - Molecular and Cell Biology of Lipids, 1811(9), pp.508–512. 2011.

Wenk, MR: *The emerging field of lipidomics.* Nature Reviews Drug Discovery, 4(7), pp.594–610. 2005.

Wieser, ME; Holden, N; Coplen, TB; Böhlke, JK; Berglund, M; Brand, WA; Bièvre, P De; Gröning, M; Loss, RD and Meija, J: *Atomic weights of the elements 2011 (IUPAC Technical Report)*. Pure and Applied Chemistry, 85(5), pp.1047–1078. 2013.

Wilm, M: *Principles of Electrospray Ionization*. Molecular & Cellular Proteomics, 10(7), p.M111.009407. 2011.

Yang, K; Cheng, H; Gross, RW and Han, X: *Automated Lipid Identification and Quantification by Multidimensional Mass Spectrometry-Based Shotgun Lipidomics*. Analytical Chemistry, 81(11), pp.4356–4368. 2009.

Yang, L; Li, M; Shan, Y; Shen, S; Bai, Y and Liu, H: *Recent advances in lipidomics for disease research*. Journal of Separation Science, 39(1). 2015.

Yang, Y-H; Lee, K; Jang, K-S; Kim, Y-G; Park, S-H; Lee, C-S and Kim, B-G: *Low mass cutoff evasion with q(z) value optimization in ion trap*. Analytical Biochemistry, 387(1), pp.133–5. 2009.

Zhao, Z and Xu, Y: *An extremely simple method for extraction of lysophospholipids and phospholipids from blood samples*. Journal of Lipid Research, 51(3), pp.652–659. 2010.

Zheng, L; Kind, RT; Decuypere, S; Freyend, SJ Von; Coombs, GH and Watson, DG: *Profiling of lipids in Leishmania donovani using hydrophilic interaction chromatography in combination with Fourier transform mass spectrometry*. Rapid Communications in Mass Spectrometry, 24, pp.2074–2082. 2010.

Zhu, C; Dane, A; Spijksma, G; Wang, M; van der Greef, J; Luo, G; Hankemeier, T and Vreeken, RJ: *An efficient hydrophilic interaction liquid chromatography separation of 7 phospholipid classes based on a diol column*. Journal of Chromatography A, 1220, pp.26–34. 2012.

Zook, DR and Bruins, AP: *On cluster ions, ion transmission, and linear dynamic range limitations in electrospray (ionspray) mass spectrometry*. International Journal of Mass Spectrometry and Ion Processes, 162(1-3), pp.129–147. 1997.

Zubarev, RA and Makarov, A: *Orbitrap Mass Spectrometry*. Analytical Chemistry, 85(11), pp.5288–5296. 2013.

APPENDIX

PUBLICATION RECORD (SEPTEMBER 2016)

Triebl, A; Weissengruber, S; Trötzmüller, M; Lankmayr, E and Köfeler, HC: Quantitative analysis of N-acylphosphatidylethanolamine molecular species in rat brain using solid-phase extraction combined with reversed-phase chromatography and tandem mass spectrometry. Journal of Separation Science, 39(13), pp.2474–2480. 2016.

Meshcheryakova, A; Svoboda, M; Tahir, A; Köfeler, HC; Triebl, A; Mungenast, F; Heinze, G; Gerner, C; Zimmermann, P; Jaritz, M and Mechtcheriakova, D: Exploring the role of sphingolipid machinery during the epithelial to mesenchymal transition program using an integrative approach. Oncotarget, 7(16), pp.22295–323. 2016.

Sala, P; Pötz, S; Brunner, M; Trötzmüller, M; Fauland, A; Triebl, A; Hartler, J; Lankmayr, E and Köfeler, HC: Determination of Oxidized Phosphatidylcholines by Hydrophilic Interaction Liquid Chromatography Coupled to Fourier Transform Mass Spectrometry. International Journal of Molecular Sciences, 16, pp.8351–8363. 2015.

Tripolt, NJ; Leber, B; Triebl, A; Köfeler, H; Stadlbauer, V and Sourij, H: Effect of Lactobacillus casei Shirota supplementation on trimethylamine-N-oxide levels in patients with metabolic syndrome: An open-label, randomized study. Atherosclerosis, 242(1), pp.141–144. 2015.

Triebl, A; Trötzmüller, M; Eberl, A; Hanel, P; Hartler, J and Köfeler, HC: Quantitation of phosphatidic acid and lysophosphatidic acid molecular species using hydrophilic interaction liquid chromatography coupled to electrospray ionization high resolution mass spectrometry. Journal of Chromatography A, 1347, pp.104–10. 2014.

ORAL PRESENTATIONS

Triebl, A; Trötzmüller, M; Leithner, K and Köfeler, HC: High resolution tandem mass spectrometry in cancer metabolism research. 27th MassSpec Forum Vienna, Feb. 23rd 2016, Vienna, Austria. (awarded Biemann-Viehböck-Award for the best oral presentation of a Young Scientist)

Triebl, A; Trötzmüller, M; Hartler, J; Thallinger, GG and Köfeler, HC: Automated identification of lipids using MS2 data. MassSpec Forum Vienna 2015, 17.02.-18.02.2015, Vienna, Austria.

POSTERS

Triebl, A; Trötzmüller, M and Köfeler, HC: Determination of N-Acyl-Phosphatidylethanolamines using SPE and HPLC-SRM Detection. 5th European Lipidomic Meeting, 2nd – 4th September 2015, Swansea, United Kingdom.

Triebl, A; Trötzmüller, M; Hartler, J; and Köfeler, HC: Triglyceride analysis of complex biological samples using HPLC-HR/AM-MS/MS. 4th European Lipidomic Meeting, September 22 - 24, 2014, Graz, Austria. (awarded Poster Award for second best poster presentation)

LIPID STANDARDS

Supplementary Table 1: Lipid standards used for generation of tandem mass spectra.

Lipid species	*sn*-1	*sn*-2	*sn*-3	Name
PI 25:0	12:0	13:0	-	1-dodecanoyl-2-tridecanoyl-sn-glycero-3-phospho-(1'-myo-inositol) (ammonium salt)
PI 31:1	17:0	14:1	-	1-heptadecanoyl-2-(9Z-tetradecenoyl)-sn-glycero-3-phospho-(1'-myo-inositol) (ammonium salt)
PI 37:4	17:0	20:4	-	1-heptadecanoyl-2-(5Z,8Z,11Z,14Z-eicosatetraenoyl)-sn-glycero-3-phospho-(1'-myo-inositol) (ammonium salt)
PI 43:6	21:0	22:6	-	1-heneicosanoyl-2-(4Z,7Z,10Z,13Z,16Z,19Z-docosahexaenoyl)-sn-glycero-3-phospho-(1'-myo-inositol) (ammonium salt)
PC P-36:1	(P)	18:1	-	1-(1Z-octadecenyl)-2-oleoyl-sn-glycero-3-phosphocholine
PC P-38:4	(P)	20:4	-	1-(1Z-octadecenyl)-2-arachidonoyl-sn-glycero-3-phosphocholine
PC P-40:6	(P)	22:6	-	1-(1Z-octadecenyl)-2-docosahexaenoyl-sn-glycero-3-phosphocholine
PE P-36:1	(P)	18:1	-	1-(1Z-octadecenyl)-2-oleoyl-sn-glycero-3-phosphoethanolamine
PE P-38:4	(P)	20:4	-	1-(1Z-octadecenyl)-2-arachidonoyl-sn-glycero-3-phosphoethanolamine
PE P-40:6	(P)	22:6	-	1-(1Z-octadecenyl)-2-docosahexaenoyl-sn-glycero-3-phosphoethanolamine
LPC 13:0	13:0	-	-	1-tridecanoyl-2-hydroxy-sn-glycero-3-phosphocholine
LPC 14:0	14:0	-	-	1-myristoyl-2-hydroxy-sn-glycero-3-phosphocholine
LPC 15:0	15:0	-	-	1-pentadecanoyl-2-hydroxy-sn-glycero-3-phosphocholine
LPC 16:0	16:0	-	-	1-palmitoyl-2-hydroxy-sn-glycero-3-phosphocholine
LPC 18:0	18:0	-	-	1-stearoyl-2-hydroxy-sn-glycero-3-phosphocholine
LPC 18:1	18:1	-	-	1-oleoyl-2-hydroxy-sn-glycero-3-phosphocholine
LPE 14:0	14:0	-	-	1-myristoyl-2-hydroxy-sn-glycero-3-phosphoethanolamine
LPE 16:0	16:0	-	-	1-palmitoyl-2-hydroxy-sn-glycero-3-phosphoethanolamine
LPE 18:0	18:0	-	-	1-Stearoyl-2-Hydroxy-sn-Glycero-3-Phosphoethanolamine
LPE 18:1	18:1	-	-	1-oleoyl-2-hydroxy-sn-glycero-3-phosphoethanolamine
PS 32:0	16:0	16:0	-	1,2-dipalmitoyl-sn-glycero-3-phospho-L-serine (sodium salt)
PS 34:0	17:0	17:0	-	1,2-diheptadecanoyl-sn-glycero-3-phospho-L-serine (sodium salt)
PS 34:1	16:0	18:1	-	1-palmitoyl-2-oleoyl-sn-glycero-3-phospho-L-serine (sodium salt)
PS 34:2	16:0	18:2	-	1-palmitoyl-2-linoleoyl-sn-glycero-3-phospho-L-serine (sodium salt)
PS 36:0	18:0	18:0	-	1,2-distearoyl-sn-glycero-3-phospho-L-serine (sodium salt)
PS 36:1	18:0	18:1	-	1-stearoyl-2-oleoyl-sn-glycero-3-phospho-L-serine (sodium salt)
PS 36:2	18:0	18:2	-	1-stearoyl-2-linoleoyl-sn-glycero-3-phospho-L-serine (sodium salt)

PS 36:2	18:1	18:1	-	1,2-dioleoyl-sn-glycero-3-phospho-L-serine (sodium salt)
LPS 16:0	16:0	-	-	1-palmitoyl-2-hydroxy-sn-glycero-3-phospho-L-serine (sodium salt)
LPS 17:1	17:1	-	-	1-(10Z-heptadecenoyl)-2-hydroxy-sn-glycero-3-[phospho-L-serine] (sodium salt)
LPS 18:0	18:0	-	-	1-stearoyl-2-hydroxy-sn-glycero-3-phospho-L-serine (sodium salt)
LPS 18:1	18:1	-	-	1-oleoyl-2-hydroxy-sn-glycero-3-phospho-L-serine (sodium salt)
PC 31:1	17:0	14:1	-	1-heptadecanoyl-2-(9Z-tetradecenoyl)-sn-glycero-3-phosphocholine
PC 32:0	14:0	18:0	-	1-myristoyl-2-stearoyl-sn-glycero-3-phosphocholine
PC 32:0	16:0	16:0	-	1,2-dipalmitoyl-sn-glycero-3-phosphocholine
PC 32:0	18:0	14:0	-	1-stearoyl-2-myristoyl-sn-glycero-3-phosphocholine
PC 32:1	18:1	14:0	-	1-oleoyl-2-myristoyl-sn-glycero-3-phosphocholine
PC 34:0	16:0	18:0	-	1-palmitoyl-2-stearoyl-sn-glycero-3-phosphocholine
PC 34:0	17:0	17:0	-	1,2-diheptadecanoyl-sn-glycero-3-phosphocholine
PC 34:0	18:0	16:0	-	1-stearoyl-2-palmitoyl-sn-glycero-3-phosphocholine
PC 34:1	16:0	18:1	-	1-palmitoyl-2-oleoyl-sn-glycero-3-phosphocholine
PC 34:1	18:1	16:0	-	1-oleoyl-2-palmitoyl-sn-glycero-3-phosphocholine
PC 36:0	18:0	18:0	-	1,2-distearoyl-sn-glycero-3-phosphocholine
PC 36:1	18:0	18:1	-	1-stearoyl-2-oleoyl-sn-glycero-3-phosphocholine
PC 36:1	18:1	18:0	-	1-oleoyl-2-stearoyl-sn-glycero-3-phosphocholine
PC 36:2	18:0	18:2	-	1-stearoyl-2-linoleoyl-sn-glycero-3-phosphocholine
PC 36:2	18:1	18:1	-	1,2-dioleoyl-sn-glycero-3-phosphocholine
PC 40:0	20:0	20:0	-	1,2-diarachidoyl-sn-glycero-3-phosphocholine
PC 40:6	18:0	22:6	-	1-stearoyl-2-docosahexaenoyl-sn-glycero-3-phosphocholine
PC 48:2	24:1	24:1	-	1,2-dinervonoyl-sn-glycero-3-phosphocholine
PE 32:0	16:0	16:0	-	1,2-dipalmitoyl-sn-glycero-3-phosphoethanolamine
PE 34:0	17:0	17:0	-	1,2-diheptadecanoyl-sn-glycero-3-phosphoethanolamine
PE 34:1	16:0	18:1	-	1-palmitoyl-2-oleoyl-sn-glycero-3-phosphoethanolamine
PE 36:0	18:0	18:0	-	1,2-distearoyl-sn-glycero-3-phosphoethanolamine
PE 36:1	18:0	18:1	-	1-stearoyl-2-oleoyl-sn-glycero-3-phosphoethanolamine
PE 36:2	18:0	18:2	-	1-stearoyl-2-linoleoyl-sn-glycero-3-phosphoethanolamine
PE 36:2	18:1	18:1	-	1,2-dioleoyl-sn-glycero-3-phosphoethanolamine
PE 36:4	16:0	20:4	-	1-palmitoyl-2-arachidonoyl-sn-glycero-3-phosphoethanolamine
PE 36:4	18:2	18:2	-	1,2-dilinoleoyl-sn-glycero-3-phosphoethanolamine
PE 43:6	21:0	22:6		1-heneicosanoyl-2-(4Z,7Z,10Z,13Z,16Z,19Z-docosahexaenoyl)-sn-glycero-3-phosphoethanolamine
PG 32:0	16:0	16:0	-	1,2-dipalmitoyl-sn-glycero-3-phospho-(1'-rac-glycerol) (sodium salt)
PG 34:0	17:0	17:0	-	1,2-diheptadecanoyl-sn-glycero-3-phospho-(1'-rac-glycerol) (sodium salt)
PG 34:1	16:0	18:1	-	1-palmitoyl-2-oleoyl-sn-glycero-3-phospho-(1'-rac-glycerol) (sodium salt)
PG 36:0	18:0	18:0	-	1,2-distearoyl-sn-glycero-3-phospho-(1'-rac-glycerol) (sodium salt)

PG 36:1	18:0	18:1	-	1-stearoyl-2-oleoyl-sn-glycero-3-phospho-(1'-rac-glycerol) (sodium salt)
PG 36:2	18:1	18:1	-	1,2-dioleoyl-sn-glycero-3-phospho-(1'-rac-glycerol) (sodium salt)
PG 36:2	18:0	18:2	-	1-stearoyl-2-linoleoyl-sn-glycero-3-phospho-(1'-rac-glycerol) (sodium salt)
DG 24:0	12:0	12:0	-	1,2-didodecanoyl-sn-glycerol
DG 32:0	16:0	16:0	-	1,2-dipalmitoyl-sn-glycerol
DG 34:0	18:0	16:0	-	1-octadecanoyl-2-hexadecanoyl-sn-glycerol
DG 34:1	16:0	-	18:1	1-Palmitin-3-Olein
DG 36:0	18:0	18:0	-	1,2-dioctadecanoyl-sn-glycerol
DG 36:2	18:1	-	18:1	1,3-di-(9E-octadecenoyl)-glycerol
DG 36:4	18:2	-	18:2	1,3-di-(9Z,12Z-octadecadienoyl)-glycerol
DG 38:0	20:0	18:0	-	1-eicosanoyl-2-octadecanoyl-sn-glycerol
TG 48:0	16:0	16:0	16:0	1,2,3-trihexadecanoyl-glycerol
TG 50:0	16:0	16:0	18:0	1,2-dihexadecanoyl-3-octadecanoyl-sn-glycerol
TG 50:0d5	16:0	18:0	16:0	1,3(d5)-dihexadecanoyl-2-octadecanoyl-glycerol
TG 50:0d5	19:0	12:0	19:0	1,3(d5)-dinonadecanoyl-2-dodecanoyl-glycerol
TG 50:1	16:0	16:0	18:1	1,2-dihexadecanoyl-3-(9Z-octadecenoyl)-sn-glycerol
TG 50:1	16:0	18:1	16:0	1,3-dihexadecanoyl-2-(9Z-octadecenoyl)-glycerol
TG 44:1d5	14:0	16:1	14:0	
TG 48:1d5	15:0	18:1	15:0	
TG 50:0d5	16:0	18:0	16:0	
TG 50:0d5	19:0	12:0	19:0	
TG 51:1d5	17:0	17:1	17:0	LM6000 (Avanti Polar Lipids)
TG 58:7d5	20:2	18:3	20:2	
TG 58:10d5	20:4	18:2	20:4	
TG 60:1d5	20:0	20:1	20:0	
TG 62:16d5	20:5	22:6	20:5	
SM 18:0				N-stearoyl-D-erythro-sphingosylphosphorylcholine
SM 18:1				N-oleoyl-D-erythro-sphingosylphosphorylcholine
SM 24:0				N-lignoceroyl-D-erythro-sphingosylphosphorylcholine
SM 24:1				N-nervonoyl-D-erythro-sphingosylphosphorylcholine
Cer 16:0				N-palmitoyl-D-erythro-sphingosine
Cer 17:0				N-heptadecanoyl-D-erythro-sphingosine
Cer 18:0				N-stearoyl-D-erythro-sphingosine
Cer 18:1				N-oleoyl-D-erythro-sphingosine
Cer 20:0				N-arachidoyl-D-erythro-sphingosine

Supplementary Table 2: LIPID MAPS quantitative internal standards (Avanti Polar Lipids Inc., Alabaster, AL, USA).

Lipid species	IUPAC name
PC 25:0	1-dodecanoyl-2-tridecanoyl-*sn*-glycero-3-phosphocholine
PC 31:1	1-heptadecanoyl-2-(9Z-tetradecenoyl)-*sn*-glycero-3-phosphocholine
PC 37:4	1-heptadecanoyl-2-(5*Z*,8*Z*,11*Z*,14Z-icosatetraenoyl)-sn-glycero-3-phosphocholine
PC 43:6	1-henicosanoyl-2-(4Z,7Z,10Z,13Z,16Z,19Z-docosahexaenoyl)-sn-glycero-3-phosphocholine
LPC 17:1	1-(10Z-heptadecenoyl)-2-hydroxy-sn-glycero-3-phosphocholine
PE 25:0	1-dodecanoyl-2-tridecanoyl-sn-glycero-3-phosphoethanolamine
PE 31:1	1-heptadecanoyl-2-(9Z-tetradecenoyl)-sn-glycero-3-phosphoethanolamine
PE 37:4	1-heptadecanoyl,2-(5Z,8Z,11Z,14Z-eicosatetraenoyl)-sn-glycero-3-phosphoethanolamine
PE 43:6	1-heneicosanoyl-2-(4Z,7Z,10Z,13Z,16Z,19Z-docosahexaenoyl)-sn-glycero-3-phosphoethanolamine
LPE 17:0	1-heptadecenoyl-2-hydroxy-sn-glycero-3-phosphoethanolamine
PG 25:0	1-dodecanoyl-2-tridecanoyl-sn-glycero-3-[phospho-rac-(1-glycerol)]
PG 31:1	1-heptadecanoyl-2-(9Z-tetradecenoyl)-sn-glycero-3-phospho-(1'-rac-glycerol)(ammonium salt)
PG 37:4	1-heptadecanoyl-2-(5Z,8Z,11Z,14Z-eicosatetraenoyl)-sn-glycero-3-phospho-(1'-rac-glycerol) (Ammonium salt)
PG 43:6	1-heneicosanoyl-2-(4Z,7Z,10Z,13Z,16Z,19Z-docosahexaenoyl)-sn-glycero-3-phospho-(1'-rac-glycerol) (Ammonium Salt)
PS 25:0	1-dodecanoyl-2-tridecanoyl-sn-glycero-3-phosphoserine (ammonium salt)
PS 31:1	1-heptadecanoyl-2-(9Z-tetradecenoyl)-sn-glycero-3-phosphoserine (ammonium salt)
PS 37:4	1-heptadecanoyl, 2-(5Z,8Z,11Z,14Z-eicosatetraenoyl)-sn-glycero-3-phosphoserine (ammonium salt)
PS 43:6	1-heneicosanoyl-2-(4Z,7Z,10Z,13Z,16Z,19Z-docosahexaenoyl)-sn-glycero-3-phosphoserine (ammonium salt)
PI 25:0	1-dodecanoyl-2-tridecanoyl-sn-glycero-3-phospho-(1'-myo-inositol)(ammonium salt)
PI 31:1	1-heptadecanoyl-2-(9Z-tetradecenoyl)-sn-glycero-3-phospho-(1'-myo-inositol)(ammonium salt)
PI 37:4	1-heptadecanoyl-2-(5Z,8Z,11Z,14Z-eicosatetraenoyl)-sn-glycero-3-phospho-(1'-myo-inositol)(ammonium salt)
PI 43:6	1-heneicosanoyl-2-(4Z,7Z,10Z,13Z,16Z,19Z-docosahexaenoyl)-sn-glycero-3-phospho-(1'-myo-inositol)(ammonium salt)
TG	d5-TG internal standard mixture I
DG	d5-DG internal standard mixture I
Cer/Sph	ceramide/sphingoid internal standard mixture I
CL	cardiolipin internal standard mixture I

Supplementary Table 3: Lipid molecular species detected in murine liver using a 1 % class cut-off. TG and DG species were detected as $[M+NH_4]^+$ ions, PC, PE, PS, LPC, LPE and SM were analysed as $[M+H]^+$ ions, Cer and HexCer as $[M–OH]^+$, in positive polarity, while CL, PI and PG were quantified in negative ion mode as $[M–H]^–$. LPC and LPE species marked with an asterisk originate at least in part from the LIPID MAPS diacyl phospholipid internal standards.

Lipid species	*m/z*	tissue concentration (nmol/g) average+- SD	RT (min)
TG 46:0	796.73887	37.432 ± 0.756	37.1
TG 46:1	794.72322	50.697 ± 0.865	36.3
TG 47:1	808.73887	47.472 ± 3.541	36.8
TG 48:0	824.77017	69.906 ± 2.316	37.9
TG 48:1	822.75452	125.672 ± 8.124	37.2
TG 48:2	820.73887	96.660 ± 0.746	36.5
TG 49:1	836.77017	55.617 ± 3.193	37.7
TG 49:2	834.75452	41.607 ± 1.273	37.0
TG 50:0	852.80147	31.689 ± 0.831	38.7
TG 50:1	850.78582	647.567 ± 18.088	38.0
TG 50:2	848.77017	702.048 ± 11.531	37.3
TG 50:3	846.75452	301.437 ± 4.727	36.5
TG 50:4	844.73887	39.203 ± 0.826	35.8
TG 51:2	862.78582	78.342 ± 3.770	37.7
TG 51:3	860.77017	39.100 ± 0.527	37.0
TG 52:1	878.81712	325.941 ± 4.850	38.8
TG 52:2	876.80147	2805.970 ± 40.311	38.1
TG 52:3	874.78582	2372.608 ± 32.707	37.4
TG 52:4	872.77017	725.964 ± 11.204	36.7
TG 52:5	870.75452	139.081 ± 1.921	36.0
TG 53:2	890.81712	46.527 ± 2.749	38.5
TG 53:3	888.80147	48.732 ± 2.902	37.8
TG 54:1	906.84842	36.281 ± 0.938	39.6
TG 54:2	904.83277	276.179 ± 3.856	38.9
TG 54:3	902.81712	758.469 ± 6.756	38.2
TG 54:4	900.80147	602.301 ± 9.511	37.5
TG 54:5	898.78582	296.379 ± 20.560	36.8
TG 54:6	896.77017	103.147 ± 1.425	36.1; 36.4
TG 56:3	930.84842	34.984 ± 1.196	39.0
TG 56:5	926.81712	54.035 ± 9.280	37.8
TG 56:6	924.80147	49.825 ± 4.457	37.2
TG 56:7	922.78582	43.803 ± 0.962	36.7
TG 56:8	920.77017	31.669 ± 4.206	36.0
DG 30:1	556.49355	<LLOQ	24.9
DG 31:1	570.5092	<LLOQ	26.0
DG 32:0	586.5405	<LLOQ	28.5
DG 32:1	584.52485	<LLOQ	27.0
DG 32:2	582.5092	<LLOQ	25.3; 25.9
DG 33:1	598.5405	<LLOQ	28.0
DG 34:0	614.57180	<LLOQ	30.3

DG 34:1	612.55615	163.821 ± 40.686	28.8
DG 34:2	610.54050	148.628 ± 35.040	27.4
DG 34:3	608.52485	<LLOQ	25.9
DG 35:1	626.57180	<LLOQ	29.8
DG 36:0	642.60310	<LLOQ	31.9
DG 36:1	640.58745	<LLOQ	30.6
DG 36:2	638.57180	137.032 ± 28.724	29.2
DG 36:3	636.55615	90.423 ± 29.455	27.8
DG 36:4	634.54050	70.829 ± 23.119	27.2
DG 37:4	648.55615	<LLOQ	28.1
DG 38:2	666.60310	<LLOQ	30.9
DG 38:3	664.58745	<LLOQ	29.8
DG 38:4	662.57180	80.313 ± 13.889	29.1
DG 38:5	660.55615	<LLOQ	27.6
DG 38:6	658.54050	34.588 ± 14.119	26.7
DG 40:2	694.63440	<LLOQ	32.5
DG 40:6	686.57180	<LLOQ	28.6
DG 40:7	684.55615	<LLOQ	27.1
PC 32:0	734.56943	275.267 ± 9.523	24.3
PC 32:1	732.55378	140.768 ± 8.911	22.8
PC 34:0	762.60073	52.268 ± 1.795	26.5
PC 34:1	760.58508	2124.497 ± 44.780	24.9
PC 34:2	758.56943	3357.686 ± 205.325	23.2
PC 34:3	756.55378	177.327 ± 9.718	21.6; 22.2
PC 35:2	774.60073	40.937 ± 1.823	24.3
PC 36:1	788.61638	454.101 ± 3.308	27.0
PC 36:2	786.60073	2935.551 ± 90.600	25.4
PC 36:3	784.58508	871.292 ± 29.329	23.9
PC 36:4	782.56943	3391.122 ± 195.274	22.1; 23.2
PC 36:5	780.55378	220.735 ± 20.363	20.5; 21.7
PC 38:2	814.63203	57.343 ± 3.241	27.3
PC 38:3	812.61638	505.626 ± 11.120	26.1
PC 38:4	810.60073	3465.066 ± 90.358	24.5; 25.5
PC 38:5	808.58508	769.993 ± 34.510	23.7; 24.1
PC 38:6	806.56943	1692.048 ± 69.173	22.1; 22.8
PC 38:7	804.55378	34.114 ± 2.291	20.6; 21.0
PC 40:5	836.61638	41.385 ± 0.930	26.3
PC 40:6	834.60073	1205.107 ± 28.560	25.0
PC 40:7	832.58508	275.351 ± 19.482	23.2
PE 34:1	718.53813	128.793 ± 1.980	25.2
PE 34:2	716.52248	506.856 ± 10.535	23.6
PE 36:1	746.56943	56.405 ± 1.559	27.3
PE 36:2	744.55378	514.754 ± 15.100	25.8
PE 36:3	742.53813	218.470 ± 4.005	24.1
PE 36:4	740.52248	1451.545 ± 19.757	23.6
PE 36:5	738.50683	68.102 ± 2.544	22.0
PE 38:3	770.56943	121.434 ± 5.059	26.5; 27.3
PE 38:4	768.55378	3149.956 ± 66.803	25.8
PE 38:5	766.53813	935.495 ± 12.074	24.1; 24.5

PE 38:6	764.52248	2176.218 ± 47.625	22.5; 23.1
PE 40:5	794.56943	77.234 ± 2.541	25.9; 26.7
PE 40:6	792.55378	868.642 ± 17.376	25.3
PE 40:7	790.53813	434.643 ± 9.224	23.6
PE P-34:1	702.54322	<LLOQ	26.3
PE P-34:2	700.52757	<LLOQ	24.7
PE P-36:1	730.57452	<LLOQ	28.3
PE P-36:2	728.55887	<LLOQ	26.8
PE P-36:4	724.52757	75.232 ± 1.201	24.6
PE P-37:4	738.54322	<LLOQ	25.7
PE P-38:4	752.55887	75.506 ± 1.507	26.2; 26.8
PE P-38:5	750.54322	16.876 ± 1.185	25.1; 25.6
PE P-38:6	748.52757	16.207 ± 1.022	24.1
PE P-40:3	782.60582	<LLOQ	29.0
PE P-40:4	780.59017	16.676 ± 1.407	28.2; 28.8
PE P-40:5	778.57452	8.624 ± 0.823	26.5
PE P-40:6	776.55887	21.403 ± 0.869	26.3
PE P-40:7	774.54322	4.079 ± 0.146	24.5
PE P-42:5	806.60582	<LLOQ	28.5; 28.9
PE P-42:6	804.59017	<LLOQ	28.3
PS 36:1	790.55926	9.103 ± 2.522	25.0
PS 36:2	788.54361	6.765 ± 1.671	23.4
PS 36:4	784.51231	33.201 ± 1.680	21.1
PS 38:4	812.54361	709.252 ± 17.620	23.5
PS 38:6	808.51231	27.951 ± 6.636	20.7
PS 40:4	840.57491	6.920 ± 1.420	24.9
PS 40:6	836.54361	383.480 ± 21.490	23.0
PG 30:0	693.47121	<LLOQ	20.3
PG 32:0	721.50251	<LLOQ	22.6
PG 32:1	719.48686	<LLOQ	21.0
PG 34:1	747.51816	24.222 ± 1.159	23.1
PG 34:2	745.50251	<LLOQ	20.4
PG 36:2	773.53381	5.071 ± 0.423	23.8
PG 36:4	769.50251	<LLOQ	21.6
PG 38:2	801.56511	<LLOQ	25.8
PG 38:4	797.53381	<LLOQ	23.9
PG 38:5	795.51816	<LLOQ	21.1
PG 40:6	821.53381	<LLOQ	22.1
PG 40:7	819.51816	7.095 ± 0.402	20.7
PG 40:8	817.50251	<LLOQ	19.0
PG 42:6	849.56511	<LLOQ	25.5
PI 34:2	833.51855	30.958 ± 1.518	20.7
PI 36:4	857.51855	298.472 ± 7.643	20.8
PI 38:3	887.56550	168.057 ± 2.123	23.8; 24;6
PI 38:4	885.54985	2508.427 ± 66.003	23.2
PI 38:5	883.53420	80.709 ± 1.077	21.4
LPC 12:0*	440.27717	29.397 ± 2.644	1.4
LPC 13:0*	454.29282	28.200 ± 2.002	1.8
LPC 14:1*	466.29282	28.688 ± 2.858	1.6

LPC 16:0	496.33977	366.430 ± 16.416	4.3
LPC 17:0*	510.35542	90.395 ± 11.789	5.6
LPC 18:0	524.37107	343.087 ± 29.686	7.1
LPC 18:1	522.35542	53.667 ± 9.395	5.1
LPC 18:2	520.33977	60.142 ± 4.229	3.3
LPC 20:3	546.35542	4.307 ± 0.562	4.1
LPC 20:4	544.33977	103.526 ± 4.551	3.4
LPC 21:0*	566.41802	113.720 ± 12.213	12.0
LPC 22:6*	568.33977	63.518 ± 3.250	3.4
LPE 13:0*	412.24587	4.619 ± 0.353	1.9
LPE 14:1*	424.24587	4.179 ± 0.332	1.7
LPE 16:0	454.29282	37.174 ± 5.389	4.5
LPE 17:0*	468.30847	18.865 ± 3.876	5.8
LPE 18:0	482.32412	52.646 ± 8.508	7.3
LPE 18:1	480.30847	13.396 ± 4.096	5.2
LPE 18:2	478.29282	<LLOQ	3.7
LPE 20:4	502.29282	12.208 ± 1.450	3.6
LPE 21:0*	524.37107	21.043 ± 6.498	12.3
LPE 22:6	526.29282	11.195 ± 1.436	3.6
Cer 14:0	492.47751	<LLOQ	22.0
Cer 16:0	520.50881	14.650 ± 1.206	24.4
Cer 17:0	534.52446	<LLOQ	25.6
Cer 18:0	548.54011	6.101 ± 0.713	26.7
Cer 20:0	576.57141	<LLOQ	28.8
Cer 20:1	574.55576	<LLOQ	27.3
Cer 21:0	590.58706	<LLOQ	29.8
Cer 22:0	604.60271	25.361 ± 1.489	30.7
Cer 22:1	602.58706	<LLOQ	29.3
Cer 23:0	618.61836	15.134 ± 0.974	31.5
Cer 23:1	616.60271	<LLOQ	29.9
Cer 24:0	632.63401	31.710 ± 1.428	32.3
Cer 24:1	630.61836	49.654 ± 2.486	30.7
Cer 24:2	628.60271	2.925 ± 0.164	29.3
Cer 26:0	660.66531	<LLOQ	33.8
Cer 27:0	674.68096	<LLOQ	34.4
Cer 29:0	702.71226	<LLOQ	35.7
SM 16:0	703.57485	206.886 ± 15.095	21.2
SM 18:0	731.60615	93.326 ± 7.430	23.7
SM 20:0	759.63745	45.242 ± 4.321	26.1
SM 21:0	773.65310	7.951 ± 1.017	27.3
SM 22:0	787.66875	281.750 ± 33.330	28.3
SM 22:1	785.65310	17.205 ± 2.120	26.7
SM 23:0	801.68440	94.860 ± 8.781	29.3
SM 23:1	799.66875	13.435 ± 1.868	27.8
SM 24:0	815.70005	255.803 ± 16.662	30.2
SM 24:1	813.68440	522.046 ± 53.384	28.3
SM 24:2	811.66875	47.408 ± 4.899	26.7
HexCer 24:0	794.68738	18.544 ± 1.682	31.1
HexCer 24:1	792.67173	3.890 ± 1.032	30.0

HexCer 26:0	822.71868	5.291 ± 1.676	32.5
CL 70:6	1423.96495	<LLOQ	36.5
CL 70:7	1421.94930	30.636 ± 1.046	35.8
CL 72:6	1451.99625	<LLOQ	37.3
CL 72:7	1449.98060	177.286 ± 8.306	36.6
CL 72:8	1447.96495	493.021 ± 17.203	35.9
CL 74:8	1475.99625	<LLOQ	36.7
CL 74:9	1473.98060	35.404 ± 2.459	36.1

Supplementary Table 4: Lipid molecular species detected in A549 cells using a 1 % class cut-off. PC, PE, PS, LPC, LPE and SM were analysed as $[M+H]^+$ ions, Cer and HexCer as $[M–OH]^+$, in positive polarity, while CL, PI and PG were quantified in negative ion mode as $[M-H]^-$. Glycerolipids (TG, DG) were omitted from the analysis, as the concentrations detected are extremely low and could potentially result from contaminations during sample preparation. LPC and LPE species marked with an asterisk originate at least in part from the LIPID MAPS diacyl phospholipid internal standards.

Lipid species	***m/z***	**amount (nmol/10^6 cells) means ± SD**	**RT (min)**
PC 28:0	678.50683	0.432 ± 0.009	19.2
PC 30:0	706.53813	3.705 ± 0.069	21.8
PC 30:1	704.52248	2.116 ± 0.011	20.0; 20.4; 20.9
PC 31:0	720.55378	0.384 ± 0.014	23.0
PC 32:0	734.56943	6.248 ± 0.152	24.1
PC 32:1	732.55378	17.104 ± 0.212	22.4; 22.9
PC 32:2	730.53813	4.113 ± 0.048	20.6; 21.0; 21:4; 21.9
PC 33:1	746.56943	1.275 ± 0.016	23.6
PC 33:2	744.55378	0.305 ± 0.002	21.9; 22.7
PC 34:0	762.60073	0.643 ± 0.014	26.4
PC 34:1	760.58508[1]	31.400 ± 0.735	24.7
PC 34:2	758.56943	18.107 ± 1.288	23.0
PC 34:3	756.55378	2.155 ± 0.054	21.4; 21.7; 22.4
PC 35:1	774.60073	0.707 ± 0.005	25.6
PC 35:2	772.58508	0.874 ± 0.017	24.1
PC 36:1	788.61638	3.396 ± 0.059	26.8
PC 36:2	786.60073	20.177 ± 0.603	25.2
PC 36:3	784.58508	5.179 ± 0.202	23.7
PC 36:4	782.56943	2.024 ± 0.145	22.2; 23.1
PC 36:5	780.55378	0.601 ± 0.041	21.6
PC 37:2	800.61638	0.397 ± 0.007	26.2
PC 38:2	814.63203	1.469 ± 0.046	27.2
PC 38:3	812.61638	2.101 ± 0.041	25.7
PC 38:4	810.60073	1.012 ± 0.016	24.5
PC 38:5	808.58508	1.811 ± 0.097	23.6
PC 38:6	806.56943	1.757 ± 0.092	22.6
PC 38:7	804.55378	0.445 ± 0.024	20.7
PC 40:6	834.60073	0.522 ± 0.008	23.9; 24.9
PC 40:7	832.58508	1.471 ± 0.049	23.1
PE 32:0	692.52248	0.051 ± 0.006	24.6
PE 32:1	690.50683	0.958 ± 0.010	22.8; 23.3
PE 32:2	688.49118	0.144 ± 0.004	20.9; 21.4
PE 34:0	720.55378	0.077 ± 0.001	26.7
PE 34:1	718.53813	4.810 ± 0.091	25.1; 25.6
PE 34:2	716.52248	2.589 ± 0.159	23.4
PE 35:2	730.53813	0.095 ± 0.004	24.5

[1] Above ULOQ by 25 %. Value may be subject to error and should be treated with care.

PE 36:1	746.56943	2.996 ± 0.049	27.2
PE 36:2	744.55378	4.973 ± 0.361	25.5
PE 36:3	742.53813	0.629 ± 0.036	25.0
PE 36:4	740.52248	0.956 ± 0.019	23.4
PE 36:5	738.50683	0.321 ± 0.053	21.6; 21.9
PE 38:2	772.58508	0.286 ± 0.037	27.5
PE 38:3	770.56943	1.351 ± 0.039	26.5; 27.1
PE 38:4	768.55378	5.058 ± 0.145	25.7
PE 38:5	766.53813	2.472 ± 0.114	23.9
PE 38:6	764.52248	0.524 ± 0.016	22.9
PE 38:7	762.50683	0.103 ± 0.003	21.2
PE 40:2	800.61638	0.073 ± 0.001	29.6
PE 40:3	798.60073	0.124 ± 0.023	28.0; 28.4
PE 40:4	796.58508	0.090 ± 0.003	27.0
PE 40:5	794.56943	0.160 ± 0.012	25.9
PE 40:6	792.55378	0.366 ± 0.021	25.2
PE 40:7	790.53813	1.046 ± 0.035	23.4
PE 42:7	818.56943	0.091 ± 0.036	24.2
PE P-32:1	674.51192	0.780 ± 0.036	24.0; 24.4
PE P-33:1	688.52757	0.066 ± 0.002	25.1
PE P-34:1	702.54322	5.359 ± 0.102	26.2
PE P-34:2	700.52757	0.797 ± 0.012	24.6
PE P-34:3	698.51192	0.220 ± 0.007	23.9
PE P-35:1	716.55887	0.167 ± 0.004	27.2
PE P-35:3	712.52757	0.085 ± 0.003	25.0
PE P-36:1	730.57452	1.389 ± 0.029	28.2
PE P-36:2	728.55887	1.789 ± 0.043	26.6
PE P-36:3	726.54322	2.195 ± 0.016	25.3; 26.0
PE P-36:4	724.52757	6.476 ± 0.142	24.5
PE P-36:5	722.51192	1.494 ± 0.064	23.0
PE P-37:3	740.55887	0.086 ± 0.004	26.5; 27.1
PE P-37:4	738.54322	0.098 ± 0.004	25.4
PE P-38:1	758.60582	0.158 ± 0.004	30.1
PE P-38:2	756.59017	0.201 ± 0.020	28.6
PE P-38:3	754.57452	1.405 ± 0.022	27.4; 28.0
PE P-38:4	752.55887	2.540 ± 0.068	26.0; 26.3; 26.7
PE P-38:5	750.54322	2.082 ± 0.066	24.5; 24.9; 25.3
PE P-38:6	748.52757	5.028 ± 0.083	23.5; 24.0
PE P-39:6	762.54322	0.058 ± 0.010	25.1
PE P-40:3	782.60582	0.126 ± 0.007	29.0; 29.3
PE P-40:4	780.59017	0.288 ± 0.006	27.8; 28.7
PE P-40:5	778.57452	0.115 ± 0.005	26.7; 27.5
PE P-40:6	776.55887	1.213 ± 0.010	25.4; 26.2
PE P-40:7	774.54322	1.124 ± 0.014	24.4
PS 30:0	708.48101	0.047 ± 0.003	19.7
PS 32:0	736.51231	0.054 ± 0.004	22.0
PS 32:1	734.49666	0.393 ± 0.008	20.3; 20.7
PS 34:1	762.52796	2.55 ± 0.0520	22.6; 23.1
PS 34:2	760.51231	0.401 ± 0.020	20.9

PS 35:1	776.54361	0.036 ± 0.012	23.8
PS 36:1	790.55926	4.169 ± 0.338	24.8
PS 36:2	788.54361	1.366 ± 0.079	23.2
PS 36:3	786.52796	0.171 ± 0.013	21.8; 22.6
PS 36:4	784.51231	0.049 ± 0.006	21.0
PS 38:2	816.57491	0.356 ± 0.031	25.5
PS 38:3	814.55926	0.513 ± 0.039	24.1; 24.8
PS 38:4	812.54361	0.632 ± 0.064	23.3
PS 38:5	810.52796	0.142 ± 0.005	21.6; 21.8
PS 38:6	808.51231	0.035 ± 0.010	20.5
PS 40:2	844.60621	0.136 ± 0.004	27.4
PS 40:3	842.59056	0.227 ± 0.011	26.2
PS 40:4	840.57491	0.178 ± 0.014	24.7
PS 40:5	838.55926	0.065 ± 0.014	23.4; 24.3
PS 40:6	836.54361	0.450 ± 0.019	22.9
PS 40:7	834.52796	0.068 ± 0.015	21.1
PG 32:0	721.50251	0.007 ± 0.001	22.5
PG 32:1	719.48686	0.005 ± 0.001	20.8
PG 34:1	747.51816	0.040 ± 0.003	23.0
PG 34:2	745.50251	0.015 ± 0.001	21.4
PG 38:5	795.51816	0.009 ± 0.001	21.7
PG 38:6	793.50251	0.014 ± 0.001	20.5
PG 38:7	791.48686	0.009 ± 0.004	18.8
PG 40:7	819.51816	0.221 ± 0.006	21.0
PI 32:1	807.50290	0.124 ± 0.005	20.1
PI 32:2	805.48725	0.046 ± 0.002	18.2
PI 34:1	835.53420	0.548 ± 0.002	22.4
PI 34:2	833.51855	1.019 ± 0.019	20.6
PI 34:3	831.50290	0.060 ± 0.002	19.0; 20.0
PI 36:1	863.56550	0.543 ± 0.011	24.6
PI 36:2	861.54985	1.737 ± 0.017	22.9; 24.0
PI 36:3	859.53420	1.141 ± 0.030	21.4; 22.4
PI 36:4	857.51855	0.314 ± 0.004	20.8
PI 37:3	873.54985	0.207 ± 0.001	22.8; 23.6
PI 38:2	889.58115	0.397 ± 0.017	25.0
PI 38:3	887.56550	4.767 ± 0.105	24.0; 24.6
PI 38:4	885.54985	3.694 ± 0.028	22.2; 23.1
PI 38:5	883.53420	1.303 ± 0.016	21.3
PI 38:6	881.51855	0.162 ± 0.004	19.8; 20.3
PI 39:3	901.58115	0.208 ± 0.005	25.0; 25.7
PI 39:4	899.56550	0.079 ± 0.003	23.3; 23.8; 24.4
PI 40:3	915.59680	0.262 ± 0.004	26.0; 26.7
PI 40:4	913.58115	0.222 ± 0.005	24.4; 24.8; 25.4
PI 40:5	911.56550	0.173 ± 0.012	23.2; 25.4
PI 40:6	909.54985	0.795 ± 0.025	22.7
PI 40:7	907.53420	0.274 ± 0.003	20.9
LPC 12:0*	440.27717	0.044 ± 0.002	1.4
LPC 13:0*	454.29282	0.043 ± 0.007	1.8
LPC 14:0	468.30847	0.018 ± 0.006	2.4

LPC 14:1*	466.29282	0.042 ± 0.004	1.6
LPC 16:0	496.33977	0.338 ± 0.058	4.3
LPC 16:1	494.32412	0.183 ± 0.023	2.9
LPC 17:0*	510.35542	0.159 ± 0.010	5.6
LPC 18:0	524.37107	0.157 ± 0.007	7.0
LPC 18:1	522.35542	0.574 ± 0.056	5.0
LPC 18:2	520.33977	0.019 ± 0.003	3.6
LPC 20:1	550.38672	0.012 ± 0.001	7.6
LPC 20:2	548.37107	0.009 ± 0.001	5.8
LPC 20:3	546.35542	0.015 ± 0.004	5.0
LPC 20:4	544.33977	0.084 ± 0.001	4.2
LPC 21:0*	566.41802	0.181 ± 0.046	11.9
LPC 22:5	570.35542	0.009 ± 0.002	4.1
LPC 22:6*	568.33977	0.089 ± 0.003	3.5
LPE 13:0*	412.24587	<LLOQ	1.8
LPE 14:1*	424.24587	<LLOQ	1.7
LPE 16:0	454.29282	<LLOQ	4.4
LPE 16:1	452.27717	<LLOQ	3.0
LPE 17:0*	468.30847	0.033 ± 0.007	5.7
LPE 18:0	482.32412	0.024 ± 0.007	7.2
LPE 18:1	480.30847	0.064 ± 0.011	5.1
LPE 18:2	478.29282	<LLOQ	3.7
LPE 20:2	506.32412	<LLOQ	6.1
LPE 20:3	504.30847	<LLOQ	5.2
LPE 20:4*	502.29282	0.026 ± 0.005	3.6
LPE 20:5	500.27717	<LLOQ	2.7
LPE 21:0*	524.37107	0.038 ± 0.018	12.1
LPE 22:6	526.29282	0.026 ± 0.006	3.6
Cer 14:0	492.47751	0.012 ± 0.002	21.9
Cer 15:0	506.49316	<LLOQ	23.1
Cer 16:0	520.50881	0.384 ± 0.066	24.3
Cer 16:1	518.49316	0.007 ± 0.001	22.5
Cer 18:0	548.54011	<LLOQ	26.6
Cer 22:0	604.60271	0.007 ± 0.000	30.6
Cer 23:0	618.61836	0.007 ± 0.001	31.4
Cer 24:0	632.63401	0.069 ± 0.004	32.2
Cer 24:1	630.61836	0.170 ± 0.007	31.5
Cer 24:2	628.60271	0.016 ± 0.001	29.3
Cer 26:0	660.66531	<LLOQ	33.7
Cer 26:1	658.64966	0.007 ± 0.001	32.2
SM 14:0	675.54355	0.552 ± 0.009	18.4
SM 15:0	689.55920	0.343 ± 0.005	19.7
SM 16:0	703.57485	10.574 ± 0.328	21.0
SM 16:1	701.55920	0.655 ± 0.028	19.1
SM 18:0	731.60615	0.255 ± 0.009	23.6
SM 22:0	787.66875	0.557 ± 0.012	28.2
SM 22:1	785.65310	0.197 ± 0.004	27.4
SM 23:0	801.68440	0.219 ± 0.007	29.2
SM 23:1	799.66875	0.220 ± 0.008	27.7

SM 24:0	815.70005	1.599 ± 0.042	30.1
SM 24:1	813.68440	4.682 ± 0.131	28.7
SM 24:2	811.66875	0.680 ± 0.016	27.4
SM 25:1	827.70005	0.135 ± 0.005	29.7
GlyCer 24:0	794.68738	0.008 ± 0.001	31.0
GlyCer 24:1	792.67173	<LLOQ	29.9
GlyCer 26:0	822.71868	<LLOQ	32.5
CL 64:3	1345.9180	<LLOQ	36.2
CL 64:4	1343.90235	<LLOQ	35.4
CL 66:3	1373.9493	0.062 ± 0.003	37.0
CL 66:4	1371.93365	0.253 ± 0.030	36.3
CL 66:5	1369.9180	<LLOQ	35.6
CL 67:4	1385.94930	<LLOQ	36.7
CL 68:3	1401.9806	<LLOQ	37.8
CL 68:4	1399.96495	0.718 ± 0.019	37.1
CL 68:5	1397.94930	0.122 ± 0.004	36.4
CL 68:6	1395.93365	<LLOQ	35.8
CL 69:4	1413.98060	0.050 ± 0.003	37.6
CL 69:5	1411.96495	<LLOQ	36.9
CL 70:4	1427.99625	0.547 ± 0.009	37.9
CL 70:5	1425.98060	0.189 ± 0.014	37.2
CL 70:6	1423.96495	<LLOQ	36.6
CL 71:4	1442.01190	<LLOQ	38.3
CL 71:5	1439.99625	<LLOQ	37.6
CL 72:4	1456.02755	0.101 ± 0.005	38.7
CL 72:5	1454.01190	0.069 ± 0.006	38.0
CL 72:6	1451.99625	<LLOQ	37.4

Supplementary Table 5: Lipid molecular species detected in *C. elegans* embryos using a 1 % class cut-off. TG and DG species were detected as $[M+NH_4]^+$ ions, PC, PE, PS, LPC, LPE and SM were analysed as $[M+H]^+$ ions, Cer as $[M–OH]^+$, in positive polarity, while PI and PG were quantified in negative ion mode as $[M–H]^–$. LPC and LPE species marked with an asterisk originate at least in part from the LIPID MAPS diacyl phospholipid internal standards:

Lipid species	*m/z*	tissue concentration (nmol/g) average+- SD	RT (min)
TG 44:0	768.70757	0.333 ± 0.004	36.0
TG 44:1	766.69192	0.284 ± 0.012	35.3
TG 45:0	782.72322	0.573 ± 0.008	36.5
TG 45:1	780.70757	0.849 ± 0.014	35.8
TG 45:2	778.69192	0.284 ± 0.007	35.0
TG 46:0	796.73887	0.969 ± 0.018	37.0
TG 46:1	794.72322	2.144 ± 0.018	36.3
TG 46:2	792.70757	0.986 ± 0.023	35.5
TG 46:3	790.69192	0.248 ± 0.009	34.6
TG 47:0	810.75452	1.192 ± 0.038	37.4
TG 47:1	808.73887	4.135 ± 0.061	36.8
TG 47:2	806.72322	2.148 ± 0.064	36.1
TG 47:3	804.70757	0.436 ± 0.024	32.2; 35.6
TG 48:0	824.77017	1.394 ± 0.027	37.8
TG 48:1	822.75452	6.475 ± 0.058	37.2
TG 48:2	820.73887	5.939 ± 0.066	36.4
TG 48:3	818.72322	1.423 ± 0.079	35.6
TG 48:4	816.70757	0.276 ± 0.023	34.8
TG 49:0	838.78582	0.996 ± 0.011	38.2
TG 49:1	836.77017	8.530 ± 0.094	37.6
TG 49:2	834.75452	9.725 ± 0.110	37.0
TG 49:3	832.73887	3.007 ± 0.103	36.2
TG 49:4	830.72322	0.728 ± 0.036	35.4
TG 49:5	828.70757	0.412 ± 0.006	34.7
TG 50:0	852.80147	0.561 ± 0.010	38.6
TG 50:1	850.78582	10.003 ± 0.105	38.0
TG 50:2	848.77017	18.537 ± 0.234	37.3
TG 50:3	846.75452	8.472 ± 0.202	36.5
TG 50:4	844.73887	1.979 ± 0.094	35.8
TG 50:5	842.72322	1.152 ± 0.070	35.2
TG 50:6	840.70757	0.360 ± 0.038	34.5
TG 51:0	866.81712	0.467 ± 0.006	39.0
TG 51:1	864.80147	6.387 ± 0.083	38.4
TG 51:2	862.78582	17.718 ± 0.215	37.8
TG 51:3	860.77017	12.858 ± 0.310	37.0; 37.4
TG 51:4	858.75452	3.537 ± 0.147	36.3
TG 51:5	856.73887	1.894 ± 0.065	35.7
TG 51:6	854.72322	1.125 ± 0.062	35.1
TG 52:0	880.83277	0.332 ± 0.006	39.4
TG 52:1	878.81712	4.924 ± 0.039	38.8

TG 52:2	876.80147	23.532 ± 0.612[2]	38.1
TG 52:3	874.78582	20.150 ± 0.932	37.5
TG 52:4	872.77017	7.261 ± 1.011	36.9
TG 52:5	870.75452	3.556 ± 0.173	36.2
TG 52:6	868.73887	3.280 ± 0.158	35.5
TG 52:7	866.72322	0.660 ± 0.039	34.6; 35.0
TG 53:1	892.83277	2.641 ± 0.020	39.2
TG 53:2	890.81712	11.379 ± 0.247	38.6
TG 53:3	888.80147	17.434 ± 0.494	38.0
TG 53:4	886.78582	8.786 ± 0.687	37.2
TG 53:5	884.77017	5.079 ± 0.066	36.5
TG 53:6	882.75452	4.910 ± 0.175	36.1
TG 53:7	880.73887	1.753 ± 0.145	35.1
TG 53:8	878.72322	0.300 ± 0.009	34.4
TG 54:1	906.84842	1.843 ± 0.023	39.5
TG 54:2	904.83277	8.461 ± 0.059	38.8
TG 54:3	902.81712	12.928 ± 0.532	38.1; 38.4
TG 54:4	900.80147	8.603 ± 0.688	37.4; 37.7
TG 54:5	898.78582	5.356 ± 0.166	36.8
TG 54:6	896.77017	6.166 ± 0.639	36.0; 36.4
TG 54:7	894.75452	3.665 ± 0.080	35.6; 36.0
TG 54:8	892.73887	0.663 ± 0.015	34.8
TG 54:9	890.72322	0.220 ± 0.021	34.1
TG 55:1	920.86407	0.848 ± 0.026	39.9
TG 55:2	918.84842	3.354 ± 0.060	39.3
TG 55:3	916.83277	7.115 ± 0.069	38.6
TG 55:4	914.81712	4.800 ± 0.045	38.0
TG 55:5	912.80147	4.090 ± 0.024	37.3
TG 55:6	910.78582	5.366 ± 0.377	36.8
TG 55:7	908.77017	5.598 ± 0.091	36.2
TG 55:8	906.75452	2.580 ± 0.050	35.4
TG 55:9	904.73887	0.767 ± 0.029	34.6
TG 55:10	902.72322	0.536 ± 0.014	34.0
TG 56:1	934.87972	0.701 ± 0.024	40.2
TG 56:2	932.86407	1.737 ± 0.047	39.6
TG 56:3	930.84842	3.386 ± 0.057	39.1
TG 56:4	928.83277	2.555 ± 0.025	38.5
TG 56:5	926.81712	2.826 ± 0.339	37.7
TG 56:6	924.80147	3.785 ± 0.037	36.9; 37.3
TG 56:7	922.78582	4.642 ± 0.073	36.5; 36.8
TG 56:8	920.77017	2.725 ± 0.088	35.7
TG 56:9	918.75452	1.379 ± 0.059	35.0
TG 56:10	916.73887	1.096 ± 0.033	34.6
TG 57:1	948.89537	0.349 ± 0.035	40.6
TG 57:2	946.87972	0.824 ± 0.046	40.0
TG 57:3	944.86407	0.940 ± 0.017	39.4

[2] Above ULOQ by 9.2 %. Value may be subject to error and should be treated with care.

TG 57:4	942.84842	0.714 ± 0.010	38.7
TG 57:5	940.83277	0.953 ± 0.030	38.1
TG 57:6	938.81712	1.583 ± 0.051	37.5; 37.8
TG 57:7	936.80147	2.720 ± 0.039	37.1
TG 57:8	934.78582	1.584 ± 0.024	36.3
TG 57:9	932.77017	0.779 ± 0.031	35.6
TG 57:10	930.75452	1.446 ± 0.076	35.0
TG 57:11	928.73887	1.590 ± 0.048	34.4
TG 58:1	962.91102	0.355 ± 0.017	40.9
TG 58:2	960.89537	0.729 ± 0.027	40.2
TG 58:3	958.87972	0.533 ± 0.016	39.6
TG 58:6	952.83277	0.223 ± 0.007	38.0
TG 58:7	950.81712	0.383 ± 0.036	37.7
TG 58:8	948.80147	0.655 ± 0.010	36.6
TG 58:9	946.78582	1.001 ± 0.070	35.9
TG 58:10	944.77017	1.689 ± 0.077	35.2; 35.6
TG 58:11	942.75452	1.935 ± 0.365	34.4; 34.7
TG 58:12	940.73887	0.613 ± 0.018	33.9
TG 59:2	974.91102	0.291 ± 0.015	40.7
TG 59:10	958.78582	0.442 ± 0.065	35.9
TG 59:11	956.77017	0.473 ± 0.007	35.4
TG 60:14	964.73887	0.382 ± 0.015	33.4
TG 60:15	962.72322	0.437 ± 0.018	32.8
DG 30:1	556.49355	<LLOQ	24.9
DG 31:1	570.50920	<LLOQ	26.0
DG 32:0	586.54050	<LLOQ	28.4
DG 32:1	584.52485	0.557 ± 0.228	26.9
DG 32:2	582.50920	<LLOQ	25.2
DG 33:0	600.55615	<LLOQ	29.2
DG 33:1	598.54050	0.232 ± 0.012	27.6; 28.1
DG 33:2	596.52485	<LLOQ	26.2; 26.5
DG 34:0	614.57180	<LLOQ	30.2
DG 34:1	612.55615	1.535 ± 0.071	28.8
DG 34:2	610.54050	1.225 ± 0.236	27.3: 27.7
DG 34:3	608.52485	<LLOQ	25.8
DG 34:5	604.49355	<LLOQ	23.5
DG 35:1	626.57180	0.156 ± 0.010	29.5; 29.9
DG 35:2	624.55615	0.342 ± 0.033	28.4
DG 35:3	622.54050	0.282 ± 0.135	27.0
DG 35:4	620.52485	<LLOQ	25.4
DG 35:5	618.50920	0.323 ± 0.131	24.5
DG 36:0	642.60310	<LLOQ	31.8
DG 36:1	640.58745	0.317 ± 0.034	30.5
DG 36:2	638.57180	2.597 ± 0.175	29.1
DG 36:3	636.55615	1.102 ± 0.068	27.7
DG 36:4	634.54050	0.292 ± 0.053	26.1; 26.6
DG 36:5	632.52485	0.321 ± 0.021	25.8
DG 36:6	630.50920	<LLOQ	24.1
DG 37:2	652.58745	<LLOQ	30.1

DG 37:3	650.57180	<LLOQ	28.9
DG 37:4	648.55615	<LLOQ	27.5
DG 37:5	646.54050	0.420 ± 0.080	26.3; 26.7
DG 37:6	644.52485	0.600 ± 0.110	25.4
DG 38:2	666.60310	<LLOQ	30.7
DG 38:3	664.58745	<LLOQ	29.4
DG 38:4	662.57180	0.161 ± 0.023	28.2; 29.0
DG 38:5	660.55615	1.185 ± 0.225	25.3; 26.9
DG 38:6	658.54050	1.988 ± 0.214	25.5; 26.1
DG 38:7	656.52485	0.554 ± 0.194	24.6
DG 38:8	654.50920	<LLOQ	23.3
DG 39:5	674.57180	<LLOQ	28.1
DG 39:6	672.55615	0.868 ± 0.152	27.4
DG 40:4	690.60310	<LLOQ	29.7
DG 40:7	684.55615	<LLOQ	26.1; 26.6
DG 40:8	682.54050	0.44 ± 0.177	25.3; 25.7
DG 40:9	680.52485	0.943 ± 0.092	23.9; 24.3
DG 40:10	678.50920	0.356 ± 0.080	23.0
PC 30:0	706.53813	0.583 ± 0.022	21.3; 21.8
PC 31:0	720.55378	0.855 ± 0.036	22.8
PC 31:1	718.53813	0.999 ± 0.056	21.0; 21.4
PC 32:0	734.56943	2.971 ± 0.261	23.7; 24.1
PC 32:1	732.55378	4.146 ± 0.214	22.4
PC 32:2	730.53813	0.906 ± 0.046	20.6; 21.2
PC 33:0	748.58508	1.315 ± 0.072	25.1
PC 33:1	746.56943	6.662 ± 0.354	23.3; 23.8
PC 33:2	744.55378	3.241 ± 0.207	21.7; 22.1
PC 33:3	742.53813	0.646 ± 0.033	20.1; 20.5
PC 34:0	762.60073	1.468 ± 0.072	26.4
PC 34:1	760.58508	12.651 ± 1.018	24.7
PC 34:2	758.56943	11.855 ± 0.485	23.0; 23.4
PC 34:3	756.55378	2.214 ± 0.116	21.4; 22.1
PC 34:4	754.53813	1.114 ± 0.065	19.9; 20.53
PC 34:5	752.52248	2.433 ± 0.162	19.1
PC 35:0	776.61638	0.596 ± 0.036	27.2
PC 35:1	774.60073	7.029 ± 0.414	25.6; 26.0
PC 35:2	772.58508	12.504 ± 0.837	24.2
PC 35:3	770.56943	6.260 ± 0.329	22.7
PC 35:4	768.55378	3.781 ± 0.154	21.0; 21.7
PC 35:5	766.53813	8.859 ± 0.493	20.1
PC 36:0	790.63203	0.544 ± 0.034	28.4
PC 36:1	788.61638	6.982 ± 0.431	26.8
PC 36:2	786.60073	17.959 ± 0.904	25.0
PC 36:3	784.58508	12.297 ± 0.726	23.5
PC 36:4	782.56943	9.656 ± 0.435	22.0; 22.3; 23.1
PC 36:5	780.55378	19.056 ± 1.017	20.5; 21.6
PC 36:6	778.53813	2.906 ± 0.170	19.2; 19.7
PC 37:1	802.63203	1.625 ± 0.075	28.0
PC 37:2	800.61638	7.255 ± 0.352	26.3

PC 37:3	798.60073	4.591 ± 0.320	24.8
PC 37:4	796.58508	4.152 ± 0.185	23.4
PC 37:5	794.56943	11.165 ± 0.693	22.0; 22.6
PC 37:6	792.55378	11.822 ± 0.491	21.2
PC 38:2	814.63203	1.938 ± 0.263	27.1; 27.5
PC 38:3	812.61638	2.596 ± 0.128	25.4; 26.0
PC 38:4	810.60073	9.655 ± 2.285	24.0; 24.6
PC 38:5	808.58508	24.200 ± 2.692	22.8; 23.5
PC 38:6	806.56943	37.187 ± 2.396	21.1; 22.0
PC 38:7	804.55378	12.300 ± 0.582	19.6; 20.4
PC 38:8	802.53813	4.046 ± 0.189	18.8; 19.1
PC 38:9	800.52248	1.126 ± 0.055	17.5
PC 39:3	826.63203	0.459 ± 0.033	26.7
PC 39:4	824.61638	1.858 ± 0.093	25.6
PC 39:5	822.60073	5.069 ± 0.345	24.2
PC 39:6	820.58508	19.400 ± 1.346	23.5
PC 40:7	832.58508	3.317 ± 0.202	22.0; 22.5
PC 40:8	830.56943	9.005 ± 0.382	20.5; 21.1
PC 40:9	828.55378	12.876 ± 0.857	19.6
PC 40:10	826.53813	24.764 ± 2.144	18.6
PE 29:0	650.47553	0.250 ± 0.011	20.7
PE 30:0	664.49118	0.840 ± 0.027	21.7; 22.2
PE 31:0	678.50683	5.030 ± 0.241	23.1
PE 31:1	676.49118	1.558 ± 0.045	21.4; 21.8
PE 32:0	692.52248	2.549 ± 0.127	24.2; 24.6
PE 32:1	690.50683	6.107 ± 0.332	22.8
PE 32:2	688.49118	0.299 ± 0.010	21.0
PE 33:0	706.53813	3.128 ± 0.099	25.5
PE 33:1	704.52248	18.214 ± 0.642	23.6; 24.2
PE 33:2	702.50683	1.572 ± 0.076	22.1; 22.4
PE 34:0	720.55378	1.752 ± 0.094	26.4; 26.7
PE 34:1	718.53813	20.551 ± 0.953	25.0
PE 34:2	716.52248	10.984 ± 0.319	23.4; 23.8
PE 34:3	714.50683	0.538 ± 0.068	21.9; 22.4
PE 35:0	734.56943	0.875 ± 0.029	27.6
PE 35:1	732.55378	21.634 ± 0.765	25.9; 26.4
PE 35:2	730.53813	11.514 ± 0.454	24.6
PE 35:3	728.52248	1.524 ± 0.083	23.1
PE 35:4	726.50683	0.430 ± 0.020	21.3; 22.0
PE 35:5	724.49118	0.650 ± 0.027	20.5
PE 36:1	746.56943	18.872 ± 0.472	27.1
PE 36:2	744.55378	24.589 ± 0.602	25.4; 25.7
PE 36:3	742.53813	6.698 ± 0.197	23.8; 24.8
PE 36:4	740.52248	2.892 ± 0.096	22.3; 22.7; 23.5
PE 36:5	738.50683	10.137 ± 0.216	22.0
PE 37:1	760.58508	5.316 ± 0.314	28.4
PE 37:2	758.56943	6.053 ± 0.305	26.7
PE 37:3	756.55378	2.052 ± 0.115	25.2
PE 37:4	754.53813	2.023 ± 0.079	23.7; 24.4

PE 37:5	752.52248	10.660 ± 0.560	22.3; 23.0
PE 37:6	750.50683	0.742 ± 0.042	21.5
PE 38:1	774.60073	1.875 ± 0.094	29.1
PE 38:2	772.58508	2.371 ± 0.115	27.5; 27.8
PE 38:3	770.56943	2.861 ± 0.076	25.8; 26.4
PE 38:4	768.55378	4.864 ± 0.180	25.0; 25.7
PE 38:5	766.53813	14.366 ± 0.557	23.1; 24.3
PE 38:6	764.52248	4.542 ± 0.140	21.5; 22.4; 23.0
PE 38:7	762.50683	0.874 ± 0.044	21.6
PE 39:1	788.61638	1.221 ± 0.054	30.2
PE 39:4	782.56943	0.295 ± 0.010	25.9
PE 39:6	778.53813	0.881 ± 0.036	23.8
PE 40:1	802.63203	0.695 ± 0.035	30.9
PE 40:2	800.61638	0.622 ± 0.039	29.7
PE 40:5	794.56943	0.251 ± 0.013	26.5
PE 40:9	786.50683	0.63 ± 0.030	20.0
PE 40:10	784.49118	0.416 ± 0.020	19.0
PE P-33:0	690.54322	1.942 ± 0.120	26.7
PE P-34:0	704.55887	0.737 ± 0.031	27.8
PE P-34:1	702.54322	0.957 ± 0.038	26.3
PE P-35:0	718.57452	0.855 ± 0.067	28.6
PE P-35:1	716.55887	5.473 ± 0.300	25.7; 26.8
PE P-36:1	730.57452	41.576 ± 1.802	28.1
PE P-36:2	728.55887	12.838 ± 0.579	26.8
PE P-36:3	726.54322	0.769 ± 0.026	25.0; 25.4
PE P-37:1	744.59017	3.133 ± 0.230	29.3
PE P-37:2	742.57452	1.271 ± 0.046	28.1
PE P-38:1	758.60582	1.023 ± 0.053	29.9
PE P-38:2	756.59017	3.625 ± 0.185	28.4
PE P-38:3	754.57452	5.561 ± 0.396	27.4
PE P-38:4	752.55887	5.197 ± 0.178	26.0
PE P-38:5	750.54322	11.142 ± 0.633	25.3
PE O-33:0	692.55887	1.044 ± 0.082	26.8
PE O-34:0	706.57452	0.631 ± 0.042	28.0
PE O-34:1	704.55887	2.073 ± 0.084	26.3
PE O-35:0	720.59017	0.561 ± 0.029	28.8
PE O-35:1	718.57452	5.261 ± 0.173	27.7
PE O-36:1	732.59017	36.081 ± 1.868	28.3
PE O-36:2	730.57452	16.23 ± 0.401	26.5; 27.0
PE O-36:3	728.55887	0.546 ± 0.055	25.0; 25.5
PE O-37:1	746.60582	2.092 ± 0.150	29.4
PE O-37:2	744.59017	8.001 ± 0.305	27.8
PE O-37:3	742.57452	2.838 ± 0.114	26.5
PE O-38:1	760.62147	0.474 ± 0.021	30.1
PE O-38:2	758.60582	2.217 ± 0.146	28.6
PE O-38:3	756.59017	2.206 ± 0.155	27.5
PE O-38:4	754.57452	1.754 ± 0.125	26.2
PE O-38:5	752.55887	2.231 ± 0.098	25.5
PS 35:1	776.54361	0.295 ± 0.033	24.0

PS 36:1	790.55926	0.232 ± 0.042	24.7
PS 36:2	788.54361	0.154 ± 0.009	23.3
PS 36:4	784.51231	0.060 ± 0.014	20.2
PS 36:5	782.49666	2.091 ± 0.067	19.5
PS 37:1	804.57491	0.069 ± 0.017	25.9
PS 37:4	798.52796	0.079 ± 0.012	21.3
PS 37:5	796.51231	2.024 ± 0.052	20.5
PS 38:4	812.54361	0.516 ± 0.048	22.6; 23.3
PS 38:5	810.52796	5.024 ± 0.457	21.9
PS 38:6	808.51231	0.235 ± 0.011	20.0
PS 39:5	824.54361	0.190 ± 0.019	23.0
PS 40:5	838.55926	0.267 ± 0.031	24.2
PG 33:1	733.50251	0.123 ± 0.005	22.3
PG 34:1	747.51816	0.046 ± 0.002	23.3
PG 36:1	775.54946	1.302 ± 0.038	25.2
PG 36:2	773.53381	0.022 ± 0.002	23.4
PG 38:5	795.51816	0.015 ± 0.001	22.5
PI 36:5	855.50290	1.157 ± 0.017	19.3
PI 37:5	869.51855	0.235 ± 0.025	20.3
PI 38:4	885.54985	0.502 ± 0.033	23.1
PI 38:5	883.53420	13.186 ± 0.196	21.7
PI 38:6	881.51855	4.212 ± 0.028	19.7
PI 39:6	895.53420	1.274 ± 0.040	21.2
PI 40:3	915.59680	1.001 ± 0.031	20.9
PI 40:4	913.58115	0.213 ± 0.007	20.3
LPC 12:0*	440.27717	0.080 ± 0.006	1.4
LPC 13:0*	454.29282	0.079 ± 0.006	1.8
LPC 15:0	482.32412	0.023 ± 0.005	3.1
LPC 16:0	496.33977	0.374 ± 0.037	4.3
LPC 16:1	494.32412	<LLOQ	2.9
LPC 17:0	510.35542	0.025 ± 0.005	5.3
LPC 17:1	508.33977	0.072 ± 0.009	4.0
LPC 18:0	524.37107	0.248 ± 0.022	7.0
LPC 18:1	522.35542	0.192 ± 0.021	4.9
LPC 18:2	520.33977	0.091 ± 0.011	3.5
LPC 19:1	536.37107	0.097 ± 0.012	6.5
LPC 20:0	552.40237	<LLOQ	10.2
LPC 20:3	546.35542	<LLOQ	4.4
LPC 20:4	544.33977	0.054 ± 0.007	3.3
LPC 20:5	542.32412	0.081 ± 0.007	2.5
LPC 22:6	568.33977	<LLOQ	3.4
LPE 13:0*	412.24587	<LLOQ	1.8
LPE 16:0	454.29282	0.087 ± 0.011	4.4
LPE 17:0	468.30847	0.036 ± 0.006	5.5
LPE 17:1	466.29282	0.044 ± 0.005	4.1
LPE 18:0	482.32412	0.167 ± 0.016	7.2
LPE 18:1	480.30847	0.475 ± 0.042	5.0
LPE 18:2	478.29282	0.033 ± 0.002	3.6
LPE 18:3	476.27717	<LLOQ	1.0

LPE 19:1	494.32412	0.026 ± 0.005	6.6
LPE 20:1	508.33977	<LLOQ	7.8
LPE 20:2	506.32412	<LLOQ	5.9
LPE 20:3	504.30847	<LLOQ	4.5
LPE 20:4	502.29282	0.017 ± 0.002	3.4
LPE 20:5	500.27717	0.020 ± 0.002	2.6
Cer 10:0	436.41491	<LLOQ	16.5
Cer 11:0	450.43056	<LLOQ	17.9
Cer 13:0	478.46186	<LLOQ	20.6
Cer 14:0	492.47751	<LLOQ	21.9
Cer 15:0	506.49316	0.018 ± 0.002	23.0
Cer 16:0	520.50881	0.039 ± 0.005	24.3
Cer 17:0	534.52446	0.016 ± 0.002	25.4
Cer 18:0	548.54011	0.017 ± 0.001	26.6
Cer 19:0	562.55576	<LLOQ	27.7
Cer 20:0	576.57141	0.037 ± 0.002	28.8
Cer 21:1	588.57141	<LLOQ	28.7
Cer 22:0	604.60271	0.132 ± 0.003	30.6
Cer 22:1	602.58706	<LLOQ	29.3
Cer 23:0	618.61836	0.076 ± 0.003	31.4
Cer 23:1	616.60271	<LLOQ	30.6
Cer 24:0	632.63401	0.087 ± 0.006	32.2
Cer 24:1	630.61836	0.030 ± 0.002	30.6
Cer 24:2	628.60271	<LLOQ	29.3
Cer 25:1	644.63401	<LLOQ	32.2
Cer 26:0	660.66531	<LLOQ	33.7
Cer 27:0	674.68096	<LLOQ	34.4
Cer 28:0	688.69661	<LLOQ	34.9
Cer 29:0	702.71226	<LLOQ	35.6
SM 15:0	689.55920	0.388 ± 0.013	19.5
SM 16:0	703.57485	0.239 ± 0.009	21.0
SM 17:0	717.59050	0.140 ± 0.004	22.2
SM 20:0	759.63745	0.590 ± 0.036	26.2
SM 21:0	773.65310	9.045 ± 0.339	27.1
SM 22:0	787.66875	1.698 ± 0.100	28.2
SM 23:0	801.68440	0.718 ± 0.042	29.2
SM 24:0	815.70005	0.532 ± 0.033	30.1
SM 24:1	813.68440	0.329 ± 0.024	28.2

Supplementary Table 6: SRM parameters for NAPE detection and concentrations of NAPE species detected in rat brain (means and standard deviation from three separately processed samples). Q1 and Q3 resolution was 2 *m/z*, collision gas was argon with a pressure of 1.5 mtorr and retention time window 3 min around the expected retention time. CE: collision energy

	Concentration (pmol/g±SD)	**RT (min)**	**Q1 (Da)**	**Q3 (Da)**	**CE (eV)**	**Dwell time (ms)**
PE 36:2-N-19:0 (internal standard)	–	9.8	1041.80	603.48	-19	33.3
			1041.80	324.33	-29	33.3
PE 34:0-N-16:0	<LLOQ	9.1	975.81	579.53	-19	24.4
			975.81	282.28	-29	24.4
PE 34:1-N-16:0	107.65 ± 11.6	7.8	973.79	577.52	-19	22.9
			973.79	282.28	-29	22.9
PE 36:0-N-16:0	<LLOQ	10.1	1003.84	607.57	-19	33.3
			1003.84	282.28	-29	33.3
PE 36:1-N-16:0	383.36 ± 35.9	9.0	1001.83	605.55	-19	24.4
			1001.83	282.28	-29	24.4
PE 36:2-N-16:0	220.73 ± 20.2	7.9	999.81	603.53	-19	22.9
			999.81	282.28	-29	22.9
PE 36:4-N-16:0	29.99 ± 2.5	6.6	995.78	599.50	-19	23.7
			995.78	282.28	-29	23.7
PE 38:0-N-16:0	<LLOQ	11.2	1031.87	635.60	-19	56.4
			1031.87	282.28	-29	56.4
PE 38:1-N-16:0	96.05 ± 9.1	10.1	1029.86	633.58	-19	33.3
			1029.86	282.28	-29	33.3
PE 38:2-N-16:0	116.02 ± 14.5	9.0	1027.84	631.57	-19	24.4
			1027.84	282.28	-29	24.4
PE 38:4-N-16:0	302.64 ± 21.8	7.7	1023.81	627.53	-19	22.9
			1023.81	282.28	-29	22.9
PE 38:5-N-16:0	66.31 ± 1.1	6.7	1021.79	625.52	-19	23.7
			1021.79	282.28	-29	23.7
PE 40:4-N-16:0	65.51 ± 9.3	8.5	1051.84	655.57	-19	24.4
			1051.84	282.28	-29	24.4
PE 40:5-N-16:0	12.26 ± 1.4	8.0	1049.83	653.55	-19	22.9
			1049.83	282.28	-29	22.9
PE 40:6-N-16:0	115.24 ± 12.7	7.2	1047.81	651.53	-19	22.9
			1047.81	282.28	-29	22.9
PE 34:1-N-17:0	–	8.4	987.81	577.52	-19	23.7
			987.81	296.29	-29	23.7
PE 34:2-N-17:0	–	7.3	985.79	575.50	-19	22.9
			985.79	296.29	-29	22.9
PE 36:1-N-17:0	–	9.6	1015.84	605.55	-19	31.9
			1015.84	296.29	-29	31.9
PE 36:2-N-17:0	–	8.6	1013.83	603.53	-19	24.4
			1013.83	296.29	-29	24.4
PE 38:4-N-17:0	–	8.3	1037.83	627.53	-19	22.9
			1037.83	296.29	-29	22.9
PE 34:0-N-18:0	<LLOQ	10.0	1003.84	579.53	-19	33.3

			1003.84	310.31	-29	33.3
PE 34:1-N-18:0	20.61 ± 1.3	9.0	1001.83	577.52	-19	24.4
			1001.83	310.31	-29	24.4
PE 36:0-N-18:0	<LLOQ	11.2	1031.87	607.57	-19	56.4
			1031.87	310.31	-29	56.4
PE 36:1-N-18:0	63.64 ± 3.3	10.2	1029.86	605.55	-19	33.3
			1029.86	310.31	-29	33.3
PE 36:2-N-18:0	56.87 ± 6.4	9.1	1027.84	603.53	-19	24.4
			1027.84	310.31	-29	24.4
PE 36:4-N-18:0	11.26 ± 1.8	7.7	1023.81	599.50	-19	22.9
			1023.81	310.31	-29	22.9
PE 38:1-N-18:0	<LLOQ	11.3	1057.89	633.58	-19	66.7
			1057.89	310.31	-29	66.7
PE 38:2-N-18:0	17.27 ± 3	10.2	1055.87	631.57	-19	33.3
			1055.87	310.31	-29	33.3
PE 38:4-N-18:0	106.13 ± 7.7	8.9	1051.84	627.53	-19	24.4
			1051.84	310.31	-29	24.4
PE 38:5-N-18:0	28.29 ± 3	7.8	1049.83	625.52	-19	22.9
			1049.83	310.31	-29	22.9
PE 38:6-N-18:0	20.72 ± 2.4	7.2	1047.81	623.50	-19	22.9
			1047.81	310.31	-29	22.9
PE 40:4-N-18:0	18.23 ± 1.4	9.7	1079.87	655.57	-19	31.9
			1079.87	310.31	-29	31.9
PE 40:5-N-18:0	<LLOQ	9.3	1077.86	653.55	-19	25.3
			1077.86	310.31	-29	25.3
PE 40:6-N-18:0	105.68 ± 17.8	8.3	1075.84	651.53	-19	22.9
			1075.84	310.31	-29	22.9
PE 34:1-N-18:1	76.29 ± 6.3	8.0	999.81	577.52	-19	22.9
			999.81	308.29	-29	22.9
PE 36:0-N-18:1	<LLOQ	10.2	1029.86	607.57	-19	33.3
			1029.86	308.29	-29	33.3
PE 36:1-N-18:1	137.73 ± 7.4	9.2	1027.84	605.55	-19	24.4
			1027.84	308.29	-29	24.4
PE 36:2-N-18:1	138.32 ± 16.4	8.1	1025.83	603.53	-19	22.9
			1025.83	308.29	-29	22.9
PE 36:4-N-18:1	20.07 ± 1.6	6.7	1021.79	599.50	-19	22.9
			1021.79	308.29	-29	22.9
PE 38:1-N-18:1	31.63 ± 3.3	10.3	1055.87	633.58	-19	33.3
			1055.87	308.29	-29	33.3
PE 38:2-N-18:1	30.69 ± 6.2	9.2	1053.86	631.57	-19	24.4
			1053.86	308.29	-29	24.4
PE 38:3-N-18:1	<LLOQ	8.8	1051.84	629.55	-19	24.4
			1051.84	308.29	-29	24.4
PE 38:4-N-18:1	161.29 ± 26	7.9	1049.83	627.53	-19	22.9
			1049.83	308.29	-29	22.9
PE 38:5-N-18:1	40.51 ± 2.2	6.9	1047.81	625.52	-19	22.9
			1047.81	308.29	-29	22.9
PE 38:6-N-18:1	25.01 ± 1.1	6.3	1045.79	623.50	-19	25.3
			1045.79	308.29	-29	25.3

PE 40:2-N-18:1	<LLOQ	10.4	1081.89	659.60	-19	33.3
			1081.89	308.29	-29	33.3
PE 40:4-N-18:1	26.09 ± 2	8.7	1077.86	655.57	-19	24.4
			1077.86	308.29	-29	24.4
PE 40:5-N-18:1	<LLOQ	8.3	1075.84	653.55	-19	22.9
			1075.84	308.29	-29	22.9
PE 40:6-N-18:1	116.96 ± 17.7	7.4	1073.83	651.53	-19	22.9
			1073.83	308.29	-29	22.9
PE 40:7-N-18:1	11.34 ± 1	6.4	1071.81	649.52	-19	24.4
			1071.81	308.29	-29	24.4
PE 34:1-N-18:2	<LLOQ	7.1	997.79	577.52	-19	22.9
			997.79	306.28	-29	22.9
PE 36:1-N-18:2	<LLOQ	8.2	1025.83	605.55	-19	22.9
			1025.83	306.28	-29	22.9
PE 36:2-N-18:2	<LLOQ	7.2	1023.81	603.53	-19	22.9
			1023.81	306.28	-29	22.9
PE 38:4-N-18:2	10.11 ± 1.7	7.0	1047.81	627.53	-19	22.9
			1047.81	306.28	-29	22.9
PE 38:6-N-18:2	<LLOQ	5.4	1043.78	623.50	-19	40.7
			1043.78	306.28	-29	40.7
PE 40:6-N-18:2	<LLOQ	6.5	1071.81	651.53	-19	23.7
			1071.81	306.28	-29	23.7
PE 34:1-N-20:4	<LLOQ	6.9	1021.79	577.52	-19	22.9
			1021.79	330.28	-29	22.9
PE 36:0-N-20:4	<LLOQ	9.3	1051.84	607.57	-19	24.4
			1051.84	330.28	-29	24.4
PE 36:1-N-20:4	22.02 ± 6.3	8.1	1049.83	605.55	-19	22.9
			1049.83	330.28	-29	22.9
PE 36:2-N-20:4	11.47 ± 2.1	7.1	1047.81	603.53	-19	22.9
			1047.81	330.28	-29	22.9
PE 36:3-N-20:4	<LLOQ	6.1	1045.79	601.52	-19	26.2
			1045.79	330.28	-29	26.2
PE 38:1-N-20:4	<LLOQ	9.2	1077.86	633.58	-19	24.4
			1077.86	330.28	-29	24.4
PE 38:2-N-20:4	<LLOQ	8.1	1075.84	631.57	-19	22.9
			1075.84	330.28	-29	22.9
PE 38:3-N-20:4	<LLOQ	7.4	1073.83	629.55	-19	22.9
			1073.83	330.28	-29	22.9
PE 38:4-N-20:4	33.24 ± 8.5	6.9	1071.81	627.53	-19	22.9
			1071.81	330.28	-29	22.9
PE 40:4-N-20:4	<LLOQ	7.6	1099.84	655.57	-19	22.9
			1099.84	330.28	-29	22.9
PE 40:5-N-20:4	<LLOQ	7.2	1097.83	653.55	-19	22.9
			1097.83	330.28	-29	22.9
PE 40:6-N-20:4	29.85 ± 8.1	6.3	1095.81	651.53	-19	24.4
			1095.81	330.28	-29	24.4
PE 34:0-N-22:6	<LLOQ	7.5	1047.81	579.53	-19	22.9
			1047.81	354.28	-29	22.9
PE 34:1-N-22:6	<LLOQ	6.5	1045.79	577.52	-19	24.4

			1045.79	354.28	-29	24.4
PE 36:1-N-22:6	10.36 ± 2.9	7.7	1073.83	605.55	-19	22.9
			1073.83	354.28	-29	22.9
PE 36:2-N-22:6	<LLOQ	6.7	1071.81	603.53	-19	23.7
			1071.81	354.28	-29	23.7
PE 36:4-N-22:6	<LLOQ	5.4	1067.78	599.50	-19	40.7
			1067.78	354.28	-29	40.7
PE 38:4-N-22:6	16.78 ± 2.2	6.5	1095.81	627.53	-19	23.7
			1095.81	354.28	-29	23.7
PE 38:5-N-22:6	<LLOQ	5.5	1093.79	625.52	-19	36.7
			1093.79	354.28	-29	36.7
PE 38:6-N-22:6	<LLOQ	5.0	1091.78	623.50	-19	73.3
			1091.78	354.28	-29	73.3
PE 40:5-N-22:6	<LLOQ	6.9	1121.83	653.55	-19	22.9
			1121.83	354.28	-29	22.9
PE 40:6-N-22:6	19.64 ± 1.2	6.0	1119.81	651.53	-19	27.2
			1119.81	354.28	-29	27.2
PE 40:7-N-22:6	<LLOQ	5.1	1117.79	649.52	-19	61.1
			1117.79	354.28	-29	61.1

Supplementary Table 7: Exact masses and molecular formulas of PC, PE, and PI fragment ion isotopologues.

Lipid class	Type of fragment	Nominal *m/z*	*m/z* $[M–H]^-$	Molecular formula
PC	Fragment not containing glycerol	168	168.04310	$^{12}C_4{}^{13}C_0H_{11}O_4PN$
		169	169.04645	$^{12}C_3{}^{13}C_1H_{11}O_4PN$
		170	170.04981	$^{12}C_2{}^{13}C_2H_{11}O_4PN$
		171	171.05316	$^{12}C_1{}^{13}C_3H_{11}O_4PN$
		172	172.05651	$^{12}C_0{}^{13}C_4H_{11}O_4PN$
	Fragment containing glycerol	224	224.06931	$^{12}C_7{}^{13}C_0H_{15}O_5PN$
		225	225.07266	$^{12}C_6{}^{13}C_1H_{15}O_5PN$
		226	226.07602	$^{12}C_5{}^{13}C_2H_{15}O_5PN$
		227	227.07937	$^{12}C_4{}^{13}C_3H_{15}O_5PN$
		228	228.08273	$^{12}C_3{}^{13}C_4H_{15}O_5PN$
PE	Fragment not containing glycerol	140	140.01180	$^{12}C_2{}^{13}C_0H_7O_4PN$
		141	141.01515	$^{12}C_1{}^{13}C_1H_7O_4PN$
		142	142.01850	$^{12}C_0{}^{13}C_2H_7O_4PN$
	Fragment containing glycerol	196	196.03801	$^{12}C_5{}^{13}C_0H_{11}O_5PN$
		197	197.04136	$^{12}C_4{}^{13}C_1H_{11}O_5PN$
		198	198.04472	$^{12}C_3{}^{13}C_2H_{11}O_5PN$
		199	199.04807	$^{12}C_2{}^{13}C_3H_{11}O_5PN$
		200	200.05143	$^{12}C_1{}^{13}C_4H_{11}O_5PN$
PI	Fragment not containing glycerol	241	241.01184	$^{12}C_6{}^{13}C_0H_{10}O_8P$
		242	242.01520	$^{12}C_5{}^{13}C_1H_{10}O_8P$
		243	243.01855	$^{12}C_4{}^{13}C_2H_{10}O_8P$
		244	244.02191	$^{12}C_3{}^{13}C_3H_{10}O_8P$
		245	245.02526	$^{12}C_2{}^{13}C_4H_{10}O_8P$
	Fragment containing glycerol	297	297.03805	$^{12}C_9{}^{13}C_0H_{14}O_9P$
		298	298.04141	$^{12}C_8{}^{13}C_1H_{14}O_9P$
		299	299.04476	$^{12}C_7{}^{13}C_2H_{14}O_9P$
		300	300.04812	$^{12}C_6{}^{13}C_3H_{14}O_9P$
		301	301.05147	$^{12}C_5{}^{13}C_4H_{14}O_9P$